

106101

JPRS-JST-88-002

11 MARCH 1988



**FOREIGN
BROADCAST
INFORMATION
SERVICE**

JPRS Report

DISTRIBUTION STATEMENT A

Approved for public release;
Distribution Unlimited

Science & Technology

Japan

19980612 072

REPRODUCED BY
U.S. DEPARTMENT OF COMMERCE
NATIONAL TECHNICAL
INFORMATION SERVICE
SPRINGFIELD, VA 22161

DTIC QUALITY INSPECTED 6

10
92
APC

11 MARCH 1988

SCIENCE & TECHNOLOGY

JAPAN

CONTENTS

LASERS, SENSORS, OPTICS

Laser Processing Discussed in Journal Supplement

Laser Processing--Status, Perspectives [Hiromichi Kawasumi; KINO ZAIRYO, Aug 87]	1
Compound Ceramic Processing [Mamoru Okutomi; KINO ZAIRYO, Aug 87]	8
Single Crystal Growth by Laser CVD [Shigeyuki Hayashi; KINO ZAIRYO, Aug 87]	25
Fine Grain Development by Laser CVD [Kiyoshi Sawano; KINO ZAIRYO, Aug 87]	36
Superfine Grain Development by Laser [Akira Matsunawa; KINO ZAIRYO, Aug 87]	46
Hard Ceramic Film by Laser PVD [Shin'ei Mineda, Nobuo Yasunaga; KINO ZAIRYO, Aug 87]	59
Material Surface Improvement by Laser [Hiromichi Kawasumi; KINO ZAIRYO, Aug 87]	71

/9986

Laser Processing Discussed in Journal Supplement

Laser Processing--Status, Perspectives

43064001a Tokyo KINO ZAIRYO in Japanese Vol 7 Aug 87 pp 6-10

[Article by Professor Hiromichi Kawasumi, Department of Science and Engineering, Chuo University, Tokyo]

[Excerpt] 1. Introduction

Ever since the laser was invented by a researcher named T. Maiman in 1960, the powerful light beam has been put to use for processing of industrial products and for other purposes. In the 1970s, the oscillators with powerful laser outputs were developed, and this made it possible for lasers to be used for such industrial applications as welding, cutting, and making holes in industrial materials. In 1977, GM began to use powerful CO₂ gas lasers at its U.S. plant to harden the inner surface of cast-iron steering gear housing. According to the firm, the plant was processing the gear housing at a rate of 30,000 per day using 15 1-kw CO₂ laser machines. The utilization of laser machines by the major car maker showed that lasers were becoming a principal means of processing materials in the industry. A few years later, a group of researchers at MIT announced that ultraviolet lasers were very useful in processing semiconductors. Since the announcement researchers around the world have been conducting active research on the laser. Another group of researchers at MIT announced a method for producing highly uniform distribution nature Si₃N₄ powder by irradiating a mixture of ammonia gas and silane gas with CO₂ laser. The Si₃N₄ powder is gaining the attention of the ceramic industry as the material for producing auto engine parts.

Laser processing can be classified into the following four categories depending on which of the features of lasers is being utilized in carrying out processing of materials. (In a case where more than two features are involved for the processing, they were represented by the principal one at work.)

(A) Processing using high temperature generated by the bombardment of a focused laser beam having intense energy (high temperature process). (Theoretically, the diameter of the focused beam spot could be diminished to near the wavelength of the laser.)

(B) Processing using the monochromatic nature of lasers.

(C) Photochemical processing by causing a dissociation of composing elements in organic compounds, by bombarding with a high light quantum energy ultraviolet laser beam (low temperature processing).

(D) Composite processing methods: Those methods call for using more than one of the above-mentioned features at a time, or using the features by combining with chemical reactions.

(A) Processing using high temperature feature of laser light include:

i) Removal processing (making holes, cutting, trimming, marking, etc.).

ii) Welding.

iii) Surface property-changing processing (surface hardening, surface alloying, cladding, annealing, doping glazing, shock-hardening, etc.).

iv) Vapor deposition of a film of ceramics on the surface of aluminum or other materials to improve anti-wear capability.

v) Production of metal particles by bombarding with laser beams and melting a metallic material revolving at very high speeds.

vi) Growing of the monocrystal of ceramics.

(B) Processing using the monochromatic feature of laser light include:

vii) Synthesis of materials for producing ceramics (synthesis of Si_3N_4).

viii) The isolation-refining methods being utilized to obtain enriched U^{235} and Si^{30} .

(C) Examples of photochemical processing include:

ix) The formation of a thin film by decomposing organic metal compounds.

(D) Examples of composite processing include:

x) The compound plating method in which laser light is fired simultaneously in the same direction as the jet of the plating solution.

xi) The compound processing method in which the work of making holes or other kinds of processing is done on Al_2O_3 or Si material by putting them within the solution of KOH and irradiating them with lasers.

Excluding i, ii, viii, and xi, the laser processing methods itemized above could be applicable to producing functional materials in the future.

In general, high temperature processing is carried out using CO₂ or other kinds of laser light having relatively long wavelengths, by subjecting a material to laser vibrations. On the other hand, low temperature processing is conducted using shorter-wavelength lasers like the excimer laser.

2. Kinds of Lasers for Processing Use

Table 1 lists the kinds of lasers which could be used for producing functional materials. At present CO₂ lasers and YAG lasers are believed to be the only ones which could be used in industrial applications for high-temperature processing works, in view of the economy and stability of the laser system. As to the low-temperature laser processing machines, there are none available at present in the country, which can generate high energy outputs as economically as the high-temperature counterparts with the matching stability. However, it should not be long before the practical model of low-temperature high-output processing machine based on excimer lasers is developed, considering a related announcement made by a participating researcher at an industrial forum, CLEO '87, held in late April this year (1987). At the forum, C.L. Rottler of Western Research Co. announced that he had succeeded in obtaining a laser output higher than 800 J by exciting a diode with 4 kJ excimer lasers.

3. Features of Functional Material Making Methods Using Lasers

3.1 Synthesis of Ceramics Using Lasers

At present CO₂ lasers are used for synthesis of uniform ultrafine powder of Si₃N₄, a material which is drawing the attention of the industry as a new material for making ceramic auto engine parts. The Si₃N₄ powder is synthesized by irradiating a mixture of SiH₄ (silane gas) and NH₃ (ammonia gas) gas with 10.6 μ CO₂ lasers. The fine particles of Si₃N₄ result due to decomposition of the two kinds of gases into Si and N, respectively, with the irradiation, and as a result of ensuing abrupt cooling after the two decomposed elements united together. This synthesis method has the following advantages:

- 1) The materials to be processed can be heated without their contact with the heat source, and this prevents impurities finding their way into the product being synthesized. In addition, the method allows processing of a material under any kind of environment inside a chamber, as long as the chamber has a window through which the laser light can pass.
- 2) CO₂ laser light having a wavelength of 10.6 μ is absorbed by ceramics easily, and this makes it possible to synthesize Si₃N₄ powder in a relatively short time.
- 3) The said method enables conducting processing without causing localized heating of the material, and this makes it possible to obtain very fine powder of Si₃N₄ by quickly cooling after the heat processing.

Table 1. Kinds of Lasers Which Could Be Used in Industrial Processing Applications

Kinds of lasers		Wavelengths (μm)	Oscillation modes	Outputs [W] or [J]	Typical processing applications	Other remarks
CO ₂		10.6	CW	$\sim 2 \times 10^4$	Thermal treatment, welding, cutting, making holes	0.12 eV in light quantum energy
			Pulse			
TEA CO ₂		10.6	Pulse	8×10 [J]	Marking	
CO		About 5μ	CW	3000		
Ar ⁺		0.4880 0.5145	CW	20	Semiconductor processing	
Nd:YAG		1.06 (SH 0.53) (TH 0.355)	CW (Multi Mode)	1000*	Welding	2d higher harmonics 0.53 μ (14 W)
			Q-SW (Multi Mode)	150*	Welding, making holes Trimming	3d higher harmonics 0.355 μ (1.2 W)
			Q-SW (TEM ₀₀ Mode)	30*		
Nd:Glass		1.06	to 7 pulse/s	140 ⁺	Spot welding	
Alexandrite		0.70 ~ 0.78	Repeated pulses	150	Making holes	
Free electrons (FEL)		9 ~ 35	CW	$\sim 6 \times 10^3$	SPI application	
		0.64 ~ 0.655		5×10^{-4}		
Vaporized copper		0.511 0.578	Repeated pulses 6KHz	~ 150	For enriching uranium	
Pigment		0.19 ~ 4.5	Pulse	800 J	U enrichment, spectral analysis, medical applications	XeCl excimer laser excitation
Excimer	ArF	0.193	Pulse	40 ^x	Photochemical reaction	6.4 eV
	KrF	0.249		100 ^x		5.0 eV
	XeCl	0.308		300 (4KJ) \diamond	Photo etching	4.0 eV
	XeF	0.350		8 ^x		3.5 eV

* : Laser Focus Buyers' Guide (1986)

\diamond CLEO '87 Advance Program

+ : University of Tokyo Kuroda Lab materials

x : Lambda Physics Co. materials

3.2 Thin Film Making Method Using Lasers

The use of high energy particles for creating thin films in various industrial products, like ion beams which are currently used widely for that purpose, enhances the chemical reactions of the materials in those products, but the high energy particles also cause the defects within the films created by bombardment of the particles. In general, the chemical bonding of the molecules composing a solid object can be broken by applying a high energy beam with the energy level of about 10 eV. The composing electrons can be excited by applying nearly the same levels of the beam energy (Figure 1). By considering these facts, excimer lasers are drawing increasing attention of the LSI processing industry. It is now believed that the energy level of excimer lasers would be strong enough to cause proper chemical reactions needed to create a thin film, and the defects resulting from the energized particle bombardment can be restricted to very low levels.

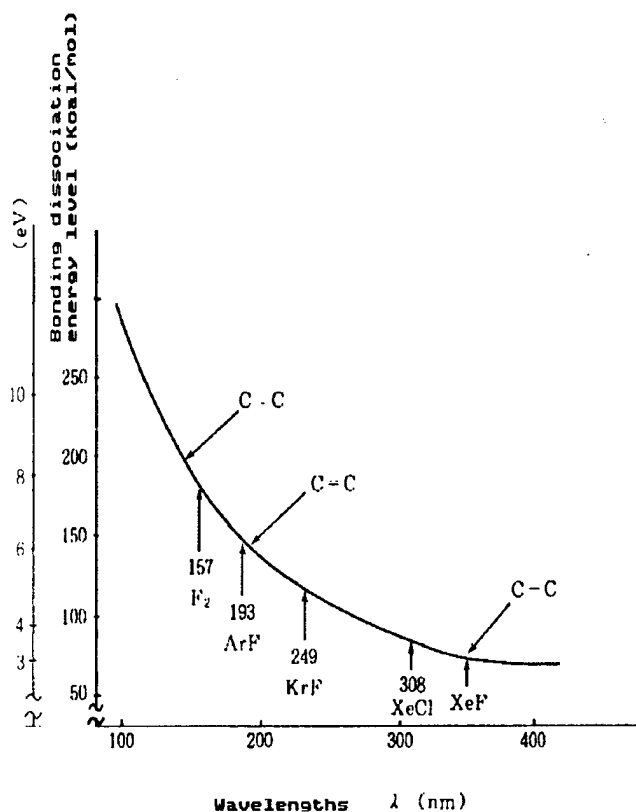


Figure 1. Relationship Between Dissociation Energy Levels of Number of Kinds of Molecules and Wavelengths of Lasers Used To Cause the Dissociation

In creating a thin film using lasers, either of the two principal features of the powerful light beam is used. Namely, the two features are the high coherence of laser light and the high purity of the light spectrum. The coherence enables the size of the light spot to be reduced to the degree of

the wavelength of the light theoretically. On the other hand, the narrowness of the spectrum width makes it possible to provide the photons of uniform energy levels, which is essential to cause needed chemical reactions in the process of creating a thin film within the environment of a specific medium.

Figure 2(a) and (b) gives the basic diagrams of the setups for experimenting with the creation of a thin film using lasers. In the setup shown in (a), the laser beam entering into the reaction chamber through the window smashes onto the surface of the material onto which a thin film is supposed to be created. On the other hand, in setup (b), the laser beam passes closer by the similar material.

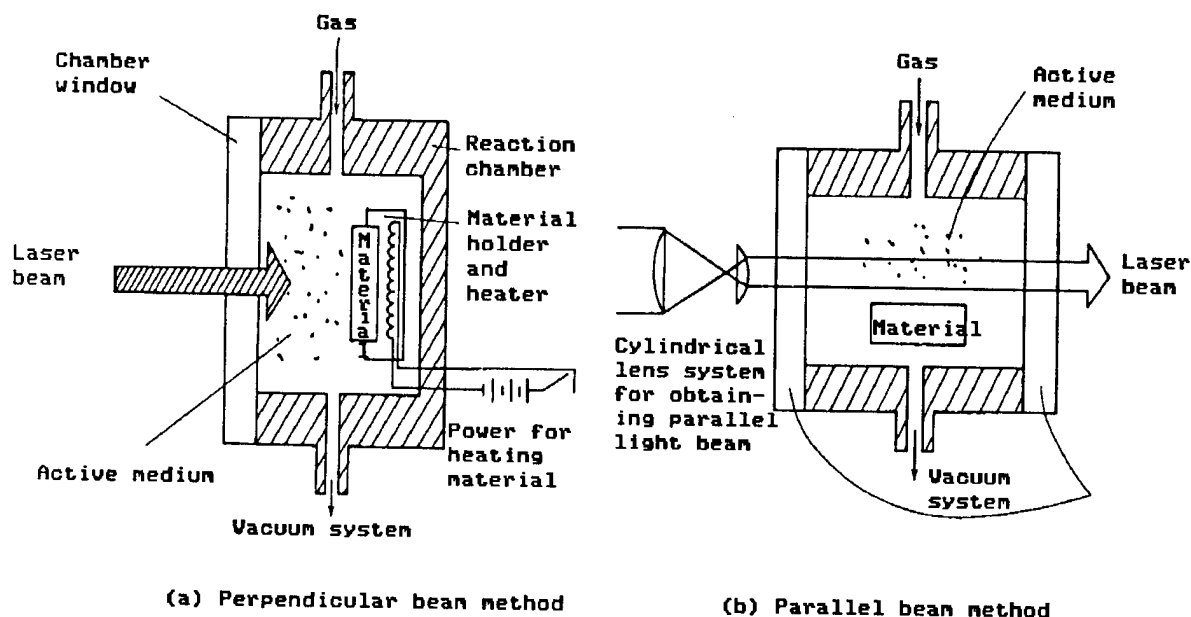


Figure 2. Two Types of Basic Setups for Forming Thin Film on Surface of Material
 (a) A method in which the laser beam enters into the processing chamber through the window perpendicular to the sample to be processed.
 (b) A method in which the beam enters into the chamber in parallel with the sample.

To form this film, either a single kind of gas or composite gases (or fluids) are simultaneously injected into the reaction chambers, which flow along the surface of the material when the material is being irradiated by lasers.

By ensuring proper selection of the wavelengths of the lasers, the kind of gas as well as the material, it is possible to attain either doping, etching, or vapor deposition of a thin film on the surface of the material with good results.

The laser chemical processing occurs when the photons in the laser light have energy levels high enough to cause the break of the chemical bonding among the molecules of the gas, and the processing is conducted as a result of the pieces of the dissociated molecules or atoms reacting with the substances on the surface of the material.

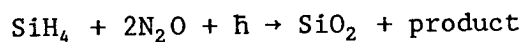
The wavelength of lasers to be utilized is decided based on the required energy level to break the chemical bonding. The processing is carried out successfully when the material and the gases involved in the processing absorb the laser energy effectively.

Table 2 lists the kinds of materials used in the experiments conducted so far, the kinds of precipitated films on the surface of those materials, and the wavelengths of lasers used in the experiments.

Table 2. Several Kinds of Thin Film Vapors Deposited on Base Materials Using Laser Chemical Processing Methods (J.G. Eden)

Base material molecules	Kinds of deposited substances	Wavelengths of lasers used λ (nm)
$\text{Mo}(\text{CO})_6$	Mo	260-270
$\text{Cr}(\text{CO})_6$	Cr	257
$\text{Al}(\text{CH}_3)_2$	Al	193, 257
$\text{SiH}_4/\text{N}_2\text{O}$	SiO_2	193
$\text{Al}_2(\text{CH}_3)_6/\text{N}_2\text{O}$	Al_2O_3	193
$\text{Zn}(\text{CH}_3)_2/\text{NO}_2$ (or N_2O)	ZnO	193 (248)

The table shows that using laser processing methods, the thin films of W and MO, the kinds which are difficult to create using conventional methods due to their high melting temperatures, can be created easily through the decomposition or organic metals. The table also shows that the laser methods are useful for forming a composite material film. The film of SiO_2 is the example. The following is the reaction formula involved in the method used to create the thin film of SiO_2 by P.K. Boyer and his research group:



They used ArF (193 nm) laser light, and reportedly they obtained the vapor deposition rate of 3,000 Å/min.

3.3 Laser Processing for Surface Properties Reform

Hardening of the surface of steel and cast iron using lasers as part of the surface properties reform has already been implemented using mass

production technology at the plants of GM. The reform is conducted by shooting laser beams at the surface of those metals by adjusting the laser light energy densities and the scanning speed so that the metal surface does not melt. Under the laser beam bombardment, the temperature on the surface rises past the A_1 transformation point. The cooling of the heated surface results due to the conduction of the heat toward nonirradiated portion of the metal under treatment. These processes can be likened to a quench hardening using neither water nor oil.

Compound Ceramic Processing

43064001b Tokyo KINO ZAIRYO in Japanese Vol 7 Aug 87 pp 11-24

[Article by Mamoru Okutomi, senior researcher at Electromagnetic Wave/Electron System Section of Denshi Gijutsu Sogo Kenkyusho; first paragraph is editorial introduction]

[Excerpt] Discussed in this chapter is the synthesis of a number of kinds of oxides having melting temperatures higher than $2,000^{\circ}\text{C}$ ($\text{ZrO}_2\text{-HfO}_2$, $\text{ZrO}_2\text{-Y}_2\text{O}_3\text{-HfO}_2$, and partially-stabilized $\text{ZrO}_2\text{-HfO}_2$ system ones) using laser sintering methods, as part of the effort to develop ceramic lasers having high strength and toughness using CO_2 lasers. Also discussed is the results of the synthesis of $\text{Al}_2\text{O}_3\text{-WO}_3$ system ceramics, which were created with the lasers being melted under nonequilibrium condition and then by being put to a steep cooling process for solidifying the melted lasers. Regarding the $\text{Al}_2\text{O}_3\text{-WO}_3$ -system ceramics thus synthesized, new kinds of compounds and monocrystals, which are not found among those that are listed on the equilibrium diagram, were recognized within the ceramics. Research has been conducted to clarify the microstructures of those compounds and crystals and to study the phase changes and mechanical strength of them.

1. Introduction

In recent years, the importance of laser instruments as industrial processing tools to carry out various jobs such as melting, welding, cutting, and making holes has been increasing. In addition, lasers are increasingly utilized to provide heat sources in various industrial applications. The principal features of lasers are the beam's high energy density, adjustability of the beam spot, and ease of handling. In conducting the processing of a material, the use of high energy beam enables high processing throughput to be attained. The high energy beam can also be used for heating a material locally. To conduct processing of a material efficiently by making use of those features of lasers, it is important to choose the right kind of laser in accordance with the kind of material to be processed and the method of conducting the processing. At present, CO_2 laser equipment is used in processing of metallic and nonmetallic materials for melting, welding, cutting, and making holes in them. Ceramics has a high absorption rate of laser energy, and for this reason lasers are beginning to be used increasingly in the heat processing of ceramics in the industry and in the R&D of various kinds of ceramics in

Table 1. Ceramics Synthesis Technology Using Lasers

Categories of synthesis technology	Conceivable synthesis methods
Synthesis of ceramics	(1) Laser sintering method (2) Ceramics synthesis method comprising laser-fusion phase (3) Self-promoted high temperature synthesis (SHS) (4) Heat-generating, decomposition synthesis (5) SHS + (4) (6) Application of nonequilibrium condition (7) Laser rheology processing method
Growth of ceramic monocrystal and surface treatment	(1) Melting-solidifying method using laser (2) Laser pull method (3) Laser Verneuil's method (4) Floating zone growth method using laser (5) Laser doping method (6) Laser heat dispersion method
Production of fine particles as material for making ceramics	(1) High-speed solid-rod spinning method (2) High-speed disk spinning method (3) Method of vibration removal of molten part of a solid rod (4) Method of gas-blow removal of the molten part (5) Method of pendant melting in the air (6) Crystal vaporization method (7) Laser thermal spraying (8) Laser plasma method (9) LCVD (10) Photochemical reactions

recent years. Table 1 lists the application fields of CO₂ laser as the heat sources in synthesizing ceramics and other related works including the growth of the single crystal. Currently, research is underway to commercialize the laser technology. The list also includes potential application fields. In research for growing and synthesizing ceramic materials conducted so far, attempts have been made to synthesize nonoxide material powders from gas phase using ceramics VD method, and to grow oxide monocrystals, monocrystal fibers, and to produce the spherical grain powder using either float zone method of molten fluid solidifying method. In all of these attempts, lasers were used to provide the heat sources. In addition, reports have been made on the synthesis of various kinds of high density ceramics (ZrO₂-HfO₂, ZrO₂-Y₂O₃-HfO₂, Al₂O₃-WO₃ systems) using laser sintering method, and on the formation of coating films on various kinds of ceramic products using laser CVD method or laser PVD method. The research for the development of new materials using CO₂ laser has begun in recent years. It is believed that the laser could be applied to the efforts in

search for the materials to create ceramics as material for developing superconductors, considering that the use of a laser would shorten the time required to produce ceramics.

The use of high power CO₂ laser light as the heat source in synthesizing ceramics has the following merits: 1) The fact that ceramics has a high absorption rate of CO₂ laser energy (wavelength: 10.6 μm) makes it possible to synthesize ceramics at shorter time; 2) the noncontact heating that the use of laser allows enables obtaining high-purity crystals of ceramics by preventing impurities from finding their way into the ceramics from the surrounding environments; 3) synthesizing of a crystal combining the features of very hard materials and high-melting temperature materials (nitrides, carbides, and borides) is possible by changing the synthesis environments. At the same time, it is also possible to synthesize ceramics containing a fusion phase; 4) the use of lasers has made it possible to grow various kinds of monocrystals of high-melting temperature nonoxide substances, which have been difficult to create until recently, by controlling the vapor pressure of the substances put under either a high pressure gas, a reduction environment, or a displacement environment; and 5) the introduction of lasers also has made it possible to create new kinds of substances and spherical-shaped particles, using the quick heating-quick cooling method and even under nonequilibrium or pseudo-equilibrium condition.

The following sections of this chapter will discuss the technology for synthesizing tough high strength ceramic materials using CO₂ laser as the heat source, including the synthesizing methods now under research. First, will be described the synthesis of a number of kinds of high melting temperature oxides with the melting points higher than 2,000°C (ZrO₂-HfO₂, ZrO₂-Y₂O₃-HfO₂, partially-stabilized ZrO₂-HfO₂), which are free of poisonous contents or radioactivity, and the synthesis of Al₂O₃-WO₃ system ceramics. Also to be discussed are the results of study of the characteristics of Al₂O₃-WO₃ system monocrystal, which were created under nonequilibrium synthesis condition.

2. Ceramics Synthesis Technology Using Laser Sintering Method

2.1 Material Preparation and Irradiation Control

The materials used for experimental creation of ZrO₂-HfO₂-system ceramics had 99.99 percent purity for ZrO₂ and HfO₂ and 99.99 percent purity for Y₂O₃, with the diameters of their grains ranging 0.5-1.0 μm for ZrO₂ and Y₂O₃ and measuring at 0.3 μm for HfO₂. The ZrO₂ (M-ZrO₂) and a far smaller amount of tetragonal ZrO₂ (T-ZrO₂). The HfO₂ had a monoclinic structure. The experimental creation involved the following combinations of materials: ZrO₂-HfO₂, PSZ (partially-stabilized ZrO₂ containing 3 %mol Y₂O₃)-HfO₂-system material, ZrO₂-Y₂O₃-system material, and ZrO₂-Y₂O₃-HfO₂.

On the other hand, in the experimental synthesis of Al₂O₃-WO₃-system ceramics, the purities and grain diameters of the material powders used were as follows: Al₂O₃--99.99 percent with an average grain diameter of

1 μm , WO_3 --99.8 percent with 0.3 μm . The synthesis can be carried out by directly irradiating those combinations of materials with lasers. But it is not practical because the direct irradiation causes the material particles to scatter due to the thermal shock resulting from the irradiation, and this makes it difficult to obtain ceramics of a desired shape. To cope with this problem, 5 percent methyl cellulose solution (distilled water) was added as a binder, and the combinations of the materials were calcined in the air after they were molded under a pressure of 100 kg/cm². The ceramics thus produced took the form of pellets with a diameter of 20 mm and a thickness of 5 mm. The calcination was conducted by putting to 600°C environment for 30 minutes for the ZrO_2 - Y_2O_3 -system and Al_2O_3 - WO_2 -system combinations, and to a 1,000°C environment for 4 hours for other combinations of materials.

2.2 CO_2 Laser System and Irradiation Condition

The CO_2 laser to be used for synthesizing ceramics is required to be able to heat the sample uniformly. The laser system used in my experimental synthesis of ceramics had a maximum output of 11.35 kw with the energy efficiency of about 20 percent. The intensity profile of the system's laser beam had a hat-shaped curve having a uniform energy density distribution (200 W/cm²). With the stability of the system, it had an output variation smaller than 2 percent after it continued to operate for 5 hours with an output of 8 kw. Figure 1 shows the outlines of the system and the irradiation setup used in the experiment. The laser system enables continuously (or in steps) changing the CO_2 laser output from zero to a required output level (the level which enables the sample to melt completely within 1 minute of irradiation) by adjusting the discharge currents, which is made possible by the sweep pattern generator built within the laser power supply. To measure laser output, cone-type calorie meters were used. As to the measurement accuracy, the meters had an error smaller than 2 percent at 10 kw output, with the ability of the reproducibility standing at 0.2 percent. The laser beam after passing through the shutter was focused using a ZnSe lens to a beam spot with a diameter of 20 mm. The samples were irradiated by being placed in the center of the carbon receptacles, each measuring 100 mm in diameter and 90 mm in height (25 mm ϕ and 40 mm deep in the inside). The laser beam was applied from the upper side of the samples. In the experimental synthesis, the laser beam was applied to the samples for a total of 60 seconds by varying the power densities to 2.7, 1.8, and 0.9 kw/cm² for creating ZrO_2 - HfO_2 -system ceramics. The measurement of the temperature on the surface of the samples while they were irradiated was conducted using a two-color pyrometer, based on AC ratio-calculating method of the two different wavelengths (0.5/0.58 μm), and two separate platinum-13 percent platinum/rhodium thermocouples. One of the thermocouples was placed above the samples at 20 mm from the surface of the carbon sample receptacles, and the other on the bottom of the receptacles.

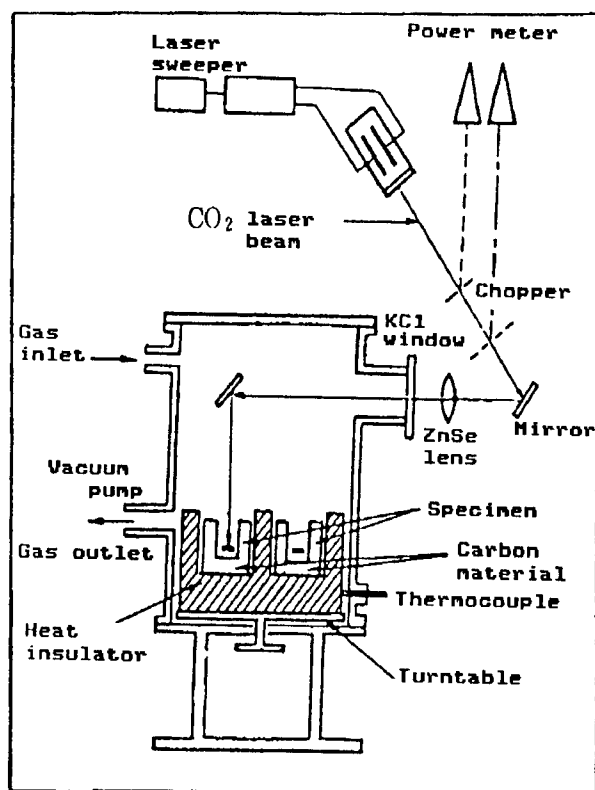


Figure 1. Laser System Experiment Outline

2.3 Observation of Synthesis Process

When the sample is struck with a laser beam, it almost instantly shines brightly and the surface begins to melt. Photo 1 [omitted] shows a series of photo frames taken by a high-speed camera (1/1,000 frames), showing the process of formation of the crystals when a 3 kw laser beam was shot at the pellet of Al_2O_3 -5 %mol CrO_3 sample. The series of frames shows the scattering of brightly shining grains when the sample material upon it was struck with a laser beam, followed by explosive scattering of the molten material on the surface of the sample due to an expansion of the air within the molded pellet due to heat from the surface. The speed of the scattering is estimated to be between 5 and 10 m/sec. It was observed that over a period up to 500 msec. from the start of laser irradiation, the scattering was seen periodically many times in every 17 msec. After 500 msec., the explosive scatterings begin to subside, and the molten sample material expands, becoming a sphere, due to surface tension. During this process, it was also observed that a spinning motion developed inside the molten mass due to thermal convection.

Figure 2(a) and (b) indicate the relationships between the surface temperatures of ZrO_2 , HfO_2 , and ZrO_2 - Y_2O_3 -system samples while they are being irradiated by lasers and the duration of the irradiation. The initial peak in the temperature surge was caused by the scattering of the molten articles from the surface of the hot sample and its having being

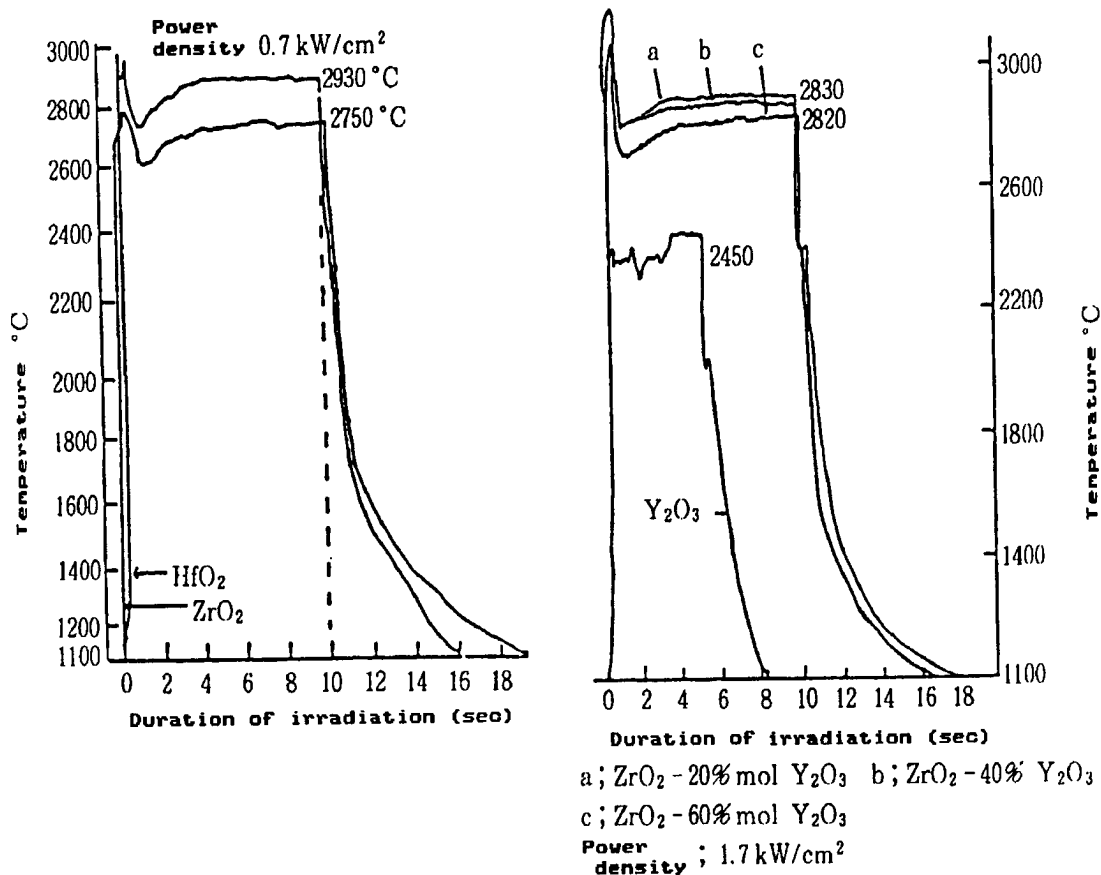


Figure 2. Curves of Surface Temperature Variations of Ceramic Samples While Being Irradiated by Lasers and After Irradiation

bombarded by a laser beam. The temperature on the surface of the irradiated sample tends to show a level which is a bit higher than the melting temperature of the sample materials themselves, as a result of measuring the temperature of the evaporated gas molecules. It is impossible to measure the time elapsed from the start of the irradiation to the melting of the sample, because it occurs so fast. Due to this, an attempt was made to calculate the time by using a model of semi-infinite field, in which the assumptions were made that the sample exists right on the path of the laser beam, that there would be no variation in the strength of laser energy, and that the sample would not move while it is heated and melted.

Under these assumptions, the temperature inside the sample at a depth X from the surface and after a duration t of irradiation can be calculated using the following equation:

$$T(X, t) = (2H\alpha_{th}t^{1/2}/K) \operatorname{erfc}\{X / \{2(\alpha_{th})^{1/2}t\}^{1/2}\}$$

In the equation, H represents the thermal energy absorbed by the sample, α_{th} denotes thermal dispersion rate, and K is thermal conduction rate. To obtain the surface temperature of the sample, assumptions are made that $X = 0$, $H = E_0(1-R)$, and $T(0, t) = T_m - T_0$. By inserting these equations into the equation, the following equation can be developed:

$$t_m = \pi K^2 (T_m - T_0)^2 / [4 \alpha_{th} \{ E_0 (1 - R) \}^2]$$

In this equation, t_m represents the time when melting of the sample begins, T_m denotes the absolute temperature at the melting point, T_0 indicates temperature on the surface of the sample when $t = 0$, α_{th} represents the thermal dispersion rate, K is the thermal conduction rate, E_0 represents the laser energy (power density) delivered to the sample, and R denotes the reflection rate from the surface of the sample.

Here, I will try to calculate the elapsed time since the start of irradiation to the beginning of the melting by supposing that the laser energy is absorbed completely by the Al_2O_3 and ZrO_2 samples. According to documents available, in the case of Al_2O_3 (2,050°C in melting temperature) $E_0 = 1.1 \text{ kw/cm}^2$, $T_0 = 293 \text{ K}$, $T_m = 2,323 \text{ K}$, when $\alpha_{th} = 1.1 \times 10^3 \text{ cm}^2/\text{sec}$ and $K = 3.3 \times 10^3 \text{ w/cm}^2\text{C}$. By using these figures, the value of t_m can be obtained to be 0.11 sec from the second equation. In the case of cubic-system zirconia it is known that the value of t_m is 0.16 sec. Those data on t_m may not be very dependable. In general, the value of t_m is believed to be in μ sec range.

3. Synthesis of Ceramics Using Laser Sintering Method

3.1 ZrO_2 - HfO_2 System

As described in the equilibrium diagram in Figure 3, phase changes occur in ZrO_2 - HfO_2 -system materials when their temperature is raised. The melting temperatures of the ceramics samples synthesized using the materials range between 2,700 and 2,860°C. The ceramics products synthesized using ZrO_2 - HfO_2 -system materials by changing mol ratio of the composing materials and by being quickly solidified after irradiation by a laser beam with a powder density of 2.7 kw/cm^2 had a semispherical shape and polycrystal structures. The ceramics thus synthesized had crystallized grains with their diameters ranging from 1 to 2 μm near the surface, and in the deeper portions the grain size reached as large as 60 μm . The ceramics had considerably more pores between those crystallized grains. Figure 4 shows the result of identification of the crystal condition on the cut face of the ceramics using microfocus X-ray diffraction method. From the results of analysis of the diffraction of the rays, it can be surmised that the mixture of $ZrO_2 \cdot HfO_2$ solid body and cubic-system ZrO_2 exists within the depth of 100 μm from the irradiated surface of the ceramics, and $ZrO_2 \cdot HfO_2$ exists in a perfect form of the solid body near the depth of 500 μm , and the mixture of $ZrO_2 \cdot HfO_2$ solid body and what is believed to be in the process of forming the solid body exists in depths ranging from 1 to 2 mm from the surface. When synthesizing ceramics using ZrO_2 - HfO_2 -system materials, the solid body of $ZrO_2 \cdot HfO_2$ is the principal thing formed within the ceramics after the materials were irradiated. However, in a sample composed of ZrO_2 and

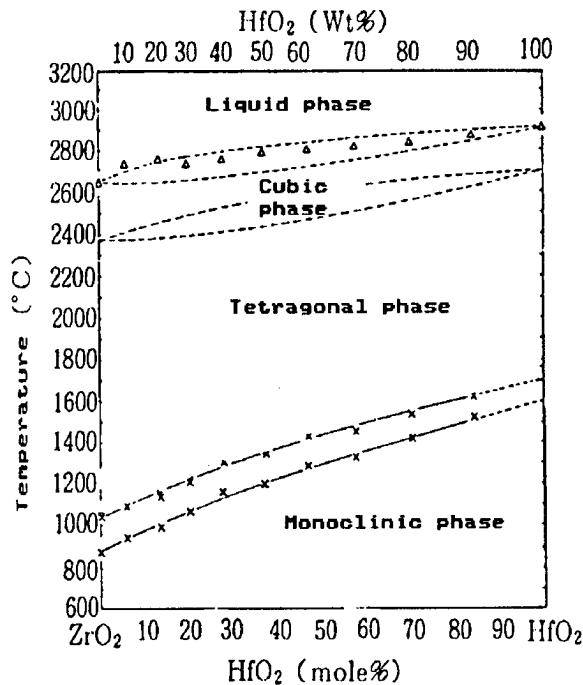


Figure 3. Equilibrium Diagram of ZrO₂-HfO₂-System Ceramic Materials
 The "x" marks in the figure represent the temperatures where the phase change between monoclinic and tetragonal system occur.
 (Results of a high temperature X-ray diffraction analysis.)

36 %mol HfO₂, significant clusters of cubic-system ZrO₂ crystals wrapped with monoclinic-system ZrO₂ crystals were observed after the material combination was irradiated by a 3 kw laser beam for 60 seconds. By using an equation derived from the X-ray diffraction analysis of ZrO₂, it was calculated that the synthesized volume of the monoclinic ZrO₂ account for 60 percent and the cubic-system ZrO₂ account for 40 percent of the synthesized ceramic product, respectively. The observation of the crystal conditions in the cut face of the ZrO₂-HfO₂ ceramics sample found many pores and cracks in the grain boundaries and within the grains (Photo 2 [omitted]). Those pores are believed to have been created by the air present within the materials, and in the process of the melting by the gas which was generated by the molten crystal. The cracks are believed to have been caused due to the phase changes under high temperature conditions, and a contraction of the crystal is believed to have contributed to aggravation of the cracks. (In ZrO₂, a phase change from monoclinic to tetragonal condition occurs at 1,000-1,100°C, and from tetragonal to cubic condition at 2,000°C. In HfO₂, a phase change from monoclinic to tetragonal condition occurs at 1,620-1,650°C range, and from tetragonal to cubic condition at 2,270°C.)

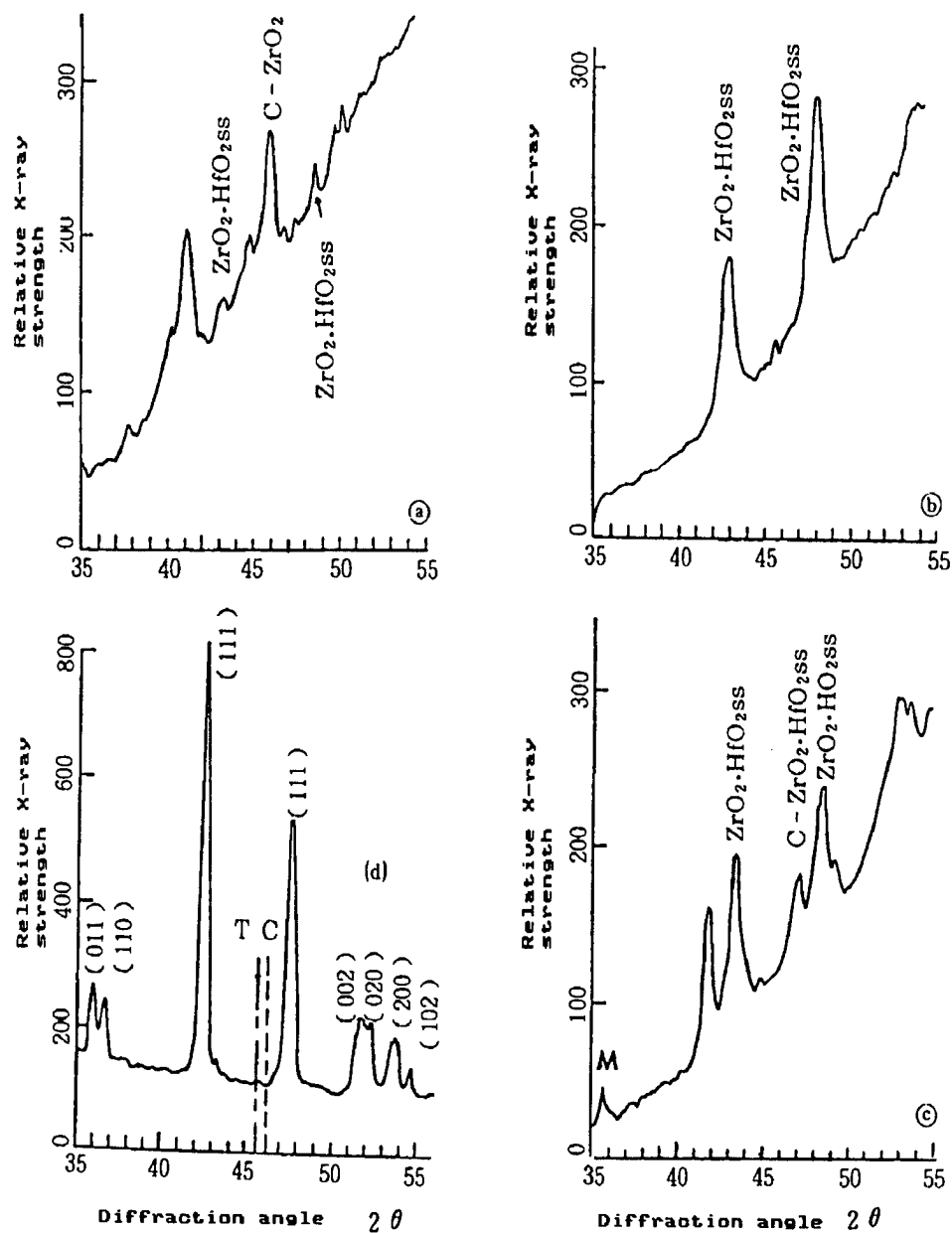


Figure 4. Cross-Section of Synthesized $\text{ZrO}_2\text{-HfO}_2$ Ceramics Sample and Results of X-Ray Diffraction Analysis of Ceramics
Diagram (d) is the result of X-ray diffraction analysis of a $\text{ZrO}_2\text{-HfO}_2$ sample which was not irradiated by lasers.

To prevent the phase change from occurring in the crystals of ZrO_2 and HfO_2 , introduction of oxides such as Y_2O_3 , CaO , or MgO into them has been studied. Experiments found that when the amount of Y_2O_3 in $\text{ZrO}_2\text{-HfO}_2$ -system material is increased, bulkier crystal grains containing cubic-phase ZrO_2 are formed. The Vickers hardness of the ceramics composed of such larger crystal grains, for example, in a 60 percent ZrO_2 -20 percent

Y_2O_3 -20 percent HfO_2 ceramics was 1,450 kg/mm², and in a 60 percent ZrO_2 -10 percent Y_2O_3 -30 percent HfO_2 ceramics the hardness reached 1,560 kg/mm². This hardness is nearly at the same levels as that of cubic ZrO_2 in ZrO_2 - Y_2O_3 -system ceramics, but lower than 1,700 kg/mm², the hardness achieved in the synthesized crystals in ZrO_2 - HfO_2 -system ceramics. The goal of this effort is to create strong ceramics having few pores, cracks and a small phase change. In view of developing such ceramics, increasing the amount of Y_2O_3 introduced into ceramic materials without limit must be avoided.

3.2 PSZ- HfO_2 System Ceramics

Partially-stabilized zirconia ceramics containing 3-6 percent Y_2O_3 displays a high toughness. The PSZ which was created using hot-press method has a bending strength of about 150 kg/mm². It is said that the strength comes from martensite transformation of the crystals between cubic and monoclinic condition. PSZ ceramics samples were also created using the laser sintering method. The structure of the synthesized crystals of the ceramics is the same as the one which was produced using the conventional sintering method, and through an X-ray analysis it was proved that the laser-sintered PSZ ceramics was composed of cubic ZrO_2 (T- ZrO_2). Shown in Photo 3 [omitted] are the photos of fracture of a molded compact of PSZ- HfO_2 -system material powders, and fractures of synthesized ceramics samples having different PS- HfO_2 materials composition ratios. The use of PSZ- HfO_2 -system materials enabled synthesizing ceramics having smaller degrees of pores in the crystallized grain boundaries and within the grains. Observation found that the diameter of the crystallized grains tended to decline as the amount of HfO_2 introduced increases. The average diameters of crystallized grains in those samples were 8 μm for a sample containing 15 %mol HfO_2 , 4.7 μm for a sample with 36 %mol HfO_2 , and 1.2 μm for a sample with 60 %mol HfO_2 . A sample with a content of 32 %mol HfO_2 had grains which were a mixture of small and significantly larger ones. In all of those synthesized ceramics samples, the solid bodies of T- ZrO_2 - HfO_2 were identified regardless of difference of the contents of HfO_2 . Figure 5 indicates the relationships between the contents of HfO_2 and variation of T- ZrO_2 volumes and changes of lattice constants in the a axis of the tetragonal ZrO_2 . When the contents of HfO_2 continue to increase, the T- ZrO_2 crystal phase changed to M- ZrO_2 phase, and in the end the solid body of $ZrO_2 \cdot HfO_2$ was formed. At the point of 32 percent HfO_2 the lattice constants of the a axis increase and as a result, the ratio of lattice constants between the c axis and the a axis is reversed. It is believed that this was caused as a result of a phase transition of the T- ZrO_2 occurring. In the rational formula $Y_2O_3 \cdot (Zr_{1-x} \cdot Hf_x)O_2$, it is conceivable that part of the Zr was displaced with Hf. In T- ZrO_2 crystals, it is believed that the solid body is generated by the formation of M- ZrO_2 crystals as a result of a decline of the volume of T- ZrO_2 crystals and then by diffusion of Hf to the places of the Zr ions of the ZrO_2 , just like the displacement and diffusion process of Hf to the places of the cations in T- ZrO_2 crystals.

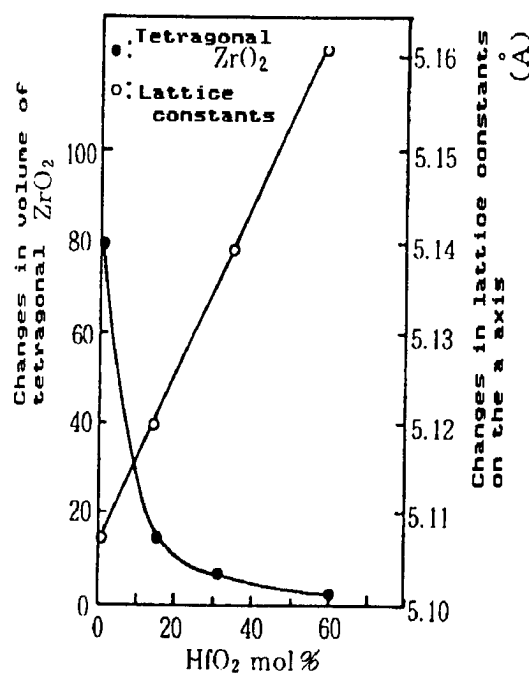


Figure 5. Changes of Volume of Tetragonal V and Lattice Constants on a Axis of V in Partially-Stabilized ZrO₂ in Accordance With Changes of HfO₂ Contents

3.3 Evaluation of ZrO₂-HfO₂-System and PSZ-HfO₂-System Ceramics

In ZrO₂-HfO₂-system ceramics, pores and cracks tend to occur within the synthesized crystals. In these experiments, Y₂O₃ was introduced into the ceramics which were synthesized to prevent the occurrence of a phase change in the crystals of the ceramics. In the experiments, 3 %mol Y₂O₃ was added to V material, and as a result a partially-stabilized ZrO₂-HfO₂ sintered body having little pores and a small grain-size distribution was obtained. The hardness of the synthesized crystals differed in accordance with the contents of HfO₂. In ZrO₂-HfO₂-system ceramics, high degrees of hardness were achieved when the contents of HfO₂ remained in 32-36 %mol range. In the case of PSZ-HfO₂-system ceramics, the hardness decreased significantly when the contents of HfO₂ declined below 25 %mol or increased higher than 39 %mol. When the contents were changed from 25 to 39 %mol, the hardness changed over 1,700-1,800 kg/mm². This hardness is only next to Al₂O₃ ceramics which has a hardness of 2,000 kg/mm². Figure 6 shows the relationships between the contents of HfO₂ and the hardness. In a strength test conducted using a diamond-tipped listed indenter loaded with more than 50 kg of weights, cracks developed from near the indent scar in the ZrO₂-HfO₂-system ceramics samples, but no cracks appeared in the PSZ-HfO₂-system samples. Table 2 lists the results of measurements of the melting temperatures, crystal phases and hardness of a number of kinds of the crystals of synthesized ceramics. The melting temperatures listed adopted the surface temperature when the surface of the samples melting was being

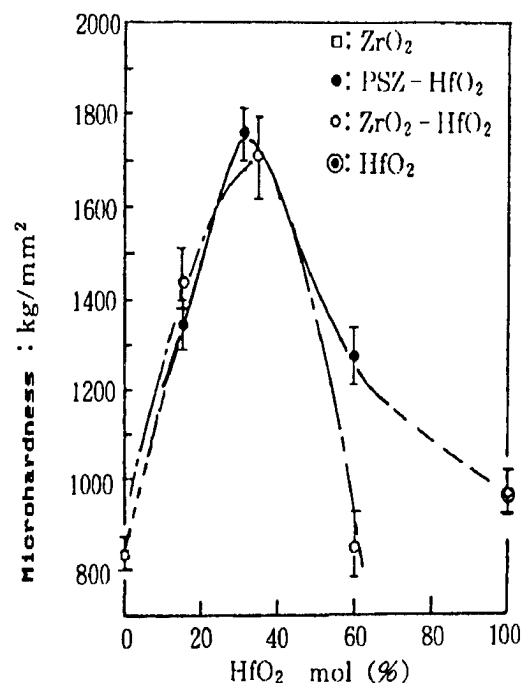


Figure 6. Relationships Between Contents of HfO_2 and Hardness Attained in ZrO_2 - HfO_2 -System Ceramics and PSZ- HfO_2 -System Ceramics

Table 2. Characteristics of Various Kinds of Ceramics Crystals Synthesized Using CO_2 Lasers

Samples	Contents mol %	Melting temperature °C	Crystal phases	Hardness kg/mm ²
ZrO_2	---	2,750	M - ZrO_2	840 ± 45
HfO_2	---	2,930	M - HfO_2	970 ± 50
Y_2O_3	---	2,680	C - Y_2O_3	920 ± 50
ZrO_2 - HfO_2	15 HfO_2	2,800	M - ZrO_2 · HfO_2 ss	1430 ± 90
	36 HfO_2	2,800	C - ZrO_2 , ZrO_2 · HfO_2 ss	1700 ± 90
	60 HfO_2	2,850	M - ZrO_2 · HfO_2 ss ZrO_2 · HfO_2 ss	1660 ± 90
ZrO_2 - Y_2O_3	3 Y_2O_3	2,750	T - ZrO_2 , M - ZrO_2	830 ± 50
PSZ - HfO_2	16 HfO_2	2,750	T - ZrO_2 , ZrO_2 · HfO_2 ss	1360 ± 90
	36 HfO_2	2,750	T - ZrO_2 , ZrO_2 · HfO_2 ss	1750 ± 60
	60 HfO_2	2,850	T - HfO_2 , ZrO_2 · HfO_2 ss	1280 ± 60

PSZ: Partially stabilized
 ZrO_2 (ZrO_2 - 3 % mol Y_2O_3)

M: Monoclinic crystal phase
T: Tetragonal crystal phase
C: Cubic crystal phase
ss: Solid solution

bombarded by a laser beam. The method of using temperature causes an error of ± 2 percent in the temperature range of 2,000 to 3,500°C from the actual melting temperatures. But anyway, measurement of the surface temperature clearly tells that an increase in the contents of HfO_2 causes the

temperature shifting to a higher side. To investigate the thermal characteristics of the sample under high temperature condition, a differential thermal analysis was conducted in the air by pulverizing the sample. As a result, it was found that the monoclinic ZrO_2 turned to tetragonal ZrO_2 accompanied by an endothermic reaction, and while from the tetragonal state to the monoclinic ZrO_2 accompanied by an exothermic reaction. On the other hand, similar crystal phase shifts were observed in ZrO_2 - HfO_2 -system ceramic samples, when they were subjected to similar analytical conditions. As regards the phase transition temperatures, a transition behavior quite similar to that of the sintered bodies created using arc method was observed in the ceramic samples. However, in PSZ- HfO_2 -system ceramics no phase changes were detected, indicating the ceramics' better stability at high temperature. Table 3 was compiled based on the data obtained by conducting a DTA analysis, and lists temperatures at which phase transitions from monoclinic to tetragonal state as well as from tetragonal to monoclinic state start, together with temperatures at which the transitions stop.

Table 3. Results of Differential Thermal Analyses of Thermal Characteristics of Various Kinds of Ceramics Synthesized Using Lasers
(Temperature at which phase changes start and then end.)

Synthesized crystals	Monoclinic state Starting temperatures	→ Tetragonal state Ending temperatures (°C)	Tetragonal state Starting temperatures	→ Monoclinic state Ending temperatures (°C)
ZrO_2 *	1156	1224	1106	1008
ZrO_2 - 3 mol % Y_2O_3	1152	1208	1056	996
ZrO_2 - 15 mol % HfO_2	1144	1216	1104	1040
ZrO_2 - 60 mol % HfO_2	1216	1240	1230	1126
PSZ - 15 mol % HfO_2	-	-	-	-
PSZ - 60 mol % HfO_2	-	-	-	-

* Untreated

ZrO_2 - Y_2O_3 - HfO_2 -system ceramics has high melting temperatures, and it has nearly the same hardness as that of Al_2O_3 ceramics. These features of the ceramics make it suitable for use as mechanical structural material and in other applications where the material is required to have good anti-wear and high-temperature abilities. By controlling the contents of Y_2O_3 , it may be possible to use the ceramics as an abrasive. To see the applicability of the ceramics as the abrasive grains, an experiment in which stainless steel was polished using the grains was conducted. The powder of the ceramics, with the diameter of the powder grains ranging 5-10 μm , for use in the polishing was produced by crushing the ceramics into powder using an automatic milling machine. The polishing was conducted using the wet lapping method in which the ceramic powder was furnished only once during the polishing. Figure 7 shows the relationships between the hardness of a number of kinds of ceramics crystals and the

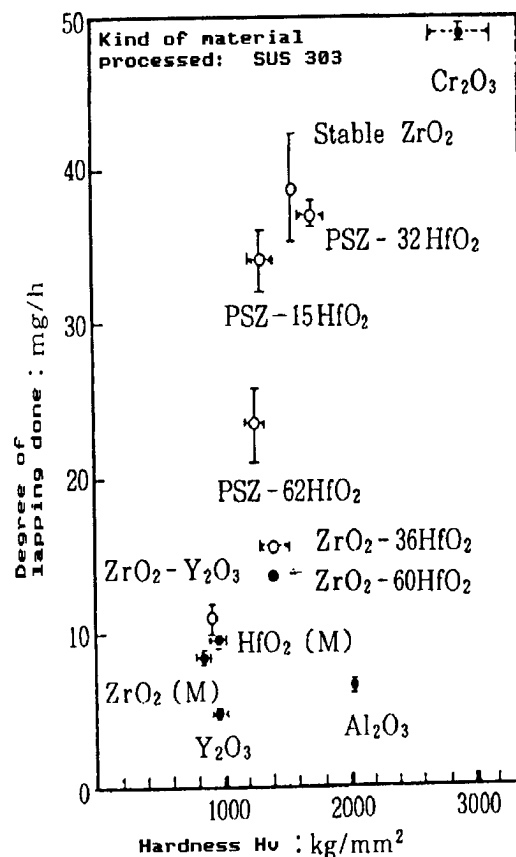


Figure 7. Evaluation of Lapping Performance of Powder Grains of Various Kinds of Ceramics Synthesized Using Laser Sintering Methods
 Revolving speed of lap and sample: 30 rpm
 Powder grain diameters: 2-4 μm
 Lap density: 50 percent furnished only once
 Lapping condition: pressure; 0.6 kg/cm²

degrees of processing done, when the powders of those crystals are used for various processing purposes. Among those crystals, the powder of PSZ-HfO₂-system ones with the HfO₂ content of 15 and 32 %mol, respectively, exhibited particularly good lapping results when they were used in processing of SUS303 stainless steel. It was found that low chemical affinities between the powder grains and the steel contributed to attaining the high lapping rates.

As described so far in this section the PSZ-HfO₂-system ceramics makes good material for producing heat-resisting material for use in furnaces and structural material, and can be applied to polishing and grinding tools by controlling the amounts of additives introduced into the ceramics.

3.4 Synthesis of Al_2O_3 - WO_3 -System Ceramics

As regards the research related to Al_2O_3 - WO_3 -system ceramics, research on chemical reactions between the two different materials at a temperature of $2,500^\circ\text{C}$ was conducted, and the equilibrium diagram of the Al_2O_3 - WO_3 system was obtained (Figure 8). The two kinds of materials, when made to react with each other, change to liquid phase at temperatures higher than $1,230^\circ\text{C}$. This makes it possible to conduct reaction tests involving those two kinds of substances using an electric furnace. But the use of the furnace requires a comparatively long time to conduct the test, and by using the furnace method it is difficult to obtain the solidified phase of WO_3 due to evaporation of the substance during the test. To cope with this problem, lasers were used to synthesize ceramics by melting the material using lasers and quickly solidifying the melted materials. The ceramics thus synthesized contained new kinds of compounds which cannot be found on the Al_2O_3 - WO_3 -system equilibrium diagram, and it was found that new types of monocrystals were generated within the ceramics. In the following, the results of a study on the characteristics of the synthesized ceramics will be discussed.

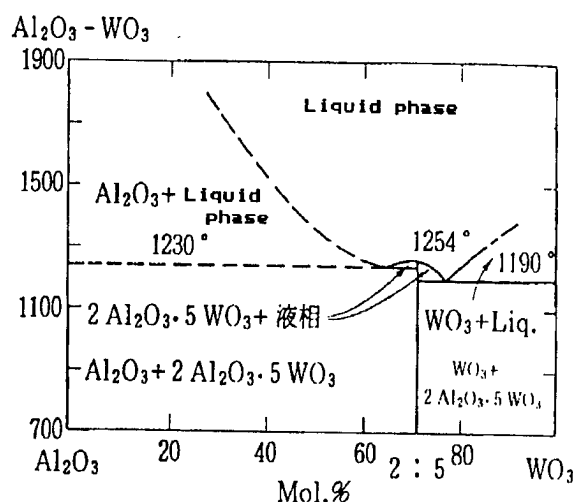


Figure 8. Equilibrium Diagram of Al_2O_3 - WO_3 -System Ceramics

What was interest in the process of synthesizing ceramics was a phenomenon, in which a mountain-shaped ceramic crystal grew toward the direction from which the laser beam came (Photo 4(a) [omitted]), when the pelletized samples of Al_2O_3 -40 %mol WO_3 -system and Al_2O_3 -50 %mol WO_3 -system materials were irradiated by lasers at output power density of 2.5 kw/cm^2 for 5 minutes. The growth speed amounted approximately to 1.2 mm/min . No similar growth phenomenon was observed in other samples with a different mixture ratio of the materials. In those samples, the melted mixture solidified to form semispherical ceramics due to surface tension. The ceramics had bluish color on the surface, and checking of a cross section (a face perpendicular to the growth direction of the crystal) found that the ceramics was composed of a monocrystal with little distortions (Photo 4(b) [omitted]). The checking was conducted using microfocus X-ray Laue method.

There is a possibility that the synthesized ceramics is made up of an alumina monocrystal, due to evaporation of the WO_3 contents under laser irradiation because of their higher vapor pressure than that of Al_2O_3 . To investigate the possibility, the grown monocrystal was compared with a sapphire using the right-angle scattering method of laser Raman spectroscopic analysis. As a result, the peaks of W, which are higher than the peak strength of Al, were observed in the data obtained through the analysis of the monocrystal. This indicated that the monocrystal apparently contains tungsten, and in that respect the monocrystal was a completely different one from Al_2O_3 monocrystal. The tungsten-containing monocrystal had a core structure which looked like a cluster of pillars (Photo 5 [omitted]), and it was encircled by more irregular but still pillar-shaped crystal structures.

The structural analysis of the monocrystal, which was conducted by crushing the crystal into powder and using the X-ray diffraction method, found that the monocrystal was quite a different one from the monocrystal of Al_2O_3 - 5WO_3 which can be formed at a lower temperature. The comparison of (hkl) and the spacing (d) between their measurement values and values obtained through calculations using ASTM values (a, b, c, α , β , γ), in addition to separation of $K\alpha$ rays from the X-ray diffraction pattern found that Al_2O_3 - 3WO_3 monocrystal had: a space group of rhombic system belonging to Pnca; the lattice constants of $a = 9.104$, $b = 12.580$, and $c = 9.057$ Å; α , β , $\gamma = 90$ degrees; and 0.104 Å in the volume of the unit lattice. Table 4 shows the relationships between the (hkl) and the spacing values of the Al_2O_3 - 3WO_3 monocrystal obtained through measurement and similar values of the laser-synthesized crystals obtained through calculations.

The cause and processes of the crystal of Al_2O_3 - 3WO_3 continuing to grow while the material sample of the crystal is being irradiated by lasers are believed to be as follows: First, moments after the irradiation starts the material sample melts completely, and the heat of the melted sample is dissipated by the carbon stand on which the sample is put; this causes a temperature gradient to appear within the molten material, promoting the precipitation of a crystal core having a growth direction; once the core appears, the crystal continues to grow as a result of the heat escaping through the solid-liquid-state interface on the molten sample. As regards those Al_2O_3 - WO_3 -system products having other composition ratios of the materials, particularly noteworthy here is the polycrystalline phase feature of the new compound Al_2O_3 - 3WO_3 , in addition to the synthesized Al_2O_3 - 5WO_3 listed on the equilibrium diagram. According to calculations conducted based on the ratios of the strength of the standard diffraction rays, the synthesized volumes of Al_2O_3 , Al_2O_3 - 3WO_3 , and Al_2O_3 - 5WO_3 at 70 %mol WO_3 level are estimated at 88, 79.3, and 11.9 percent in that order, respectively, and it was recognized that much of the Al_2O_3 - 3WO_3 was synthesized. At 90 %mol WO_3 level, it was observed that noodle-shaped polycrystals were formed, and this resulted from the above-mentioned crystal phase having been affected by WO_3 . Table 5 lists various crystal phases and hardness of a number of kinds of ceramics synthesized using lasers, along with the temperatures on the surface of the material samples while being irradiated. From those data listed in the table, it was learned that the monocrystal of Al_2O_3 - 3WO_3 having high hardness can be

Table 4. Results of Identification of $\text{Al}_2\text{O}_3\text{-3WO}_3$ Crystals With Identification Conducted Using X-Ray Diffraction Method

n	hkl	Calculated values (Å)	Measured values (Å)
1	020	6.289652	6.302000
2	111	5.728023	5.733000
3	121 R	4.497530	4.507000
4	102	4.057942	4.058000
5	112	3.861969	3.860000
6	031	3.805122	3.807000
7	022	3.675151	3.677000
8	131	3.512888	3.511000
9	202	3.216866	3.217000
10	040	3.144826	3.146000
11	230	3.089718	3.088000
12	013	2.935758	2.937000
13	222	2.864011	2.866000
14	311	2.814610	2.816000
15	123	2.068604	2.067000
16	240	2.590735	2.591000
17	232	2.552292	2.551000
18	312	2.478412	2.478000
19	250	2.203986	2.205000
20	411	2.182110	2.182000
21	233 R	2.159371	2.162000
22	313	2.114075	2.114000
23	214	2.003082	2.003000
24	252	1.981757	1.982000

Table 5. Melting Temperature, Crystal Phases, and Microhardness of $\text{Al}_2\text{O}_3\text{-WO}_3$ -System Ceramics Synthesized Using Lasers

Material composition mol%	Melting temperature °C	Crystal phases	Hardness HV : kgf/mm ²
$\text{Al}_2\text{O}_3\text{-20 WO}_3$	2100	Al_2O_3 , $2\text{Al}_2\text{O}_3\cdot 5\text{WO}_3$	1760 ± 50
$\text{Al}_2\text{O}_3\text{-30 WO}_3$	2100	$\text{Al}_2\text{O}_3\cdot 3\text{WO}_3$	2010 ± 50
$\text{Al}_2\text{O}_3\text{-40 WO}_3$ *	2100	Al_2O_3 , $2\text{Al}_2\text{O}_3\cdot 5\text{WO}_3$	2190 ± 50
$\text{Al}_2\text{O}_3\text{-50 WO}_3$ *	2100	single $\text{Al}_2\text{O}_3\cdot 3\text{WO}_3$	3700 ± 50
$\text{Al}_2\text{O}_3\text{-60 WO}_3$	2100	Al_2O_3 ,	1780 ± 50
$\text{Al}_2\text{O}_3\text{-70 WO}_3$	2100	$2\text{Al}_2\text{O}_3\cdot 5\text{WO}_3$	1150 ± 50
$\text{Al}_2\text{O}_3\text{-80 WO}_3$	2100	$\text{Al}_2\text{O}_3\cdot 3\text{WO}_3$	1030 ± 50
$\text{Al}_2\text{O}_3\text{-90 WO}_3$	2100	WO_3	1000 ± 90

* Synthesis of monocrystal

synthesized only when the contents of WO_3 are confined between 40 to 50 %mol levels. The hardness surpassed that of Al_2O_3 monocrystal, and is equivalent to 3,700 kg/mm² in Vickers hardness.

So far in this chapter, the synthesis of Al_2O_3 - WO_3 -system ceramics using lasers has been discussed. From the experiments for the synthesis, it was found that the ceramics crystal which was synthesized by melting the materials and then quickly solidified under nonequilibrium state contains Al_2O_3 - 3WO_3 , a new compound which cannot be found on the state diagram. It was also found that the monocrystal of Al_2O_3 - 3WO_3 was possible to create only when WO_3 was confined between 40 to 50 %mol range.

4. Conclusion

So far in this chapter, the synthesizing technology of oxide ceramics aimed at developing tough and high strength new ceramics, as an example of the application of CO_2 laser to industrial usage to provide high-temperature heat sources, has been discussed. The discussion also touched the material characteristics of ZrO_2 - HfO_2 and ZrO_2 - Y_2O_3 - HfO_2 -system ceramics. In addition, the finding of new compounds and monocrystals by synthesizing Al_2O_3 - WO_3 -system ceramics under nonequilibrium condition, which had not been found on the state diagram, was also described. This finding suggests a possibility that there could be similar kinds of still unknown crystals in other systems of reaction which have their melting points at lower temperatures. In view of this, synthesizing crystal, especially under nonequilibrium condition, will become more interesting in the future.

In producing ceramics, the use of lasers makes it possible to carry out sintering speedily, and this will be particularly convenient in synthesizing different kind of ceramics, to study the characteristics of ceramic materials by changing the material composition in the laboratory. The kinds of ceramics discussed in this chapter could be utilized in industrial applications as heat resisting material for use in furnaces and structural ceramics, and for grinding and polishing applications. But for utilization of those ceramics on a commercial basis, a further improvement of the characteristics must be made. There is a possibility that the use of lasers in ceramics synthesizing could produce results which have been unknown. In view of this, lasers would become an important tool in the development of new industrial materials in the future.

Single Crystal Growth by Laser CVD

43064001c Tokyo KINO ZAIRYO in Japanese Vol 7 Aug 87 pp 25-32

[Article by Shigeyuki Hayashi, assistant professor, Tohoku University; researcher at the university's Metal Material Research Laboratory; first paragraph is editorial introduction]

[Excerpt] CO_2 gas laser proves to be a superb heat source for use in various applications. Using the laser, thin monocrystals with a diameter of less than 1 mm were grown. This chapter will discuss the processes for creation of the crystals, including a report on related work done by a U.S.

research group. CO₂ laser can be used with various kinds of substances, and in the future it could be used for the growth and synthesis of thin films, fibers, and fine particles of various materials.

1. Introduction

During the past 30 years or so since Dr Maiman succeeded in oscillation of a ruby laser in 1960, various kind of lasers--solid, liquid, and gas lasers--have been invented. Today, the superior optical characteristics of those lasers are used in various fields, including communications, measurement, information processing, industrial processing, medical applications, and nuclear fusion. Among those various kind of lasers developed so far, the CO₂ laser which oscillates at a wavelength of 10.6 μm had been attracting the attention of researchers for many years as a very promising heat source, for the laser's capability of generating high energy output at high efficiency. In 1970, two researchers, D.B. Gasson and B. Cockayne, attempted to create monocrystals of such high-melting temperature oxides as Al₂O₃ (melting temperature $T_m = 2,050^\circ\text{C}$) and Y₂O₃ ($T_m = 2,450^\circ\text{C}$) using a CO₂-N₂-He laser. Then another researcher, J.S. Haggerty, tried to grow the single crystals of oxides and carbides in the environments of the air, Ar, Cl₂, H₂, and CH₄ using a 200 W CO₂ laser. The attempts were made by changing the density of the laser beam energy, the angle of incidence, the growth speed, and the growth direction. C.A. Burrus and J. Stone succeeded in growing Nd:YAG ($T_m = 1,950^\circ\text{C}$) to the length of about 0.5 cm with a diameter of 50 μm by controlling the growth direction, and they also succeeded in attaining a CW laser operation using the crystal at room temperature. While in Japan, in 1977 K. Takagi and M. Ishii announced the results of their joint research on the microvoids created within the single crystal of sapphire by growing the crystal of sapphire.

The fact that those typical experiments of growing monocrystals using lasers were made in the 1970s indicates that the level of the basic technology for growing monocrystal using lasers was already reaching a considerably high standard then. Among those researchers the purpose of growing the monocrystals differed. But what was common to their practices was the fact that all of the monocrystals grown by them were smaller than 2 mm in diameter, in most cases around 100 μm . It can be said that the ability of creating a single crystal with such a small diameter using lasers demonstrates clearly the features of laser heating. The technology for producing a very thin diameter crystal with good reproducibility can be applied to producing not only optical fibers but also a monocrystal of very high purity using very tiny amounts of expensive materials, so that it can be used in the research of substance properties.

In the following sections of this chapter, the modified pedestal growth method (LHPG) involving laser heating, and the effects of using the method on the solidification of the molten materials, crystal growth process, crystal structures, crystal defects, and the generation of new substances will be discussed. Along with the discussion, the results of research by a U.S. group headed by Stanford University Professor R.S. Feigelson, who has

been active in the research for growth of fiber crystals in recent years, will be introduced.

2. Crystal Growth Setup and Growth Method

The laser heating systems which are popularly used now have much in common in their features. Because of this, the outlines of the laser heating system installed at the CMR of Stanford University will be discussed in the following. The Stanford system incorporates 50 W CO₂ lasers, and it can be used with various kinds of samples, including oxides, borides, and metals which have low laser energy absorption rates. The ratio of He, N₂, and CO₂ gas in the laser system is about 3:1:1, with the composition being able to be changed slightly when the output range is switched. As processing environments, the facility allows choosing of either the air, vacuum or Ar environment. By making the diameter of the material rods ($<1\text{mm}\phi$) to be processed smaller, the system enables locally melting materials having melting temperature reaching up to around 2,700°C. The diameter of samples which the system can handle ranges from 50 to 1,500 μm with a length of 200 mm. The sample can be moved at stepless speeds ranging from 0.1 mm to 100 mm/min. The controlling of the diameter as well as the length of the sample can be carried out manually or automatically while observing the sample under a stereoscopic microscope (maximum magnification: 70 times). The Stanford system allows recording of the process of crystal growth in video cassette tapes. This would enable a researcher to study the dynamics of the formation of crystals any time by playing back the recorded tapes, and this would greatly help a researcher engaged in crystallography in furthering their research.

Now changing topics, two different examples of arranging samples and laser optical systems will be introduced in the following.

(1) The arrangement shown in Figure 1 is the one which was tried by C.A. Burris and Y. Stone. The simplicity and usefulness of the arrangement account for its being used with various kinds of materials even today. Figure 1(a) indicates that a single laser beam was split into two beams, and they are being fired at the tip of a feed from two directions, after the beams were narrowed to 200 $\mu\text{m}\phi$ using ZnSe lenses. The figure indicates that the irradiation of the feed at the top caused molten liquid of the feed material in semispherical shape to be formed. As the seed, either single crystals having controlled orientations, polycrystals or some other substances can be used. Figure 1(b) shows pulling up a seed at a steady speed, after it was lowered to get its lower tip in touch with the molten part on the top of a feed below and when forming a stable molten zone between the feed and the seed. In the process of the crystal growth, the diameter of the crystal is controlled to be within one-half to a one-fourth of the diameter of the feed.

While the crystal is being grown, the feed is moved vertically and the laser power is adjusted carefully so that the same shape of the molten zone can be maintained throughout the growth process. When the fixed feed is heated either from one direction or two directions, there would appear a nonuniform distribution of temperature within the molten zone. If this

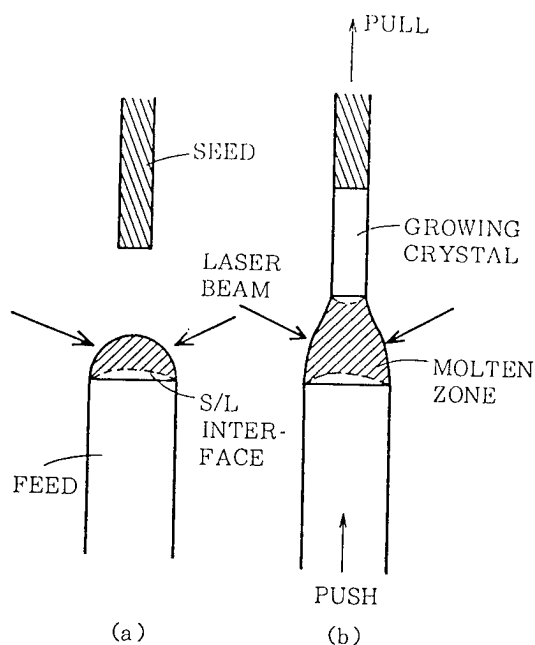


Figure 1. Crystal Growing Method Incorporating Simultaneous Laser Beam Firing From Two Directions Tried by C.A. Burris and J. Stone
(a) Top of feed melts; (b) Growth of crystal is underway.

nonuniform distribution poses any problems, the feed should be revolved to ease the nonuniformity.

(2) The setup for growing a crystal using CO₂ laser beam shown in Figure 2 is more sophisticated. This growing method was developed by M. Fejer, et al., and since it was developed the method has been used frequently. The arrangement of the seed and feed is the same as in the Burris-Stone method. The optical system is as follows: 1) A laser beam from the oscillator with the beam having a circular cross section is split into two beams and then their traveling directions are changed 90 degrees by a set of cone-shaped reflecting mirrors; 2) then these horizontally-moving beams have their directions changed 90 degrees again, this time upward, by a set of concentric-circle reflecting mirrors, which are set slanted by 45 degrees upward; 3) these beams are then reflected toward the feed in focused beams by a set of concentric elliptical reflectors to bombard the feed. The merit of the Fejer's laser shooting system is that it enables a higher uniformity of the temperature distribution within the molten zone to be achieved, because the setup allows a larger circumference of the zone exposed to laser beams. This higher uniformity, coupled with more effective use of the beam power which the setup allows, makes it possible for the system to melt substances having a higher melting temperature and a larger diameter. The drawbacks of the system are a longer time needed to adjust the beam traveling paths properly prior to using the system, and a higher cost of the system due to the sophisticated optical system.

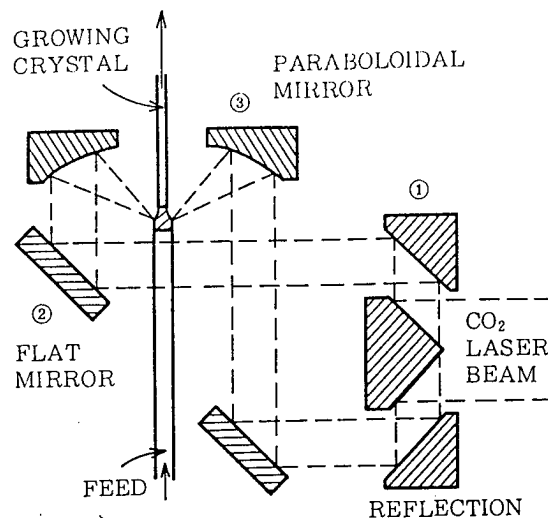


Figure 2. Crystal Growing Method Used by M. Fejer, et al.

3. Sample Diameter, Shape, and Length of Molten Zone

The crystal grown from the molten material tends to contain crystal grain boundaries, stacking faults, dislocations, void, and other dotted defects. But when the size of the crystal grown is made much smaller, those defects decrease markedly and the condition of the crystal nears perfection. This means that the properties of the crystal, which are delicately affected by the crystal structure, approach their ideal values. For example, according to S. V. Tsivinsky, the dislocating density N within a grown crystal is given by the following equation:

$$N = \frac{\alpha}{b} \left(\frac{dT}{dZ} \right)_0 - \frac{1}{D} \frac{2\tau_c}{Gb}$$

In the equation, α represents the linear expansion coefficients, b Burgers vector, $(dT/dZ)_0$ the temperature gradient in the direction of crystal axis in the interface, D the diameter of a sample material, τ_c the critical shear stress, and G denotes the rigidity. The equation tells that the dislocation density decreases when D becomes thinner, and when the D declined to a certain diameter, a crystal with no dislocation within it results. The correctness of the equation has been ascertained by experiment. In fact, a crystal with no dislocation has been created successfully by reducing the value of D . As described thus far, a reduction of the diameter of the sample material causes a change in the quality of a crystal grown from the material.

Lasers prove useful particularly in the growth of a thin-diameter crystal having high melting temperature, as the energy density of the beam can be increased by narrowing the diameter of the beam down to about 100 μm using long focal distance lenses. But the use of lasers for growing crystal poses some technical problems. When trying to grow a single crystal having a diameter less than 1 mm, controlling of the molten zone must be implemented with greater care for stability. In many cases, the volume of the molten zone ($\pi r^2 l$) is around 10^{-5} cc, and this makes the micro-scale convection and the flow of (Marangoni) to be ignored. It is considered that the molten zone can be maintained in the shape only by the surface tension of the molten liquid. Inside the molten zone dispersion of the atoms is occurring. It was W. Heywang who conducted an in-depth study on the safety [as published] of the molten zone.

He found that in a thin-diameter crystal, the longest length of stable molten zone (l_{max}) increases in proportion to the diameter d of the crystal, while in a larger-diameter crystal, the l_{max} has a critical value of $2.84 (\tau/\rho g)^{1/2}$.

τ represents the surface tension,
 ρ denotes the density of the molten liquid, and
 g represents gravitational acceleration.

Rayleigh and W.G. Pfann proved that under weightlessness state l_{max} equals πd . S.R. Corriell, et al., found that the stability of the molten zone of a thin crystal under a gravity is dictated by dimensionless factors represented by Bond number $B = \rho g d^2 / 4\tau$. On the other hand, K.M. Kim, et al., ascertained the correctness of their theory by successfully growing the thin crystals of sapphire and silicon in accordance with the theory and obtaining desired results. According to the results of the instant experiment, the stability was achieved when the ratio of diameters of the sample and the material was chosen at 1:2.5 or so, almost the same ratio announced by Feigelson, et al. It is important to adjust the laser beam energy properly to maintain the same diameter of the molten zone just above and beneath the solid-liquid state interface (Figure 3 [omitted]). This is particularly important when a substance having a high rate of reflection of laser beam, such as metal, is being melted. In such a substance, a slight unwanted change in the shape of the molten zone causes a drop of temperature in the zone, leading at times to solidification of the zone. To avoid this, the shape of the molten zone must be kept strictly at a stable condition throughout the laser processing.

4. Various Kinds of Single Crystal

In principle, the monocrystal growing methods using lasers as the heat sources described in the preceding sections are the variations of (band) melting method, and this makes all the advantages of the F-Z method being found in the growing methods. Those advantages are the controllability of growth direction using a seed crystal, no need for the crucible, easing of compositional overcooling due to steep temperature gradient, possibility of doping of dissimilar atoms, and ability of creating alloy. As an example of creating alloy, Figure 4 indicates the process of making Co-Fe alloy

using laser beams. In the figure, laser beams are projected at the tip of Co and Fe material rods ($\sim 0.5 \text{ mm}\phi$) bound in parallel to produce the molten liquid of Co-Fe alloy for growing the single crystal of the alloy. The composition of the grown alloy can be changed by adjusting the diameters of the material rods involved. To produce the alloy of high material

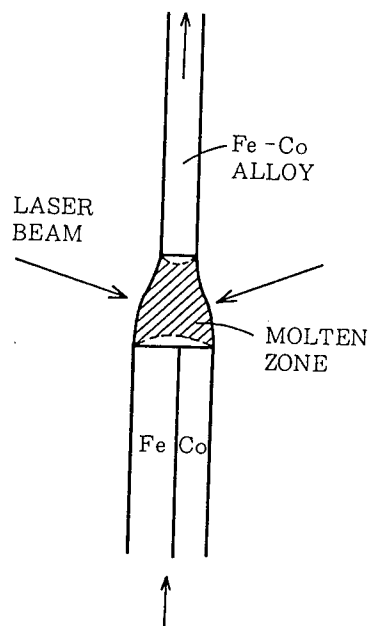


Figure 4. Growth Method of Single Crystal of Co-Fe Alloy

uniformity it is important to conduct the growing very slowly. As described in a preceding passage of this chapter, the laser heating creates a very steep temperature gradient ($\sim 1,000^\circ\text{C}/\text{cm}$) in the heated material because the laser beam is focused on a very tiny area of the material. This can result in causing cracks on the material sample while it is heated, and at times the sample is destroyed. The cracks can be prevented from developing by using the seed of high quality and by growing crystal longer. While growing a crystal, voids can be formed within the crystal at times. It is believed that the voids are created due to an instability on the solid-liquid state interface, and to prevent them from developing, it is necessary to slow down the growth speed. As other problems which could affect the quality of grown crystal, there are the appearance of opaque or whitish portions within the crystal. In each of those cases, conducting a heat treatment after crystal was grown properly is very important to increase the completeness of the crystal. In the following, several instances of growing the crystals of various kinds of materials will be introduced.

(1) Volatile materials

The crystal of the materials which have high melting temperatures and produce high vapor pressure when melted cannot be grown without using a high-pressure crystallizing furnace. Without using such a furnace, the crystal of MgO ($T_m = 2,800^\circ\text{C}$) cannot be grown due to violent evaporation of

the molten liquid. On the other hand, under molten liquid condition $\text{Gd}_2(\text{MoO}_4)_3$ ($T_m = 1,157^\circ\text{C}$) exists being decomposed into Gd_2O_3 and MoO_3 , and MoO_3 evaporates briskly. In this experiment to grow the crystal of $\text{Gd}_2(\text{MoO}_4)_3$, more than enough MoO_3 was added to the material to compensate for the evaporation. As a result, the crystals of $\text{Gd}_2(\text{MoO}_4)_3$ with a diameter of 200-600 μm and a length of about 10 cm were grown at a rate of 3.5 mm/min.

(2) Decomposing and melting substances

Under a particular temperature, a completely different kind of solid substance is created as a result of reactions between a liquid and a solid materials; conversely, under a particular temperature, a solid substance decomposes into a liquid and solid substances; the reactions involved in those processes are called peritectic reactions. Peritectic has no particular melting temperature, and due to this it cannot be grown directly from the molten liquid of the material. Due to this, usually a peritectic can be grown by precipitating it from the material using a fusing agent. Another method of creating a peritectic is by promoting the precipitation of the crystal from the molten liquid of the materials by introducing a required ingredient into the material mixture. The single crystal growing method using lasers can also be applied to the growth of a peritectic. Figure 5 gives the state diagram of a peritectic compound (a), and two separate growth processes (b) and (c) of the crystal. The state diagram indicates that a peritectic compound having a material composition C_1 triggers a peritectic reaction between a liquid B with a composition C_3 and a solid body D with a composition C_4 at temperature T_2 . One method of growing the single crystal of the peritectic (C_1) is to move along the molten zone of a substance having a composition C_2 gradually vertically, by sandwiching it between the solid bodies of C_1 material. This causes the feed above the molten zone to melt, and makes the crystal of the feed material precipitate beneath the zone (Figure 5(b)). Figure 5(c) indicates another method. In the method, a several molten zones are created over the length of the feed having a composition C_1 ; then the movement along of those zones slowly causes the precipitation of a crystal having a composition C_4 appearing at first, with this composition gradually changing closer to that of C_3 as the zones move along further; and the change continues until a steady state is reached after a peritectic reaction with the crystal having the composition C_4 . While those changes in the composition of the molten zones are occurring, a temperature shift in the molten zones occurs from T_1 to T_2 in parallel with the changes, and the precipitation of C_4 crystal is followed by its change to C_1 crystal through the peritectic reaction. Due to those changes involved, the speed of crystal growth must be kept very slow.

In the following, the growth of $\text{Y}_3\text{Fe}_5\text{O}_{12}$ (YIG) crystal will be introduced as an example of growing a peritectic. According to the Fe_2O_3 - Y_2O_3 -system crystal state diagram, the peritectic temperature of the crystal is $1,555^\circ\text{C}$. The crystal growing was conducted by YIG crystal as the seed and the feed using laser beams. The feed contained an excessive amount of Fe_2O_3 so that the feed melts well below $1,555^\circ\text{C}$. The result was that a YIG crystal containing an excessive amount of Fe_2O_3 in striations was obtained

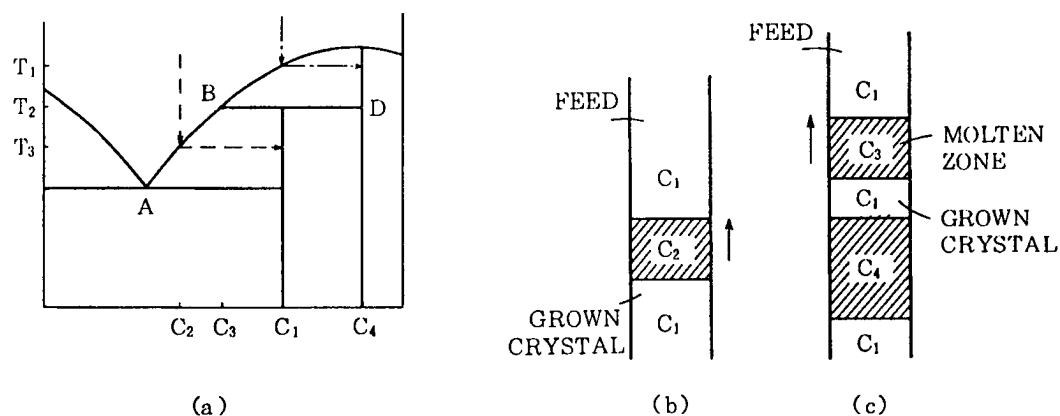


Figure 5. Growth of Crystal of Peritectic Compound

- (a) A typical state diagram
- (b) A case of putting a crystal having a material composition C_2 between feed rods, and then moving it along after it melted
- (c) A case of moving along the molten zones of feed (C_1)

when the growing was carried out at a speed of 0.25 mm/min. The growing speed should be set at the maximum speed at which the molten zone can be moved along without changing the shape under the right temperature condition. The striations are believed to be removed by further slowing down the crystal growing speed. Consequently, that method used to grow the $Y_3Fe_5O_{12}$ (YIG) crystal can easily be used for growing thin single crystals of peritectic compounds.

(3) Substances having facets

In general, when a crystal is grown using the floating zone melting method, the shape of the substance at the solid-liquid interface bulges out to the side of melted portion. In metal which has small latent heat for melting, the interface runs almost along the curved isothermal face. But in a substance having a large latent heat value, there is an instance that part of the interface move away from the isothermal face to form a low exponential lane (facet), as shown in Figure 6. On the facet, the density of impurities increases and a domain called core is created within a grown crystal, due to creeping growth of crystal on the plane. Presence of the domain seriously affects the uniformity of a crystal, and this poses a big problem in growing crystal from molten materials. According to a report by R.S. Feigelson, et al., on the results of their research involving Nd:YAG, the core was formed when the diameter of a grown crystal was 500 μm , but when the diameter was reduced below 200 μm the core disappeared, improving uniformity of the composition of the crystal. Usually, the solid-liquid state interface exhibits a sharply curved line under laser heating; considering this, the results of research by Feigelson, et al., suggest that there is a critical value as regards the dimensions of the facet.

(4) Metallic substances (Co and Fe)

The crystal growing method discussed above cannot be applied effectively to the substances like metal, which have low laser absorption ability and high

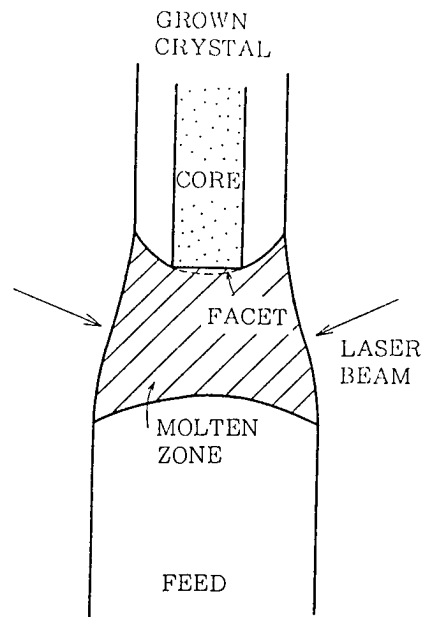


Figure 6. Condition of Solid-Liquid State Interface Having Facet

thermal conductivity. In the following, the results of experiment to grow the monocrystal of Co and Fe using lasers, which this author conducted, will be introduced. The feed was created by making wires of Co and Fe with each having a diameter of 0.5 mm, and then chemically treating them to make the surface rugged. The diameter of the seed was made as thin as about 100 μm . The reason was to avoid an incident in which the molten zone instantly solidifies upon contact with a thick seed rod, due to occurrence of a large heat transfer to the seed rod. (Once the solidification occurs, it becomes very difficult to melt the solidified portion again. This is because of the necessity for a time-consuming fine adjustment of the position of the stage to bring the seed and feed in place, after they moved away from the laser beams due to the thermal expansion caused by applying heat again.) When such a thin seed does not snap upon touching the molten zone, growing of the monocrystal starts by adjusting the ratio of diameters of the seed and feed to around 1:2.5. The use of laser power levels which were a bit higher than appropriate caused the shapes of the molten zones to be less than ideal. Figure 7 describes the shapes of those molten zones pretty accurately. Figure 7(a) indicates that a thinner surface layer of the Fe sample compared with the degree of melting in the Co sample was melted by laser beams, under conventional arrangement of the seed and feed. Figure 7(b) indicates that a sapphire rod was placed on an experimental basis in parallel to the feed, and melting of the feed was effected by the heat from the sapphire after the rod was irradiated by laser beams.

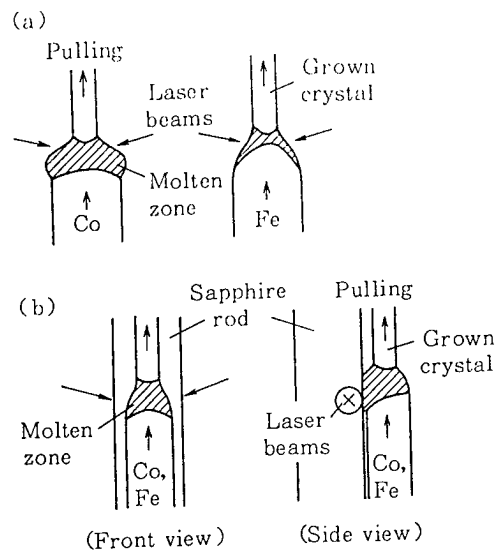


Figure 7. Two Ways of Arranging Feed and Seed in Growing Crystals
 (a) Conventional arrangement
 (b) Samples being placed in parallel to a sapphire rod

The introduction of the sapphire rod contributed to stabilizing the molten zone, and allowed reducing laser power levels to open half that required in the case of (a). Figure 8 [omitted] shows a single crystal of Co thus obtained, and the Laue spots of the crystal. The Laue spots indicate that the crystal has a high degree of perfectness. Figure 9 [omitted] shows a grown Fe crystal and the etching patterns on the surface of the crystal. From the Laue photos, the Fe crystal was judged to be monocrystal. So far, there have been few instances where the single crystal of Fe was created from the molten liquid. From X-Ray diffraction analysis of many of the crystal samples grown, it was found that both in Co and Fe, crystals had grown to all directions by the same degrees uniformly.

(5) Other kinds of substances

Ferroelectric substance LiNbO_3 is a crystal which has good nonlinear optical characteristics. It has a melting temperature peculiar to the substance, and LiNbO_3 is mass-grown using the conventional pull method. When the single crystal is grown in various diameters using laser beams, the domain structures change in accordance with change of diameter. Figure 10 indicating several domain structures on the C face (c axis is the growth direction), was copied from documents on similar articles.

- (a) represents concentric domain structure,
- (b) is regarded almost as single domain structure, and
- (c) represents complete single domain structure.

It was found that when crystal was grown in the direction of the a axis, the crystal assumes two domain structure.

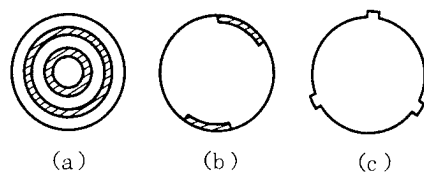


Figure 10. Domain Structure Types of LiNbO_3 Crystal on Its C Face

- (a) Crystal diameter: 1 cm
- (b) Crystal diameter: $700 \mu\text{m}$
- (c) Crystal diameter: $150 \mu\text{m}$

ScTaO_4 crystal belongs to monoclinic-system crystals in its crystal structure. However, D. Elwell, et al., succeeded in growing ScTaO_4 crystal belonging to metastable phase tetragonal-system crystals in growing monocrystal using lasers as the heat source. The crystal having such a phase is believed to have been realized as a result of very steep temperature gradient involve in the heating method.

5. Conclusion

So far in this chapter, the outline of the efforts to grow thin single crystals of various kinds of substance using CO_2 laser beams has been discussed. A thinner crystal tends to have a higher perfectness of the crystal. There is a possibility that the properties of a crystal change as the dimensions of the crystal diminish. For those reasons, it is expected that research on creation of thin films and growing of fibers for industrial applications would be stepped up in the future.

Under the circumstances, the importance of CO_2 laser would increase considering the capability of the laser, which can heat and melt substances under various processing environments.

Fine Grain Development by Laser CVD

43064001d Tokyo KINO ZAIRYO in Japanese Vol 7 Aug 87 pp 33-39

[Article by Kiyoshi Sawano, researcher at No 1 Material Research Center of Nippon Steel Corp.'s No 1 Technical Institute; first paragraph is editorial introduction]

[Excerpt] Demands for superfine grains of various materials have been increasing, and they have been put into practical industrial applications in various fields. Laser CVD is one of the methods for producing such grains, and the method is attracting industry attention. In this chapter, the principles and features of CVD method and a laser CVD system will be introduced. In addition, the properties of the grains produced, the synthesizing mechanism and the examples of application of the grains to practical usages will be described.

1. Introduction

The superfine grains of various materials find applications in production of pigments, catalysts, and ceramics. The characteristics of the grains for those applications must be evaluated from: 1) chemical composition and purity; 2) phase composition; 3) shape of primary grains and their grain size distribution pattern; 4) shape of agglomerated grains, their hardness, and their grain size distribution pattern; 5) condition of crystallization and density of the structural effects; and 6) surface condition. In producing the superfine grains, those elements must be controlled properly in accordance with the requirements in their applications.

Many scientists have been doing research on synthesizing the superfine grains using CVD method, a method which enables the controlling. In the research conducted so far, metals and nonoxide ceramics were the principal kinds of material involved in the synthesizing efforts. Among a number of CVD methods, laser CVD method attracts particular attention due to its ability of synthesizing the superfine grains having almost ideal powder characteristics. This is made possible due to the laser CVD method's advantageous features, including the ability of heating only the reaction gases and forming a very confined reaction zone, enabling high controllability of the reaction.

In the following sections of this chapter, the synthesizing of superfine grains using laser CVD method, including the method's principles and features, a synthesizing system, characteristics of synthesized grains, and the synthesizing mechanism involved, will be discussed.

2. Principles of Laser CVD

A gas has a nature of absorbing particular wavelengths of light when it is exposed to infrared or ultraviolet light. There is a possibility that in exposing a gas to a laser beam, a reaction could occur when the wavelengths of infrared or ultraviolet laser beam and the absorption wavelengths of the gas coincides. In connection with this, Table 1 lists the wavelengths of a number of kinds of infrared and ultraviolet lasers together with their photo energies. Figure 1 shows the infrared ray (IR) absorption position in the IR spectrum of SiH_4 and the position of usable wavelength ($10.6 \mu\text{m}$) of CO_2 laser in the laser spectrum.

SiH_4 has a major absorption band near the wavelength of CO_2 laser, and this means that it would be possible to cause a fairly large absorption by controlling the pressure and the temperature involved.

Gases exhibit different phenomena depending on which kind of laser light they absorbed--infrared laser light or ultraviolet laser light. In irradiating gases with excimer laser which has a comparatively short wavelength, in many cases the photon energy level is higher than the uniting energies in those gases. Under such a condition, gas can easily be photodissociated when it was irradiated with laser light. In case the photodissociation cannot be realized with a single run of the dissociation

Table 1. Wavelengths of Various Kinds of Lasers and Their Photon Energies

Kind of laser	Media for generating laser light	Wavelengths (nm)	Photon energies (eV)
Excimer laser	ArF	193	6.4
	KrF	249	5.0
	XeCl	308	4.0
	XeF	350	3.5
Infrared laser	YAG	1,060	1.17
	CO	5,000	0.25
	CO ₂	10,600	0.12

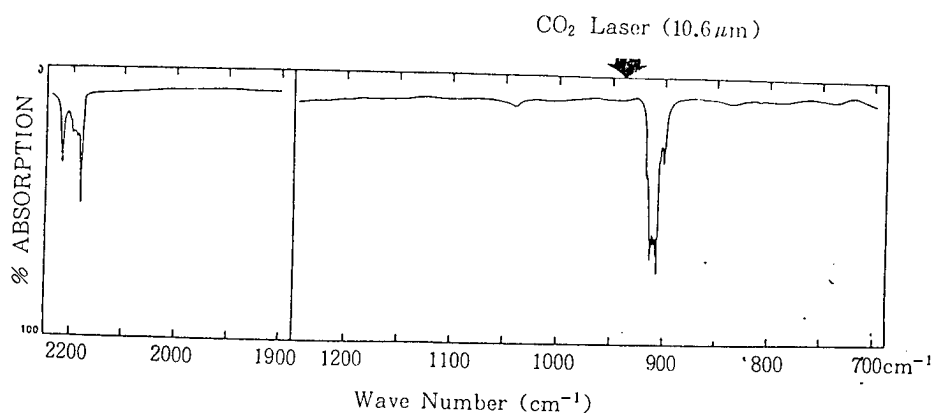


Figure 1. IR Spectrum of SiH₄ and Usable Wavelength of CO₂ Laser in Laser Spectrum
(IR value(s): at 14K Ar matrix)

reaction, repeating the same process once again by increasing the strength of laser light could achieve a photodissociation. Photodissociation reactions in gases using lasers can be induced at a considerably lower temperature than the decomposition temperatures of them.

On the other hand, infrared lasers, particularly far infrared CO₂ laser has a lower photon energy level. This means that when a gas was irradiated with such a infrared laser, it is not photodissociated but the temperature of the gas rises as a result of the absorbed laser energy shaking the bonding mechanism of the gas. Consequently, a reaction occurring under this condition is a thermal reaction caused by the laser-induced heat, and this makes it possible to apply basically the conventional chemical reaction theory to the reaction. Due to this reason, the kinds of gas in which thermal decomposition can be caused easily even under comparatively low temperature are used in the CO₂ laser CVD method.

In order to synthesize the fine particles of a substance using a CVD method, it is necessary to realize the condition of an oversaturation of the synthesis environment with gases needed to synthesize the particles, to promote the formation of the homogeneous core in the reaction space. The degree of oversaturation is not static, but it is a value which is dictated by such factors as the decomposition speed of a gas, equilibrium vapor pressure of a solid substance formed, the temperature, the pressure of gases involved, and the stay time. It is difficult to calculate the saturation degree precisely. For this reason, it was proposed to use the equilibrium constant ($\log K_p$) of the reaction for the formation of a solid substance, as the index of the degree of the saturation and to indicate the possibility of formation of the fine particles. For the solid substance to be formed, it is said that the value of the $\log K_p$ must be higher than 3 or so. What has been discussed in this paragraph concerns thermal chemical reactions, and can also be applicable to CO_2 laser CVD, but not to the ultraviolet laser CVD.

3. Features of Laser CVD

It is believed that no one has ever succeeded in synthesizing the fine particles using excimer laser. This is because excimer laser is not suitable for synthesizing uniform particles as it is a pulse laser, and because of nonavailability of a high-powered excimer laser system. In the following, the features of CO_2 laser CVD will be briefly described.

Laser CVD method has high efficiency in the utilization of laser energy, because the reaction gas, being irradiated by a laser beam, generates heat and as a result reacts itself. Because the gas is excited only when it is exposed to a laser beam, it is possible to quickly heat and cool the gas, enabling it to form the superfine grains while forming only small agglomerations. In addition, the use of lasers enables synthesis of the fine grains under a more stable condition, because the high controllability of laser in its beam power, beam diameter, and the cross-section profile of the beam enables it to achieve more precise controlling of the synthesizing process. In laser CVD, the laser energy is introduced into the reaction chamber through a sealed window on the wall of the chamber. The merits of this are that: 1) the tightly sealed chamber makes it possible to control the reaction environments within the chamber more precisely; 2) almost no contaminants find their way into the environment from the cool chamber walls due to evaporation of the material forming walls; and 3) it is easy to conduct process measurements and observe the synthesizing process by installing proper-sized windows for those purposes on the walls.

Among the drawbacks of the method are, the kind of reaction gas must be chosen so that it has the absorption wavelength corresponding to that of the laser being used. Another disadvantage is that the smaller power outputs of laser systems available now compared with other exciting means, including plasma, make them unsuitable for use in mass production of the fine grains.

4. Laser CVD System

Figure 2 shows the diagram of a CO₂ laser CVD system for synthesizing the fine powders. In the system, a CO₂ laser beam meets the flow of the reacting gas at right angles in the center of the chamber, and reactions occur at the point where they meet. The laser beam is introduced into the chamber through the window of KCl in the system horizontally. Prior to the laser beam meeting the flow of reactant, the strength, the diameter of the beam, and the beam profile are adjusted to proper levels and shape using ZnSe lenses. The system has a maximum laser output of 180 w and the diameter of the beam can be adjusted between 2 and 6 mm ϕ . In order to stabilize the heat history, an experiment to synthesize fine powders was conducted by making the cross section of the laser beam into a rectangular shape and the width wider than that of the flow of reactant, and favorable results were obtained.

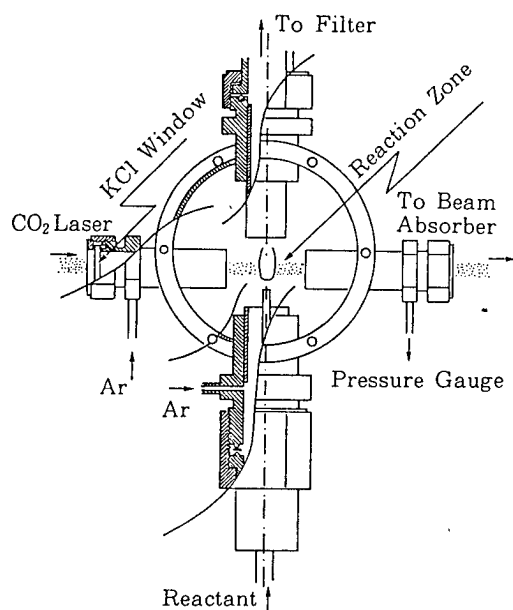


Figure 2. Diagram of Laser CVD Fine Grain Synthesizing System

The reacting gas is led into the chamber through a nozzle with a diameter of about 1 mm ϕ at the bottom of the chamber. Outside the flow of the reactant exists a flow of an inactive gas (consisting mainly of Ar to arrest the powder synthesized and for the purpose of controlling the environment within the reaction chamber. Thanks to the flow of the inactive gas, the powder synthesized can be arrested by the filters installed at the top of the chamber without sticking to the chamber windows and the walls. The pressure within the chamber can be adjusted by a drain vacuum pump on the system and the control valves installed between the filters. Usually, the pressure is maintained at a certain level between 0.2 and 1 atm.

Photo 1 [omitted] shows the main part of the CVD system described above. The reaction chamber has a cylindrical shape with the two ends sealed with SiO₂ glass. Through one of the windows, the beam of He-Ne laser is led

into the chamber to the region where the powder is being formed, and the laser light which was scattered or passed through the synthesis region is measured. Detector of the scattered light is placed in the foreground right of the He-Ne laser generator, and another detector for sensing the passed laser light is at the opposite side of the reaction chamber from the scattered light detector. By assuming that the complex index of refraction of the synthesized grains is known, and that each of the grains scatters the light independently and laser light scattered by a single grain does not interfere with light scattered by another grain, the diameter of the synthesized grains and their number density can be calculated from the strengths of the passed and scattered laser light. Conversely, it is also possible to grasp qualitatively a change in the index of refraction of the grains (melting, reaction products, etc.) at the reaction region.

5. Fine Grains Synthesized Using Laser CVD Method

As described in a preceding section of this chapter, at present CO_2 laser is the only kind of laser utilized in CVD applications. The results of experiments to be discussed in the following sections were all obtained using the CO_2 laser system.

5.1 Si Powder

Si powder can be synthesized by causing a thermal decomposition reaction of SiH_4 gas. The powder can be formed at high efficiencies at a reaction temperature higher than about $1,000^\circ\text{C}$. The yield of the powder is close to 100 percent. The powder formed at a reaction temperature of around $1,000^\circ\text{C}$ takes a form of chained grains with a number of such chains forming an aggregation of the grains. The primary grains assume the form of polycrystal and their grain diameter ranges from 20 to 40 nm. When the reaction temperature goes up beyond $1,200^\circ\text{C}$, spherical grains with their diameter ranging from 100 to 200 nm begin to appear, and the rate of appearance of such larger grains drastically increases as the temperature ascend higher. The emergence of the spherical grains is attributed to melting of synthesized grains. The emergence of the spherical grains causes the grain size distribution pattern of the synthesized grains to have two major peaks, as shown in Figure 3.

In synthesizing of Si from In_4 under certain conditions the grain size and the number density of the Si powder could have been measured, by measuring the strengths of the scattered and passed light of He-Ne laser beam, thanks to the simplicity of the material system involved and the known value of the complex index of refraction of Si formed. By scanning the reaction area within the chamber with the laser beam, it was possible to measure changes of the index and the density at various reaction areas above the reactant nozzle. Figure 4 indicates the results of such a measurement. The figure indicates that the diameter of the synthesized grains increase in proportion to the time (position) but the number density decline.

Results of the measurement suggest the following things. In general it is believed that the growth of the grains in a CVD method is as a result of the formation of the homogeneous cores and their growth in size afterwards.

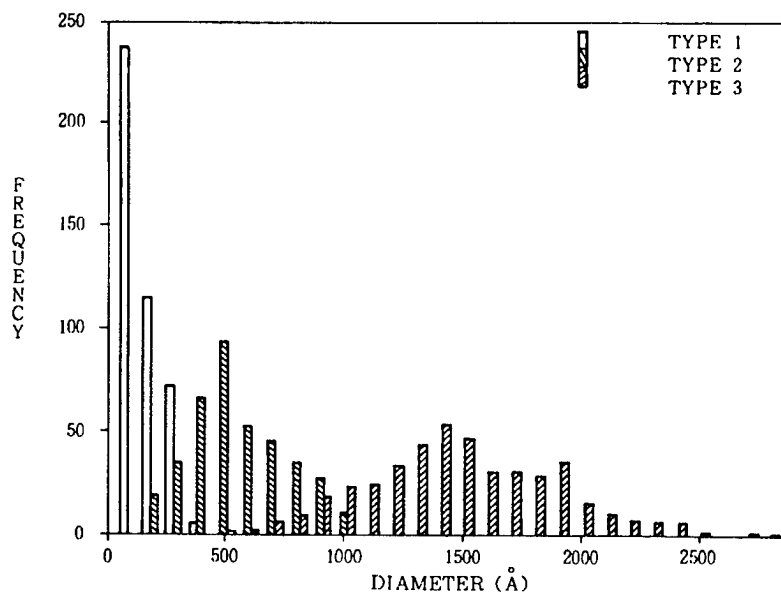


Figure 3. Grain Peak Distribution Pattern of Si Powder Containing Spherical Grain
(Note: Type 1 represents nonagglomerated small-diameter grains; Type 2 is agglomerated grains, and Type 3 represents spherical grains formed through the melting process.)

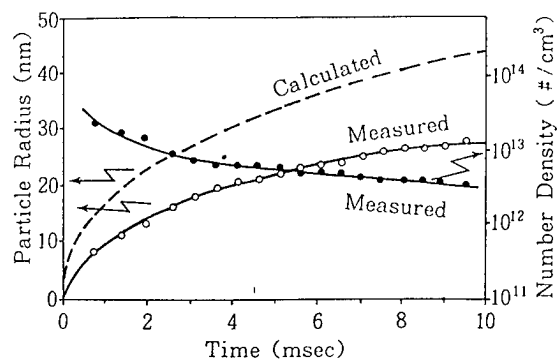


Figure 4. Changes of Diameter of Si Powder Grains and Their Number Density in Reaction Area as Time Elapses
The "calculated" curve indicates the calculation results of the growth of the grains due to collision and coalescence of the grains.

In this model of assumption, the number density of the grains increases, but no decline occurs. In SiH_4 , a gas which can easily be decomposed and has a high decomposition speed, almost all of the gas decomposes into countless number of cores with their size close to the atoms, when the homogeneous cores are formed. Consequently, the growth of the cores after the decomposition occurs as a result of coalescence among those cores, rather than due to decomposition of additional SeH_4 gas. Due to this, the number density declines as the growth of the grains proceeds. This process is similar to a model for explaining process of the formation of carbon

black from hydrocarbons, and the decline can be calculated quantitatively by assuming the values of some parameters needed for the calculation. The results of such calculations are shown in Figure 4. The "calculated" curve in the figure shows a pattern of increase which resembles pretty closely that of the "measured" curve.

Under the condition in which melting of synthesized Si grains occurs, the aforementioned assumptions for calculating the grain diameter and the number density by measuring the strengths of the scattered and passed light of the He-Ne laser beam become no longer usable, making it impossible to calculate them. In such a case, the confirmation for accuracy of the model is done using the data obtained by measuring the grain diameter of the synthesized powder. The author's experiment showed that the measurement results and the calculated results coincided well.

The Si powder thus synthesized can be used as the material for producing reaction-sintered silicon nitride. For treatment, scattering and molding of silicon nitride powder, the material grains for producing the powder is preferred to have monodispersion, high purity, submicron size, isotropic shape (sphere) and no agglomerations. As the grains meeting those requirements, the melt-synthesized grains are more suitable. It has been ascertained that using the grains, production of reaction-sintered silicon nitride having better uniformity and higher mechanical characteristics than silicon nitride made using conventional method is possible.

5.2 SiC Powder

The synthesis of SiC powder was conducted using a number of different kinds of reaction gases such as $\text{SiH}_4\text{-CH}_4$, $\text{SiH}_4\text{-C}_2\text{H}_4$, and CH_3SiH_4 . In all of those gases almost completely pure SiC powders were obtained, by adjusting the synthesis conditions to their optimum. The size of those powder grains was in submicron levels, and in those powders which took crystallized forms, the type of the crystal was $\beta\text{-SiC}$. As regards the mechanism of formation of the grains, differences were observed between the single reaction gas and the mixture of two different gases.

In every case of synthesizing using the mixtures of gases, the formation of SiC powder went through two stages of reactions--first the formation of Si grains as a result of selective decomposition of SiH_4 , followed by the formation of SiC through reaction with the hydrocarbons. The occurrence of this two-stage reaction was ascertained from the changes in the levels of the passed and scattered light of the He-Ne laser beam scanning the reaction region, the characterization of synthesized powders, and relations between reaction temperature and reaction parameters. In the two-stage reaction, the formation of SiC calls for very great activation of the reaction parameters, and the formation process is believed to have something to do with the decomposition of the hydrocarbons. The activation can be enhanced either by increasing the strength of the laser beam, increasing the stay time of the reaction gas by decreasing the flow speed of the gas, and by increasing the reaction chamber pressure. The start of the formation of SiC can be known with a change of the reaction temperature. Figure 5 shows the relationship between the flow volumes

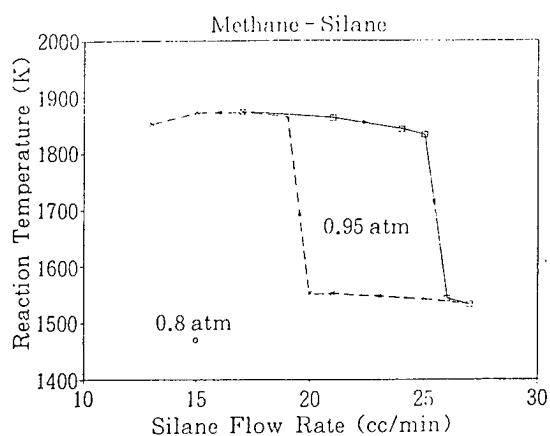


Figure 5. Relationships Between Flow Volumes of Reactant and Reaction Temperatures
(Flow volume of CH_4 is identical with that of SiH_4 . Arrows indicate changes in the flow volumes of the reactant.)

of reactant and the reaction temperatures in the SiH_4 - CH_4 -system gases. In the figure, as the flow rate decreases there is a point where the reaction temperature abruptly shoots up. The flow volume-reaction temperature relation curve of the SiH_4 - CH_4 -system gas has a hysteresis, as shown in the figure. It is believed that the hysteresis appears as a result of maintenance of a reaction for a certain duration, once the reaction atmosphere was activated by a heat-generating reaction in the process of formation of SiC . The particles formed during a reaction at a temperature of $1,200^\circ\text{C}$ are mostly Si particles containing no SiC . While at a reaction temperature of around $1,500^\circ\text{C}$ after an abrupt increase of the temperature, almost all of the Si particles are turned into SiC grains and there remain few Si particles in the reaction region. Due to those mechanism of reactions, the kind of hydrocarbons to be used affects the fashion of the reactions occurring and influences greatly the properties of synthesized powder. CH_4 is more stable than C_2H_4 . When the former is used under similar synthesizing condition, SiC grains with a larger diameter can be obtained, due to the growth of them through collisions and coalescence among Si particles up to a higher temperature without the particles turning into SiC , compared to using C_2H_4 . Table 2 lists difference in the size of synthesized grains between CH_4 and C_2H_4 . When CH_4 is used, the synthesized SiC powder grains have few agglomerations and semispherical shapes due to melting of the Si particles prior to their turning into SiC (Photo 4 [omitted]). The reason why the grains having complete spherical shape are not formed from the spherical Si particles is believed to be due to the formation of polycrystals resulting from formation of a plural number of the cores within the particle, when it turns into an SiC grain.

In CH_3SiH_3 gas which contains both Si and C within a single molecule, SiC grains are believed to be formed via the processes of the gas turning into a high polymer as a result of polymerization, elimination of the hydrogens and then via the process of crystallization. The powder grains

Table 2. Differences in Diameter of Synthesized SiC Powder Grains When Two Different Hydrocarbons Used for Synthesis
(SiH₄ was used for both of the hydrocarbons listed below as Si source.) (Average grain diameter (nm))

Hydrocarbons	Reaction temperatures (°C)	TEM	BET
CH ₂	1,620	51	56
C ₂ H ₄	1,650	38	31

synthesized in the reaction temperature ranging from 700-1,000°C have amorphous structure, while at temperatures higher than 1,400°C the synthesized grains become crystallized β -SiC. The diameter of the grains is rarely affected by the reaction temperature, and it remains at 30-40 nm range.

By using the SiC powder thus synthesized, SiC sintered bodies were made. In the preceding section, it was mentioned that powder for producing a sintered compact is preferred to have no agglomerations and spherical grain shape. So as the material gases for synthesizing SiC powder, the SiH₄-CH₄ combination was chosen. The combination enables synthesizing SiC grains having highly spherical shape by the two-stage reactions, by growing the Si particles and then melting them. As sinter promotion agents, B and C were added, it was ascertained that B can be added uniformly by mixing B₂H₆ with the material gases. C can be added by controlling the mixing ratio of SiH₄ and CH₄. The experiment to produce sintered ceramics using the SiC powder, synthesized using the above-mentioned method, proved that the powder has high performance.

5.3 Si₃N₄ Powder

Si₃N₄ cannot be formed from SiH₄ and N₂ as the reaction gases. On the other hand, Si₃N₄ is formed from the combination of SiH₄ and SiH₄ and NH₃, but in this case an excessive amount of NH₃ is needed. The Si₃N₄ of stoichiometric composition can be obtained only when each of the reaction pressures, the strength of laser beam, and the ratio of NH₃/SiH₄ are high enough. When a significant decline in any of these values occurs, isolated Si particles begin to appear within the synthesized powder. Table 3 gives the conditions for obtaining Si₃N₄ of stoichiometric composition.

Table 3. Synthesis Conditions Under Which Pure Powder of Si₃N₄ Obtained

Laser strength (W/cm ²)	Reaction pressure (atm)	Ratio of NH ₃ /SiH ₄	Flow volume of SiH ₄ (cm ³ /min)	Reaction temperature (°C)
1 x 10 ⁵	0.5	9	5	1,030

The Si_3N_4 powder grains obtained under the conditions listed in Table 3 took the form of either amorphous or compound of α and β type grains. The grain diameter was small ranging from 10 to 20 nm. Synthesis of such small diameter grains is believed to be as the result of NH_3 decomposing and reacting to form Si_3N_4 even under relatively low temperature. In order to synthesize powder more suitable for making ceramics, research is underway to introduce NH_3 in the way to cause the two-stage reactions physically.

6. Conclusion

So far in this chapter, synthesis of superfine grains of various substances using CO_2 laser CVD method has been discussed. In actuality, the method has potential greater than what has been discussed in this chapter. In addition to the Si-system materials discussed in this chapter, there are many kinds of other gases and low-boiling-point fluids, which have major points of absorption of laser energy in their absorption wavelength spectra. This would make it possible to synthesize many more kinds of useful materials using them. In actuality, attempts have been made to synthesize TiO_2 , B, and TiB_2 using lasers. When the required conditions are met, it is possible to synthesize fine powder using non- CO_2 lasers. In the future, it is expected that a further progress would be made in the synthesis of the superfine grains using laser and nonlaser CVD methods. With this prospect, high hopes are placed on the laser CVD method's establishing a firm position as a principal CVD method, by taking advantage of the advantages of the laser method.

To conclude this chapter, gratitude is expressed to Dr John S. Haggerty of the MIT, who offered useful materials in writing this article, and to those who also helped in various ways in writing the article.

Superfine Grain Development by Laser

43064001e Tokyo KINO ZAIRYO in Japanese Vol 7 Aug 87 pp 40-49

[Article by Akira Matsunawa, professor at Osaka University, researcher at the university's Welding Engineering Institute; first paragraph is editorial introduction]

[Excerpt] Among existing means for providing practical heat sources, lasers are attracting attention as a powerful heat source, which can deliver a power density which is nearly the same with, or higher than that of an electron beam. By bombarding with such a high-density beam, it is possible to evaporate any kind of material instantly. In this chapter, recent developments in the production of superfine grains of a number of kinds of substances using lasers, including the features of high-power, high-density lasers, the evaporation characteristics of irradiated materials, the condensation process of evaporated atoms, and the feature of produced power grains, will be discussed.

1. Introduction

The superfine grains of substances, which exhibit the physical and chemical nature different from bulk substances, are attracting industry attention as new functional materials, due to the characteristics peculiar to such grains. Recently, emphasis in research on those grains has been shifting from studying their properties to developing production methods and application fields for the grains. The methods for producing those superfine grains could be divided into two categories: The one is to split a bulk material into smaller and smaller bits, and the other is to reconstruct to a desired grain size after breaking a bulk material into atomic or molecular level elements (condensation method). For each of those methods, physical and chemical processes have been proposed to produce the fine grains, and there are many instances of pioneering research on the methods.

In view of energy required to obtain the fine grains, the splitting method has an edge over the condensation method. But in the splitting method, it is very difficult to crush bulk material into submicron sizes, where the fine grains begin to show the properties different from the bulk material. For this reason, researchers now put emphasis on the development of the condensation method based on physical evaporation, for the formation of superfine grains with their diameter smaller than 1 nm [as published].

The evaporation method calls for raising the temperature of a substance higher than its evaporation or sublimation temperature. The principles involved for obtaining fine grains using this method seem quite clear and simple. But in actuality, much has yet to be unraveled as to the principles. In fact, little has been clarified about the cluster evaporation, which is believed to be playing an important role in the process for the formation of superfine grains by the evaporation method. However, putting this problem aside, it is a well-known fact that evaporation of a substance is realized by heating it to a high temperature. Various heating methods have been studied so far for creating superfine grains. For example, many researchers have been conducting research on the development of evaporation-within-gas method, which used direct or indirect heating by Joule heat, direct heating by plasma or arc, or heating with an electron beam or a laser beam. By using the high-frequency heating method, plasma jet method or active plasma arc method, it is said that production of the fine grains on a commercial basis could be possible. The drawbacks of the induction heating method are the high grain production costs and the difficulty of evaporating the substances of high melting temperature. The drawback of the plasma jet method is the possibility of the molten material being blown away by the jet. The problems with the active plasma arc method are the comparatively larger size of the produced powder grains, and in the case of some kinds of metallic materials, unwanted superfine grains of hydride are formed.

The following are the principal conditions required for producing superfine grains using the evaporation method: 1) Clean working environments free of impurities; 2) good controllability of grain size and grain size

distribution pattern; 3) high yield and high grain formation efficiency; and 4) ease in catching formed fine grains.

It can be said that the superfine grain production methods using lasers satisfy the above conditions fairly well. As regards the laser evaporation method, M. Kato and Ueda, et al., in the early 1970s reported on the results of their experiments, in which they produced the superfine grains of oxides by irradiating various kinds of oxides and evaporating them using CO₂ laser beams. But for some years after their announcements were made, emphasis on research for development of evaporation method was put on the resistor heating method and arc heating method. This resulted in few announcements having been made on the results of research on laser evaporation method, despite the fact that significant progress was made in the development and the propagation of larger-output lasers since the latter half of the 1970s. Attempts to form superfine grains chemically using lasers were made by Haggerty, et al., in 1981. They succeeded in synthesizing the superfine grains of SiC and Si₃N₄ by irradiating the mixture of SiH₄ gas and C₂H₄ gas as well as the mixture of SiH₄ gas and NH₃ gas with a CO₂ laser beam, and by inducing reactions as a result of those mixtures' absorption of the laser energy.

The following sections of this chapter will introduce the latest developments in the production of superfine grains using laser heating and evaporation methods.

2. Laser Beam as a Heat Source

The most salient feature of lasers as a heat source is their capability of achieving extraordinarily high spatial power density at the point where the light converges. Table 1 lists the maximum power densities attained by a number of different kinds of heat sources. The table shows that an electron beam is the only practically available heat source which can match the power of lasers. When bombarded by such a powerful laser beam, almost any kind of substance on the earth evaporate in a very short time and it would not even be difficult to reach the plasma condition. A big difference between an electron beam and a laser beam is that the former is used mainly under vacuum environments, while the latter can be used under varied kinds of environments ranging from vacuum condition to high pressure environments of various kinds of gases.

Table 1. Maximum Power Densities Attained by Number of Heat Sources

Heat sources	Power densities (kw/mm ²)
Oxyacetylene	10 ²
Oxyhydrogen flame	3 x 10 ²
Argon arc	10 ³
Electron beam (CW)	10 ⁵ - 10 ⁸
Electron beam (pulse)	10 ⁶ - 10 ⁸
Laser beam (CW)	10 ² - 10 ⁸
Laser beam (pulse)	10 ⁶ - 10 ¹²

In addition, other features of lasers as a heat source are the ability of maintaining impurity-free processing environments by noncontact heating, the easy controllability of the beam power density by manipulating the beam converging system, and the ability of heating metallic and nonmetallic materials with comparatively high efficiencies. Those features make laser beams a very attractive heat source.

On the other hand, a problem in using lasers with metal as a heat source is the low efficiencies of heat input into metal, due to high degrees of surface reflection (small levels of heat absorption). Figure 1 shows the reflection rates of a laser beam on the surface of various kinds of metal (mirror-surface finish) under room temperature change in accordance with the wavelengths.

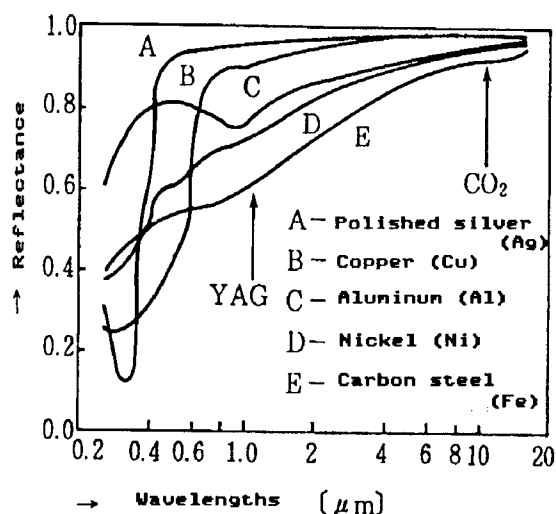


Figure 1. Reflectance-Wavelength Characteristics of Laser Beam in Different Metals

In general, the reflectance ratio increases as the wavelength increases. The wavelengths of CO₂ laser (wavelength: 10.6 μm) and YAG laser (1.06 μm), two kinds of practically used lasers capable of generating high outputs, belong to infrared range, and they have low efficiencies in heating the surface of metal. Even with the same kind of material, the surface reflectance ratio differs depending on the surface conditions and the temperature in which the material is placed. The absorption rate increases when the degree of roughness on the surface increases and the surface temperature is higher. The absorption efficiency increases when the degree of the surface irregularities is closer to the wavelength of the laser beam. But even with those efforts to improve the absorption rate, the absorption rate actually attained in processing of metal material is very low. This calls for the development of laser systems having a higher power output and a shorter wavelength of the beam. However, in practical application, the reflection problem is offset by the greater merits of using lasers. the use of lasers permits attaining much higher power

density than density attained using conventional arc heating method, and lasers allow an easier control of the power density.

3. Evaporation Phenomena

When a substance is bombarded by a high power density laser beam, the surface melts in a very short time, and soon strong evaporation of the substance begins. Usually, when the evaporation is occurring, a brightly luminous flame, called laser plasma or laser plume, is observed rising upright from the surface of the bombarded substance. Figure 2 [omitted] shows such a flame rising from the surface of a pure Ti metal plate, when the metal surface is bombarded by a pulse YAG laser beam at an angle less than 90 degrees. For a long time it was believed that the flame was high-density, high-temperature plasma made up mainly of the components of the evaporating substance. However, it was found recently that the nature of the flame seems to vary slightly depending on the wavelengths of lasers being used.

Figure 3 [omitted] shows the spectrum of the plume which appeared when a metal target was bombarded by a pulse YAG laser beam (peak output: about 10 kw). The bright line spectrum consists mostly of the atomic lines of the target material (Ti atoms in the case of Figure 3 spectrum), and less bright monovalent ion lines can also be observed on the spectrum. What is noteworthy here is the fact that among those atomic lines (neutral lines), the spectrum lines called resonance line present themselves as absorption lines as a result of strong self-absorption. This indicates that the plume is the high-density vapor composed mainly of the atoms of the target material, with the temperature of the plume nearly at the evaporation temperature of the material. On the other hand, according to the results of a spectrum analysis in irradiating a metal sample with a 5 kw-class continuous CO₂ laser beam, the ion line of the gas in the vicinities were also detected along with the polyvalent metal ion lines. But whether or not the ion lines of such a gas can be detected depended on the kinds of gas present in the irradiation atmosphere. This analysis result indicates that in irradiating the metal with a CO₂ laser beam, the plume generated is made up of high-density, high-temperature metal plasma. The reason why the difference occurs in the component structures in the vapor plume after the atomic vapors were generated, depending on the difference of the kinds of lasers used, is because the degree of absorption of the photons by the atoms varies in accordance to the frequencies (wavelengths) of the lasers.

Depending on whether a plume of the evaporated vapor generates a neutral vapor flow or a plasma current, differences result in the ways of interaction between the laser beam and the target substance, affecting the degree of laser energy reaching the surface of the substance. When the frequency is low (long wavelengths) the plasma absorption loss is high, while when the frequency is high (short wavelengths) scattering loss caused by the grains goes up.

How fast a substance can be evaporated by irradiating it with a laser beam is a point of interest, in view of how fast the superfine grains can be synthesized using lasers. So far, there were few instances where the

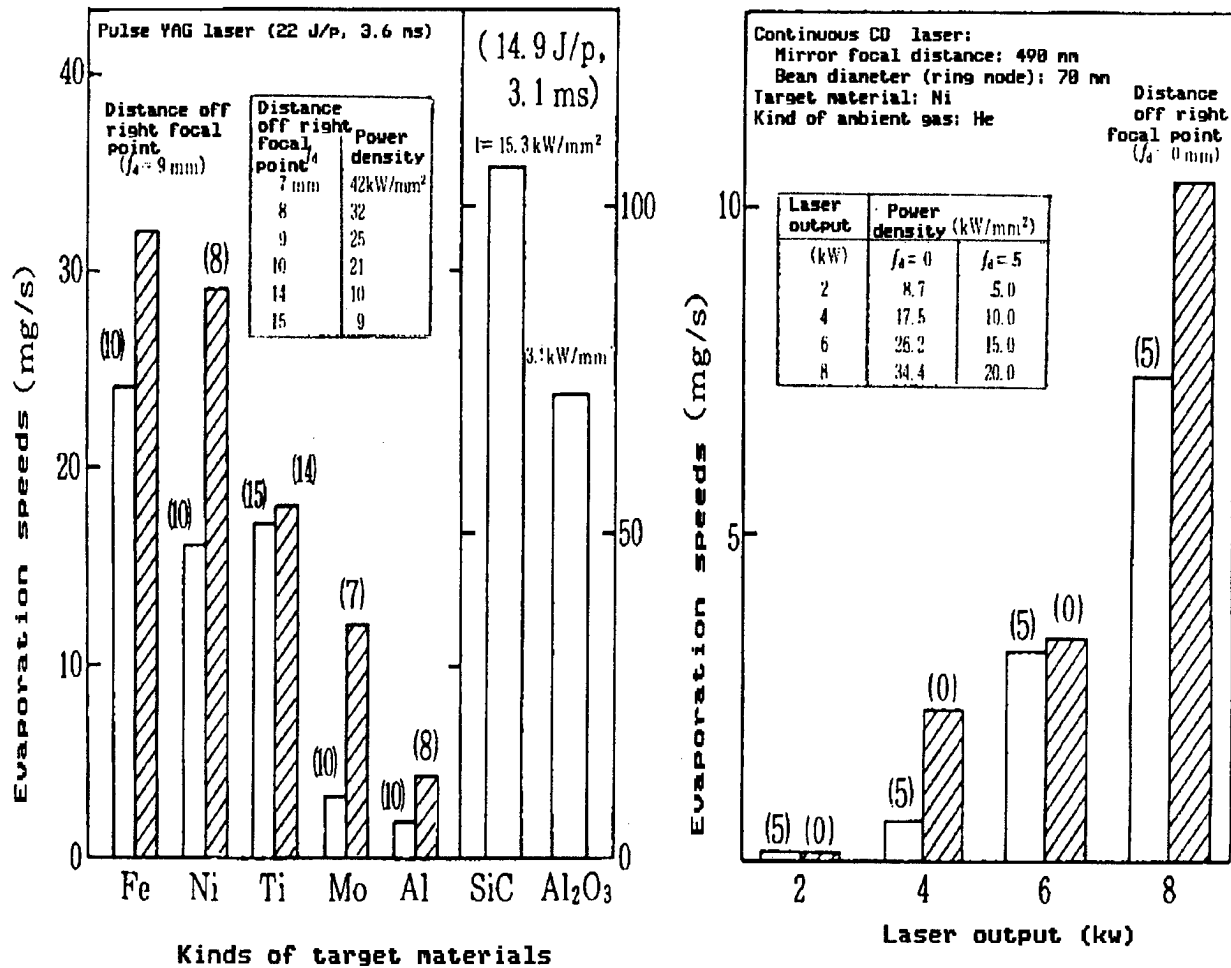


Figure 4. Evaporation Speeds of Different Materials When Bombarded by Pulse YAG Laser Beam and Continuous CO₂ Laser Beam

measurement was conducted extensively and systematically. Figure 4 gives the results of measurement of the evaporation speeds of a number of kinds of materials using a pulse YAG laser (mean maximum output: 200 w, pulse width: 0.24-3.1 ms, peak output : 10 kw) and a continuous CO₂ laser produced better results than the CO₂ laser in the degrees of evaporation per a unit irradiation power density. This is due to the fact that a laser beam having a shorter wavelength can be absorbed by metal more easily, with a smaller absorption loss by the plasma allowing more laser energy to reach the material surface.

4. Processes for Formation of Superfine Grains

Not much research has been conducted to clarify the processes involved in the formation of the superfine grains using laser evaporation method. The following discussion is based on the results of a related research, which the author conducted using a pulse YAG laser system.

The photos in Figure 5 [omitted] indicate the process of the growth of a plume when a pulse YAG laser beam was fired perpendicularly at the surface of the target material. The pictures were taken using a special super-high speed photographic technique called "shadowgraph," with an exposure time of about 50 ns ($1 \text{ ns} = 10^{-9} \text{ s}$). The photos indicate the evaporation starting moments after the irradiation started. They also show that a column of vapor (plume) rapidly growing upright from the surface of the target material. As is clear from the photos, the plume is made up of the inner core section and the outer "sheath" section surrounding the core. The results of a spectral analysis indicate that the core section is made up mainly of atomic vapor of the target material, and the sheath section of compressed gas surrounding the core. When the power density of the laser beam was increased a little more, a turbulence began to appear in the plume of vapor. When the power was boosted extremely high, a column of molten substance shot up from the molten surface of the target material, as shown in Figure 6 [omitted]. The shooting up of the molten liquid causes the formation of the grains (spatter) with a diameter of more than $10 \mu\text{m}$, due to surface tension instability. The occurrence of the spatter is not desirable in view of formation of the superfine grains. Figure 7 shows the appropriate laser irradiation conditions for producing the grains. The applicable range of the irradiation conditions change in accordance with the kinds of the target material and the material's surface conditions. Consequently, it is necessary to adjust the irradiation condition in accordance with changes of those conditions in the target material. As shown in Figure 5 [omitted], the plume caused by a laser irradiation is highly directional. Depending on the irradiation conditions, the speed of the plume shooting up from the material surface changes from a few tens of meters per second to near the speed of sound traveling in the air.

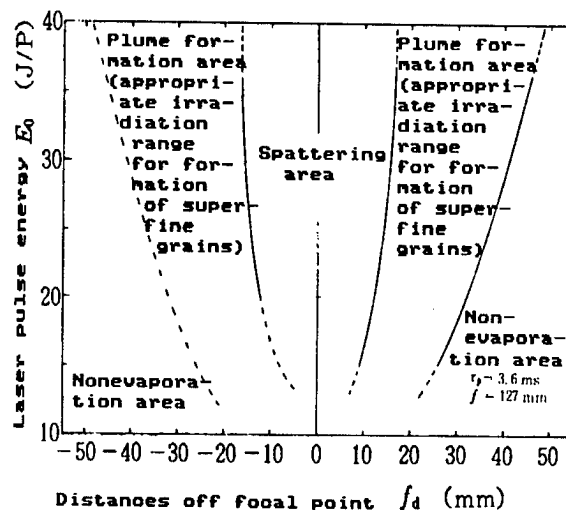


Figure 7. Appropriate Laser Irradiation Conditions for Evaporating Titanium Target Material

In the meantime, how the atomic vapor (cluster vapor is believed also included in the vapor) generated by laser beam irradiation can be turned into the superfine grains has been a point of interest from both academic aspect and controlling the diameter of the synthesized grains. Figure 8 shows the diagrams of the setup for measuring various optical characteristics of the plume. The setup enables measuring the strength of the probe laser beam after it passed through the plume, the strength of specific bright line spectrum, and the strength of scattered irradiation laser beam simultaneously.

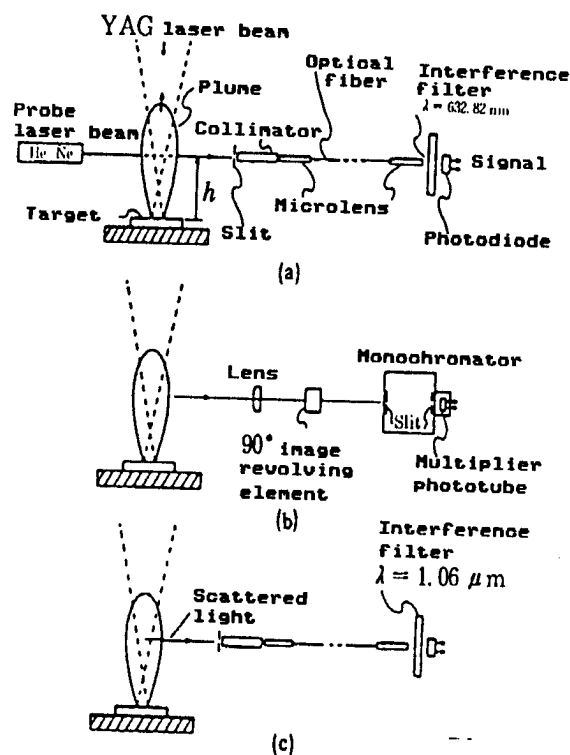


Figure 8. Method for Measurement of Various Optical Characteristics of the Plume

- (a) Method for measuring laser light transmission factor
- (b) Spectrum line strength measurement method
- (c) Method for measurement of strength of scattered irradiation laser beam

Figure 9 gives the results of the measurement of the optical characteristics of the plume at a certain height from the target material surface using the above-mentioned method, and the output waveform of the pulse laser beam. As is clear from the figure, a dip in the transmission factor of the probe laser beam, indicating the presence of an evaporated gas in the path of the beam, appears a while after the irradiation of the target material begins. The figure also shows that the evaporation continues until the irradiation laser output goes down to a critical level. The figure also shows that the strength of the luminous phenomenon when the

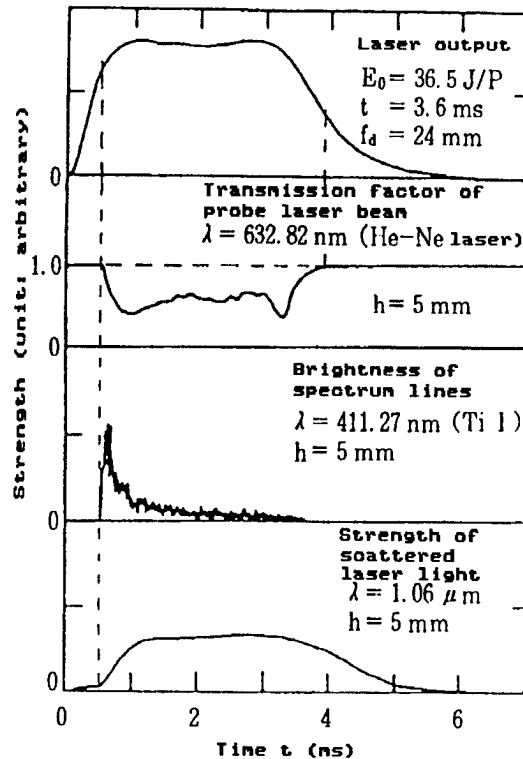


Figure 9. Optical Characteristics of Plume and Irradiation Laser Output Waveform

plume flares up registers the peak immediately after the evaporation starts, and then rapidly attenuates. In other words, this apparently means that the atomic vapor coming from the evaporated target material is in the state of being excited for a very short time, and for most of the rest of the irradiation period the vapor stays in a nonexcited state.

On the other hand, the strength of scattered YAG laser beam in the horizontal directions abruptly begins to increase when the luminous phenomenon is reaching its peak level, and the scattered laser light strength remains at a high level as long as the evaporation continues. This suggests the existence of grains within the plume larger than the atoms, which might be promoting the scattering of the incoming YAG laser beam. In fact, such grains are present within the evaporating vapor. Figure 10 [omitted] shows the photos of superfine grains with a diameter of less than 100 nm, which were caught within the vapor and observed through an electron microscope. From that observation, it is clear that fine grains with their diameter smaller than one-tenth of the wavelength of the YAG laser beam (wavelength: 1.06 μm) are being formed within the plume, and this causing the Rayleigh scattering. From the results of the measurements described, it is apparent that the atomic and cluster vapor shooting up from the laser-evaporated target material generates the superfine grains through a condensation of the vapor while it moves up in the air.

5. Features of Laser-Produced Superfine Grains

As described in the preceding section, it became clear that the superfine grains can be produced within the plume caused by bombarding a target material with a laser beam. The author's experiment to produce the grains involved a number of kinds of metals as the target material of laser beam bombardment. In the case of pure titanium which was one of those metals, the superfine grains of pure titanium with their grain diameter averaging 30 nm were formed under an inactive atmosphere of 1 atmospheric pressure, with the grains shown in Figure 10 [omitted]. Under a nitrogen atmosphere, the titanium vapor transformed into the grains of either square-shaped or rhomboid-shaped TiN with almost uniform grain diameter. It was ascertained that TiO_2 is formed when oxygen is used as the ambient gas. Using different kinds of ambient gases, as described above, it is possible to produce from various kinds of metal superfine grains of pure metals, of oxides of those metals and even fine grains of nitride ceramics. Table 2 lists the chemical structures of various kinds of superfine grains which were formed by evaporating different kinds of metals by a laser beam in the atmospheres of nitrogen and oxygen. In those grains of oxides, their chemical structures indicate that the degrees of oxidation in those grains are in the most advanced state. In the nitrogen environment, nitrides can be produced from many kinds of metals. It is apparent that all those nitrides produced form a specific composition. Among those kinds of metals tested in this research, there were also many kinds of metals which did not produce nitrides. In the case of Al, the superfine grains produced from the metal were a mixture of pure Al and nitrides. It would be a dream of scientists that they can produce superfine grains having the chemical composition they wish.

In the meanwhile, the salient feature of producing superfine grains using the laser evaporation method is that the diameter of the grains produced can be controlled easily by adjusting the pressure of the ambient gas. As shown in Figure 11, the average diameter of the grains declines when the pressure is reduced or the production environment is made vacuum. Under production of the grains using the arc heating method, it is also possible to reduce the average diameter by dropping the ambient pressure. But in the arc method, the controllable range is very narrow particularly because the size of the pole diameter is highly sensitive to changes in the ambient pressure. While in the laser evaporation method, the area of the evaporation can be changed freely without being affected by the ambient pressure. This makes it possible for the method to be able to control the diameter of the grains produced over a wide pressure condition, ranging from high vacuum environment to high pressure atmosphere. As to the reason of the declining diameter of the grains when the ambient pressure drops, as shown in Figure 9, it was found that the superfine grains are formed as a result of condensation of the atomic and the cluster vapor while it moves up in the air.

Considering the fact that under a low pressure condition, a grain within the vapor less frequently contacts other grains due to a longer mean free path, the decline of grain diameter could be explained voluntarily.

Table 2. Chemical Structures of Superfine Ceramics Grains Obtained by Evaporating Various Target Materials by Laser Beam Within an Active Atmosphere (Upper list: within a nitrogen environment; lower list: within an oxygen environment)

3										III A	IV A
										Al	Si
										Al+AlN*	Si
4	IVB	VB	VIB	VIB	VII	VII	VII	IB	II B	(FCCXII)	(Diamo)
	Ti	V	Cr	Mn	Fe	Co	Ni	Cu	Zn		Ge
	TiN	VN	β -Cr ₂ N	Mn ₄ N*	α -Fe	Co ₂ (CoO)	Ni	Cu	Zn		Ge
5	NaCl(C)	NaCl(C)	(Hexa)	(Cubic)	(BCC)	(FCCXC)	(FCC)	(FCC)	(HCP)		(Diamo)
	Zr	Nb	Mo								Sn
	ZrN	Nb ₄ N ₃ *	Mo								β -Sn
6	NaCl(C)	(Tetra)	(BCC)								(Tetra)
		Ta	W			Element					Pb
		Ta ₂ N	W ₂ (W ₃ O)			UFP produced in N ₂					Pb
6		(Hexa)	(BCC)*			Crystal structure(system*)					(FCC)

Note : *1 Al(FCC)+AlN(ZnO struc. (Hexa)) *2 Mn₄N(Cubic)+ δ -MnN(Tetra)

*3 Nb₄N₃(Tetra)+Nb₄N_{3,92}(Cubic) *4 W(BCC)+W₃O(β -W)

*5 C : Cubic ; Tetra : Tetragonal ; H & Hexa : Hexagonal ; Diamo : Diamond.

3										III A	IV A
										Al	Si
										Al ₂ O ₃ *1	—
4	IVB	VB	VIB	VIB	VII	VII	VII	IB	II B	(Cubic)	(Amor)*2
	Ti	V	Cr	Mn	Fe	Co	Ni	Cu	Zn		Ge
	TiO ₂ *3	—	Cr ₂ O ₃	r -Mn ₂ O ₃	Fe ₂ O ₃ *4	CoO	NiO	CuO	ZnO		—
5	(Tetra)	(Amor)*2	α -Al ₂ O ₃	(Tetra)	(Tetra)	NaCl(C)	(Hexa)	(Mono)	ZnO(II)		(Amor)*2
	Zr	Nb	Mo								Sn
	ZrO ₂ *5	Nb ₂ O ₅	η -MoO ₃								SnO ₂
6	(Mono)	(Mono)	(—)								(Tetra)
		Ta	W			Element					Pb
		δ -Ta ₂ O ₅	WO ₃			UFP oxides produced					PbO ₂ *6
6		(Ps.II)	(Tricl)			Crystal structure(system*)					(Orthor)

Note : *1 r -Al₂O₃(C)+ δ -Al₂O₃(—) *2 Amorphous *3 Anatase(Tetra)+Rutile(Tetra)

*4 r -Fe₂O₃(Tetra)+ ϵ -Fe₂O₃(Mono) *5 Cubic+Tetragonal+Monoclinic

*6 α -PbO₂(+PbO(Orthorhombic))

*7 C : Cubic ; Tetra : Tetragonal ; H & Hexa : Hexagonal ; Mono : Monoclinic ;

Tricl : Triclinic ; Orthor : Orthorhombic ; Ps, H : Pseudo Hexagonal

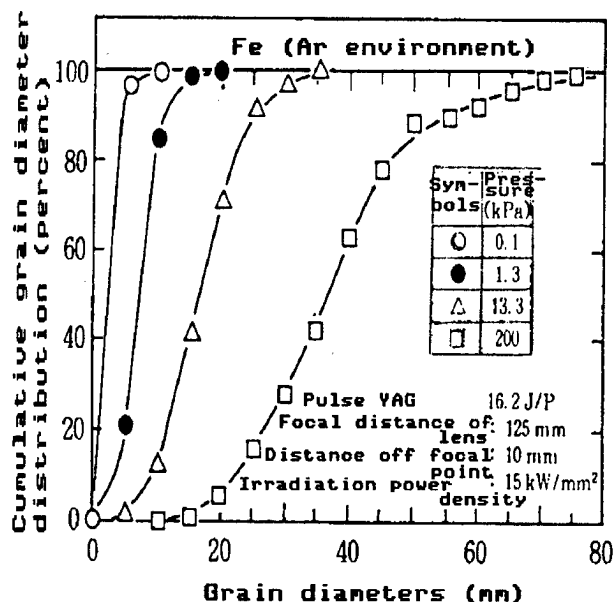


Figure 11. Controlling Diameter of Superfine Grains Produced by Changing Ambient Pressure

Using a laser beam any kind of substance can be vaporized. But it is a well-known fact that some kinds of material can be vaporized easily, but some others cannot. This means that the strength of laser energy required to vaporize differs from material to material. In using lasers for vaporizing applications, it must be taken into account that the reflection coefficient also differs from material to material. Because of this, when an alloy or a material made up of different components is used as the target material, generally the superfine grains obtained from either of those materials have material components which are different from that of the target materials. Figure 12 shows the relationship between composition of a target material and composition of superfine grains produced from the material. As the target material, Cu-Ni binary-system alloy plate and the powder of a mixture of the two kinds of metal, which were specially prepared for studying the above relationship, were used. In the case of using the Cu-Ni binary-system alloy as target material, Cu was present within the produced grains in condensed form due to Cu's having a higher evaporation rate than Ni. As explained, in obtaining the superfine grains of an alloy having a certain component ratio, it is necessary to use a target alloy, in which the ratio of the components of the alloy is adjusted properly.

6. Conclusion

This chapter has discussed the phenomena occurring when a target material is bombarded with a laser beam, and the formation of superfine grains of various materials by evaporating them with laser heat and the formation mechanism. As mentioned earlier in the chapter, there has been not much reporting on the results of research for creation of the superfine grains

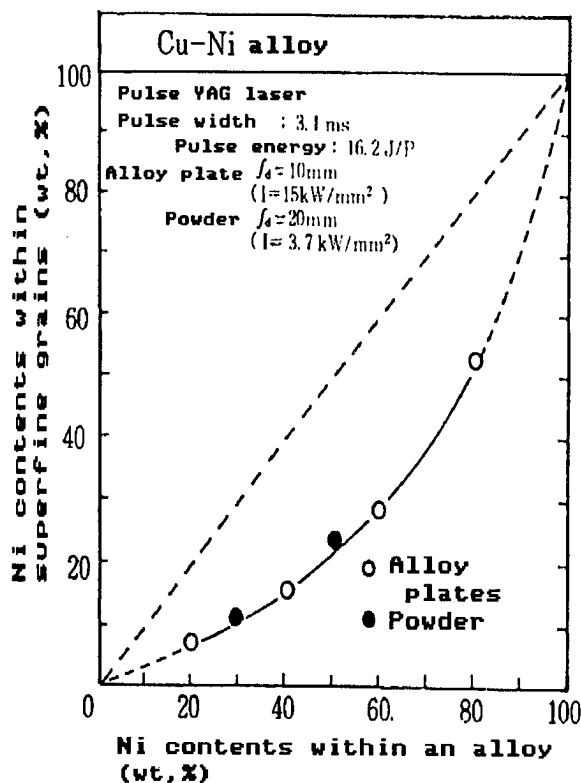


Figure 12. Chemical Composition of Superfine Grains Produced From Alloy and Powder Combined as Target Material

using laser evaporation method. Because of this, there still are many problems as regards the grain formation, which have yet to be solved through future research. Despite those problems, formation of the superfine grains using laser evaporation method would continue to be a method of interest from both an academic and engineering point of view. However, when applying the method to industrial use it must be remembered that the method has the following problem--the low conversion efficiencies from electrical input to laser beam output. This problem applies to every processing method which uses lasers as the energy sources. This is a problem inherent in lasers. Even in a CO_2 laser, which boasts the highest efficiency among lasers used today, the conversion efficiency is less than 20 percent. In producing the superfine grains, a laser with a shorter wavelength is more effective in causing the evaporation of the target material, but laser oscillation efficiency for such a laser is very low at only a few percent. Due to those problems described so far, for the time being the use of lasers for producing the superfine grain would be confined to certain limited kinds of materials, or in the production of the grains having a particular grain diameter, which cannot be obtained using other production methods.

The rest of this chapter will discuss which type of lasers--continuous laser or pulse laser--is suitable for the production of the superfine grains by evaporating the target material. Basically, grain production using the laser evaporation method calls for causing the evaporation on the

surface of the target material, and there is no need to heat the target material other than on the area of material where evaporation is intended to be caused. In the continuous heating method, an unnecessarily large pool of molten liquid is formed around the evaporation area under a quasi-stationary state. In the method, heat loss due to heat conduction to the surrounding solid parts of the laser evaporation system becomes considerably large. On the other hand, the pulse laser, when used under a proper operating condition, could allow effectively using the heat absorbed by the target material for evaporating the material surface, before the heat disperses to the surrounding areas. Due to this, it is believed that the pulse laser method is more economical to use in view of the efficiency of laser energy utilization. At present, there is no systematic data available to prove the higher efficiency of the pulse laser. The question of the efficiency has been referred to, considering that such a matter is very important in judging whether the introduction of the low efficiency laser evaporation method into practical industrial applications is commercially feasible or not.

Hard Ceramic Film by Laser PVD

43064001f Tokyo KINO ZAIRYO in Japanese Vol 7 Aug 87 pp 50-58

[Article by Shin'ei Mineda, senior researcher at Electron Processing Laboratory of Denshi Gijutsu Sogo Kenkyusho, and Nobuo Yasunaga, senior researcher at No 1 Technical Research Institute of Nippon Steel Corp.; first paragraph is editorial introduction]

[Excerpts] A new laser PVD method has been developed to deposit the film of vaporized ceramics on the surface of a substrate, by evaporating a ceramic body in revolution, by irradiating the body surface with a CO₂ laser beam from a direction of the tangential line. This method enables forming various kinds of dense and very hard ceramic film on the surface of a substrate efficiently. By introducing N ions, a super-hard film of cBN can be formed on a substrate. The laser PVD method could be used to make products which have good anti-wear, anti-heat, and anti-corrosion capabilities. In addition, the method could also be used to form a film having good electrical insulation.

1. Introduction

Active research has been made to apply ceramic coating to various kinds of products ranging from mechanical parts and electrical parts to functional as well as structural parts, to improve their anti-wear, anti-corrosion, and anti-heat capabilities. As ways of applying a ceramic film to those products, various CVD and PVD methods have been put to practical use. Which of those methods to use depends on the kind of work to be done.

In recent years, research for the development of laser CVD and laser PVD methods has been stepped up, and researchers have begun to report on the promising future of those methods. The industry puts high hopes on the progress of the research. We also have been engaged in the development of a laser PVD method using large-output CO₂ laser as heat source to evaporate

the target material. Our research is aimed at forming a film of uniform, dense, and very hard ceramics on a substrate, by evaporating a revolving ceramic body using a laser beam.

The principal features of laser PVD method are: 1) The film of ceramics can be formed on almost any kinds of materials, regardless of metallic or nonmetallic materials. Particularly, the formation is easy in the ceramic materials which have high laser light absorption rates; 2) the separation of the laser-generating unit and the processing chamber makes it possible to simplify the structure within the chamber; 3) handling a laser beam, such as branching it and causing it to scan an object, is easy. By equipping a PVD system with a material sample transporting mechanism, it is possible to coat different kinds of material with a ceramic film efficiently, or to coat a material with plural layers of ceramics; and 4) the PVD method allows a laser oscillator for a laser-based processing system also being used for a PVD system.

So far, attempts have been made to evaporate a flat-surface material sample by irradiating it with a YAG laser beam or a CO₂ laser beam. In every case of those attempts, the outputs of those lasers were less than 100 w. The problems with those laser systems were that the beam converging system tended to be easily stained, and the strength of the film formed was low due partly to instability in the deposition process. For those reasons, laser PVD method has been used only in limited fields, such as the formation of an optical thin film.

The laser PVD system which we developed enables irradiating a revolving ceramic sample with a kw-level laser beam without causing heat destruction to the sample, by firing the beam from the direction of the tangential line of the ring-shaped sample. We succeeded in developing a beam converging system less vulnerable to stain, allowing a stable vapor deposition. This enables the formation of a thin film of ceramics of a higher quality at a faster deposition speed.

In the following sections, we will introduce the basic construction of our experimental laser PVD system and its features, and will describe the deposition characteristics and the characteristics of the film formed using the system. We will also touch on examples of the system's application to forming ceramic film.

2. Basic Construction of Laser PVD System

Figure 1 gives the basic construction of the laser PVD system we built. The cwCO₂ laser beam is introduced into the vacuum chamber through the infrared lens to irradiate the ring-shaped ceramic body, rotating at a speed of 10-30 rpm, from the direction of the tangential line of the outer circumference of the ceramic body to vaporize the surface. The vaporized ceramic is then deposited on the surface of the substrate located in the left of the ceramic body. In old laser PVD systems, the ceramic vapor source material had a flat plate-like shape. The shape caused the vapor

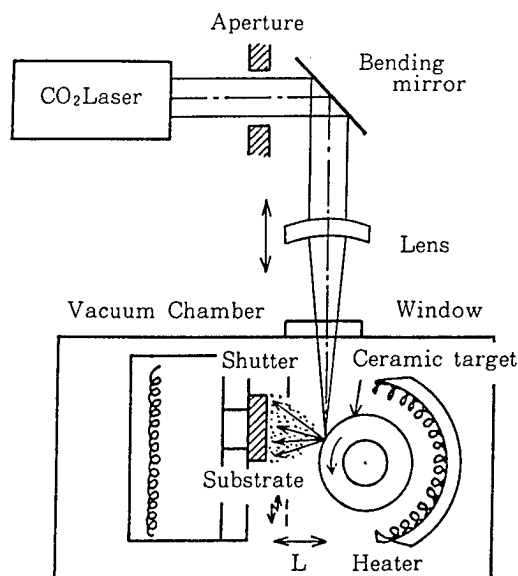


Figure 1. Basic Construction of Laser PVD System

from the material to scatter in the direction of the chamber window, through which a laser light is led into the chamber and mirrors, causing pollution. The pollution caused instability in the vapor deposition process. Our system solved these problems by making the ceramic vapor fly toward the substrate almost at the right angles with the incoming laser beam, preventing pollution of the window. In our system, a measure against heat destruction of the surface of the ceramic body due to bombardment of the surface with a powerful laser beam was taken, by heating the ceramic body to a temperature of about 800°C by an auxiliary heater. The heater on the left side of the substrate is also aimed at maintaining the substrate at a certain temperature. The shutter between the ring-shaped ceramic body and the substrate is to enable vapor deposition to begin on the substrate by opening the shutter, when the strength of laser beam hitting the ceramic body has reached a certain level.

In the following sections, we will describe the characteristics of the ceramic film-coated substrates of Mo, Cu, and Si, with the film made using various kinds of oxide ceramics and nitride ceramics, as listed in Table 1, as the revolving ceramic vapor sources.

3. Vapor Deposition Characteristics

3.1 Influence of Vacuum Degree

To find out the influence of the vacuum degree within the vacuum chamber on the characteristics of a ceramic film formed within the chamber, we conducted coating of Cu substrates with a film of Al_2O_3 under a low vacuum condition (about 1×10^{-2} Torr attained using a rotary pump) and a high vacuum condition (about 1×10^{-4} Torr achieved using an oil diffusion pump), respectively. As shown in Figure 2(a) [omitted], the film formed

Table 1. Various Ceramic Materials Used as Vapor Sources in Experiment of Coating Substrates With Ceramic Films

Ring target	composition (wt %)
Al_2O_3	Al_2O_3 99%
$3\text{Al}_2\text{O}_3 \cdot 2\text{SiO}_2$	Al_2O_3 73% SiO_2 26%
Si_3N_4	α 20%, β 80%
SiAlON	Si_3N_4 76.8 % Al_2O_3 23%
BN (1)	hBN % 95~99% Binder CaO , B_2O_3
BN (2)	hBN 60% Al_2O_3 20% SiO_2 20%

under the low vacuum condition has a pillar-structure growth similar to films formed using other nonlaser PVD methods. Such films have comparatively low hardness and adhesion power. A film formed under the high vacuum condition is transparent and has a very dense and uniform growth, as shown in Figure 2(b) [omitted].

The discussions in the following sections will concentrate on the results of experimental formation of ceramic films under high vacuum condition.

3.2 Speed of Film Formation

Figure 3 shows the relationships between irradiation laser beam powers and the speeds of deposition of the films of mullite, silicon nitride, or hBN (hexagonal system BN) on Mo substrates. In the film deposition, the distance between the substrates and the irradiation point on the surface of the ceramic ring ranged from 50 to 70 mm. The figure shows that the deposition speeds changed depending on the kinds of material on which the deposit is made. However, in each kind of material, the deposition rates increased when the irradiation power was boosted.

On the other hand, Figure 4 gives the building speeds of the films of a number of kinds of ceramics on the substrates, when the irradiation was conducted with a fixed irradiation power of 320 w and by keeping the distance between the substrates and the ceramic sources at 50 mm. It is clear from the figure that the building speed is lower for those ceramics which have a higher melting or evaporation temperature and larger thermal conductivity.

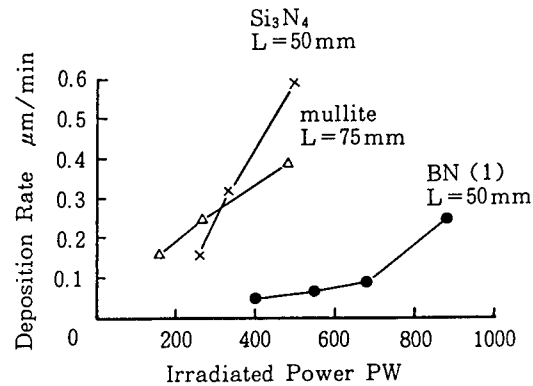


Figure 3. Relationships Between Irradiation Laser Beam Powers and Speeds of Deposition of Vaporized Ceramics

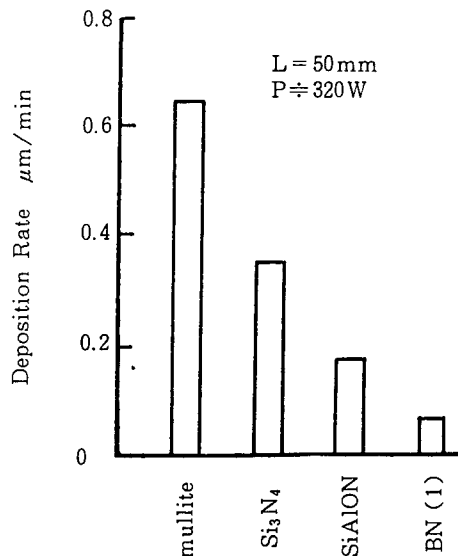


Figure 4. Differences of Building Speed of Ceramic Film on Substrates for Different Ceramics as Film Material Sources

3.3 Structure of Formed Film

An X-ray diffraction analysis of those ceramic films we created using laser PVD method found that all of them had amorphous structure. In general, ceramic films formed using PVD method have amorphous structure. This was proved by our experiments. One possible cause for the formation of amorphous structure is believed to be due to the quick cooling of the evaporated ceramic grains upon colliding with the surface of the substrate, which is maintained at a temperature ranging from 400 to 500°C.

In many cases, we found through experiment that the ceramic film composition differed from that of ceramic vapor source materials. For example, in the case of mullite, an XMA analysis found that there was more

than a fivefold difference in the contents of Si between the formed film and the ceramic material, with the film containing higher amount. On the other hand, in the case of nitride vapor source material, N contents in the film formed were substantially lower than N contents in the material. In the cases of vapor deposition of Si_3N_4 and hBN, conspicuous increases in contents of Si and B within the ceramic films formed compared with contents of N were ascertained by an ESCA analysis (Figure 5). The composition of a film is affected slightly by the irradiation conditions. But in actuality, it is difficult to control the composition significantly only by changing the conditions of laser irradiation. As we will describe in a following section, to obtain a film of a desired composition it is necessary to introduce an ion gas or other means to realize the composition.

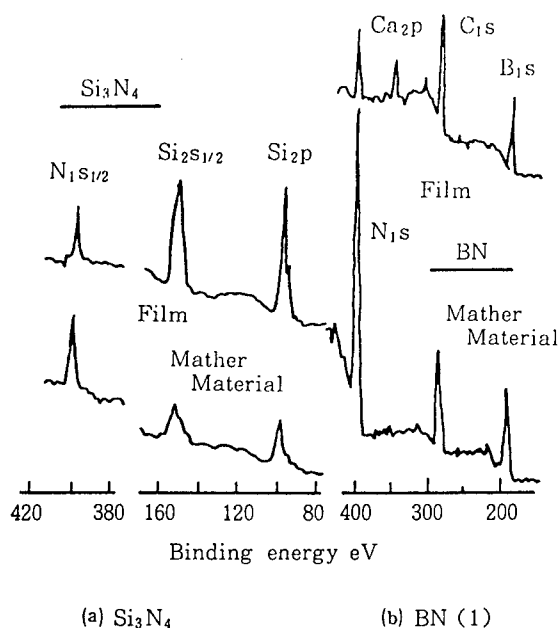


Figure 5. ESCA Spectra of Si_3N_4 (Left) and BN (Right)

3.4 SEM Observation of Film Surface

Figure 6 [omitted] shows the photos obtained by SEM observation of the fractures of four different kinds of films formed by the deposition of vaporized ceramics. It can be seen that in all of those films the vaporized ceramics are deposited uniformly and densely. The SEM photo of mullite displays sea-shell-shaped fracture most conspicuously. The shell-shaped fracture can be seen often in brittle materials. In all of those photos, no directionality of the film materials nor grain boundaries can be observed. This could be attributed to the amorphous structure of those films. From those photos, it can also be seen that almost complete adherence was realized between the substrates and the films. In the case of Si_3N_4 , it was found that the pillar-structure film tends to appear when the irradiation power is excessively large and film formation speed is too great (higher than $1.0 \mu\text{m-min}$). Similar results appeared when the film was formed by abruptly boosting the irradiation power without preheating of the

ceramic vapor source materials. Appearance of the pillar structure harms the uniformity of film and causes a deterioration of the strength of the film. For those reasons, it is believed that proper control of irradiation laser power is important to form a good film having high material density.

3.5 Strength of Film

Figure 7 gives Knoop hardness of several kinds of ceramic films each having a thickness of about $5\text{ }\mu\text{m}$. Each of the films was hardness nearly the same or higher than their source materials. Particularly noteworthy is the BN film. Its parent material hBN (hexagonal BN) is not so hard that it can be processed easily. But the film formed from the material exhibits a hardness higher than $\text{Hk } 4,000\text{ kg/mm}^2$, a hardness close to that of cBN (cubic BN). For the future, it can also be seen that even in hBN (2) with lower material purity, Knoop hardness is higher than that of Al_2O_3 . cBN has hardness next to diamond. The hardness makes the sintered body of cBN used in grinders and cutting tools for use in the processing of hard materials. Aiming at developing tools coated with the film of cBN-system ceramics, research for creating the film has been stepped up in recent years using IVD method combining ion injection method and electron beam vapor deposition method and using plasma CVD method. Despite this effort, none of these methods has been put into practical use so far. However, by using the laser vapor deposition method developed by this research, it is possible to form a film of superhard BN at a speed higher than $0.2\text{ }\mu\text{m}$ per minute, and the method would provide an effective means in promoting development of parts having better anti-wear abilities.

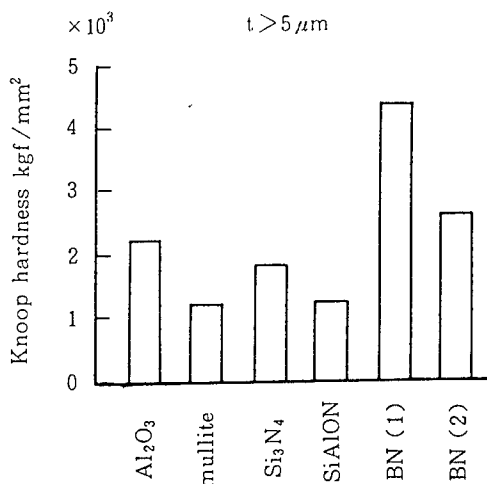


Figure 7. Knoop Hardness of Various Kinds of Ceramic Films

There is a possibility of minor differences appearing in the hardness of ceramic film formed, when the parent material samples were made using different sintering methods, even if they had the same material composition. In view of this, it is important to clarify the relationship between the characteristics of the film and that of the parent material.

4. Application of Ceramic Film

4.1 Application to Anti-Wear Parts

BN has good mechanical, heat, and chemical characteristics, and due to this, development of the technology for commercial production of BN film is awaited in many fields of the industry. The laser PVD method developed by this author enables the production of very hard BN film relatively easily. This method could be used for the production of sliding parts and other high-abrasion-resistance parts.

The following will describe the results of the test of wear and abrasion resistance of a BN film coated on an Mo substrate. The test was conducted using a dry test method. First the substrate, measuring $13 \text{ mm}^2 \times 6$ thickness in cross-section dimensions and its one broad side bulging outward (curvature: 25R), was coated with a $5 \mu\text{m}$ film of BN on the bulging side. The test was conducted in the air by pressing the coated face of the substrate against a revolving cast-iron disk under a load of 1 kgf and with an abrasion speed of 1.8 m/sec (200 rpm). The BN film was formed by irradiating a BN source material with a laser power of 800 w, and by setting the distance between the substrate and the point of laser beam bombardment on the material at 50 mm. The film thus formed had a hardness of Hk-2,000 kg/mm^2 .

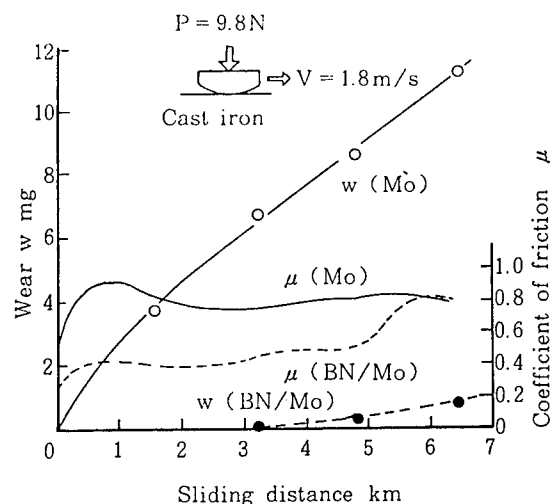


Figure 8. Comparison of Wear Performance of Mo Substrate With BN Film on Surface and One without Film

Figure 8 shows the results of the test. As seen from the figure, the overall wear rate on the BN-film coated Mo substrate is very small compared to wear rate on another Mo substrate with no such coating. Wear rate is particularly small when the wear is confined to the film--one-hundredth of the naked Mo substrate. During the initial period while the wear is still confined to the film, the friction coefficient also is small. Figure 9 [omitted] shows the rough worn face of the BN film. However, the surface

of each of the worn grooves is relatively smooth, and it can be seen that little film peeled off during the wear test. What has been described thus far is the result of a wear test conducted under a limited condition. However, those results would indicate that the laser PVD method can be used effectively for the formation of BN film on various parts and tools to improve their anti-wear capabilities.

4.2 Application of CO₂ Laser Absorber

With an increase of CO₂ laser output in recent years, the absorbers used in calorimeters and power dampers are required to have increasingly high light-proof capabilities. For application to power lasers, the absorber is required to have good laser light absorption capability, thermal conductivity, anti-hear capability, and good anti-oxidation ability. Those absorbers now available on the market have a light-proof capability of only a few hundred watts per square centimeters. Considering the possibility that the number of laser processing machines with power outputs of more than a few kilowatts would increase on the market in the future, absorbers with a greater light-proof capacity must be developed. Coating a metal substrate having a high thermal conductivity with a ceramic film having a high absorption capability of CO₂ laser beam would help create such an absorber.

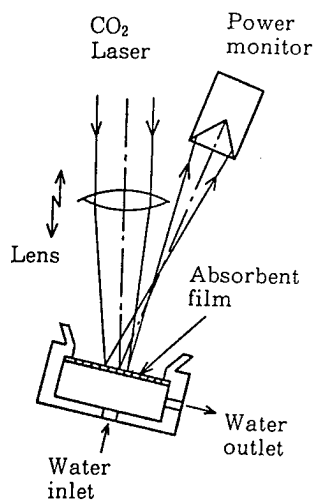


Figure 10. Setup for Measurement of Light-Proof Capability of Laser Light Absorbers

To test the light-proof capabilities of a number of kinds of coating materials, we created absorbers by coating Mo substrates, each measuring 75 mm in diameter with a thickness of 1 mm, with films of Al₂O₃, TiO₂, and Si₃N₄, respectively, using the laser PVD method we developed; we conducted light-proof tests of those substrates using a test setup shown in Figure 10. In the test, a CO₂ laser beam with a power strength of a few kilowatts was fired at those absorbers through a light-converging lens. (Those absorbers were cooled by running water with a flow rate of 4 liters per minute on their back.) Figure 11 shows the results of measurements of

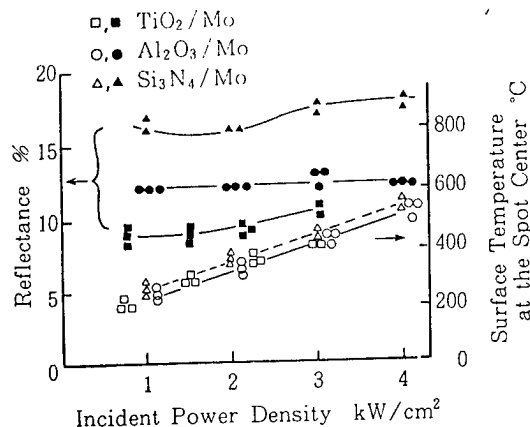


Figure 11. Laser Beam Absorption Characteristics of Several Kinds of Ceramic-Film Coated Absorbers

changes of the temperature and the reflectance of a laser beam on the surfaces of those absorbers, then the beam's power density was changed by moving the converging lens back and forth. From the figure, it can be seen that the TiO_2 absorber has the lowest reflectance and is most suitable as the absorber among them. However, the drawback of the absorber is that its reflectance varies in accordance with changes in the power density. In the case of Al_2O_3 absorber, reflectance is a little higher than TiO_2 absorber, but the reflectance remains almost constant despite changes in the power density. In all of those absorbers, no damage was observed on their surfaces after they had been subjected to on-off irradiations with a beam power of less than 4 kW/cm^2 . In general, they exhibited light-proof capabilities which are more than one digit higher than those absorbers developed so far. The output of the most powerful CO_2 laser processing machine now available anywhere is about 20 kw. It is estimated that the average power density in the near fields of such a machine is only about 2 kW/cm^2 . We are confident that those absorbers we developed could withstand direct irradiation by such a powerful laser beam well.

5. Formation of cBN Film by Adding N Ions

As we described in a preceding section, a ceramic film formed by a simple laser PVD method has an amorphous structure, and the film's stoichiometric ratio is considerably different from its parent material. For example, in the case of nitride films, N contents in the films made using the PVD method are considerably depleted, and to compensate the depletion N must be replenished. To deal with this problem, we experimentally attached a Kaufman-type ion source to a laser PVD system (Figure 12), and conducted the formation of a film by irradiating a substrate with vaporized ceramic and ions from the source simultaneously. The result was that the N/B ratio in the film formed was close to 1, and the crystallized film contained a high level of cBN.

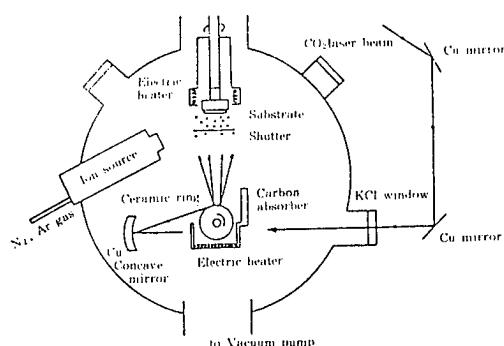


Figure 12. Schematic Drawing of Laser PVD System Equipped With Ion Source

In preparation for conducting the formation of a film, first the chamber was exhausted down to less than 1×10^{-6} Torr. Then N_2 gas was introduced into the ion gun and was ionized under a total pressure of $4-8 \times 10^{-5}$ Torr. The ions were fired at the substrate by being accelerated by a potential of about 2.5 kV. As the parent material for the formation of the film, hBN (purity: 95-99 percent) was employed. The film was built on an Si wafer and Mo substrate with the laser beam power ranging from 4000 to 1,000 w.

Figure 13 shows the ESCA spectrum of the BN film which was formed on the Si substrate at a thickness of about $1 \mu m$. Figure 13(a) shows the ESCA spectrum of a similar film formed using the simple laser PVD method. Compared with the ESCA spectrum of cBN powder (c), the peak intensity of B_{1s} in (a) is much larger, but N_{1s} is smaller. The binding energy of B_{1s} is 188 eV, and this is close to that of B metal. On the other hand, in the case of ESCA spectrum of a film (b) which was made irradiated with N ions with an acceleration voltage of 1 kV, the N_{1s}/B_{1s} peak ratio is 3.4. This value is almost identical with that of cBN powder whose ratio stands at 3.3. This means that a BN film very close to the stoichiometric ratio was formed as a result of introduction of the N ions. As regards the binding energy of B_{1s} , there is a portion which shifted a bit to the side of B metal, but for the most part it is at 191 eV, the same as that of cBN, and it can be said that the film is in the state of BN binding.

Figure 14 shows the results of X-ray diffraction analysis of the thin ceramic films, formed by changing the voltages for acceleration of the N ions. As we described earlier in this section, the film formed without using the ion gun has amorphous structure. But when N ions were introduced, a crystallized film is formed. Figure 14 shows that as the acceleration voltage increase, the contents of cBN in the film also increase. Figure 15(a) [omitted] shows the fracture of a cBN film which was formed under the acceleration voltage of 1 kV. No discernible crystal grain boundaries can be observed in Figure 15(b) [omitted]. From the figure, it is apparent that with an increase of the cBN contents the film being formed begins to have a crystallite structure. This phenomenon backs the results of the x-ray diffraction analysis.

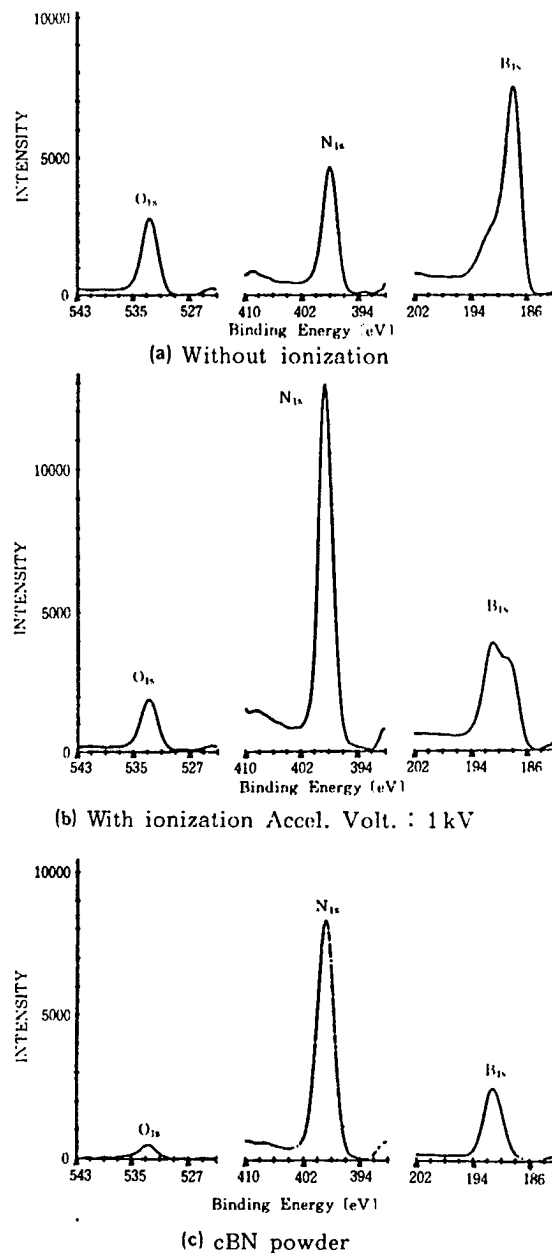


Figure 13. Results of ESCA Spectrum Analysis of BN Films

In the meantime, the Knoop hardness of those films ranged from 2,500 to 4,000 kg/mm². It is known that the hardness increases slightly when the acceleration voltage is boosted. The electrical resistance of those ceramic films we created without using N source stood at 10⁹Ω·cm. The resistance increased to 10¹¹Ω·cm when N ions were added under the acceleration of 1 kV.

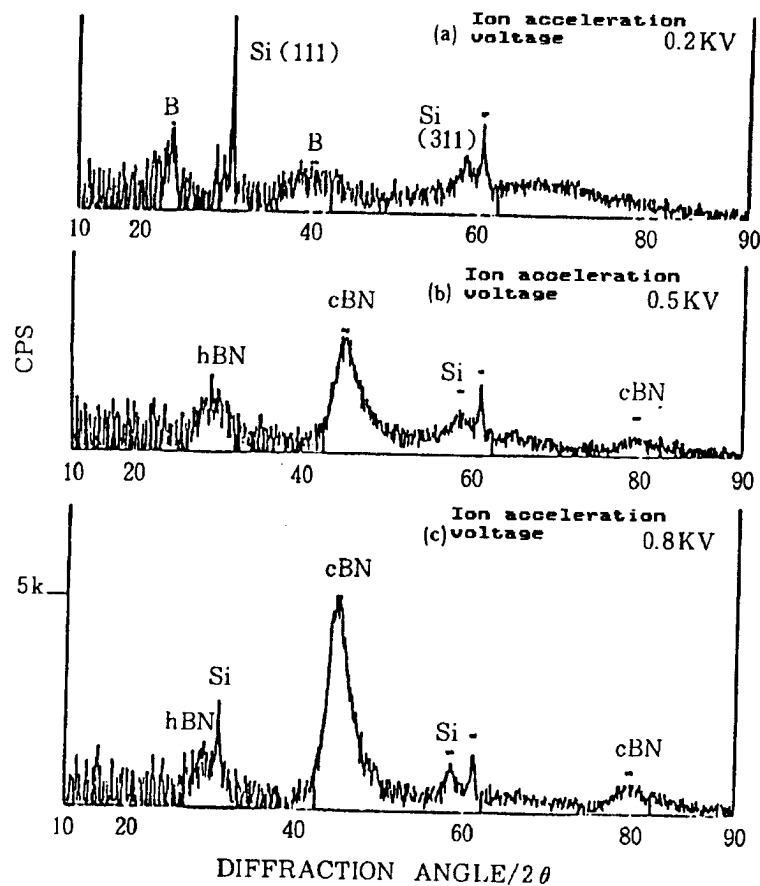


Figure 14. Results of X-Ray Diffraction Analysis of Thin Ceramic Films

Material Surface Improvement by Laser

43064001g Tokyo KINO ZAIRYO in Japanese Vol 7 Aug 87 pp 59-70

[Article by Hiromichi Kawasumi, professor, Chuo University, Science and Engineering Department; first paragraph is editorial introduction]

[Text] The methods for reforming the surface of industrial materials can be classified by the processing conditions roughly into thermal processing method, compound processing method, and light excitation processing method. This chapter will examine the surface reform technology of steel, which is currently used in the steel and automobile manufacturing industries as a mass-production technology, from a viewpoint of thermal conduction and metallurgical technology. It will also touch on what must be taken into account in introducing the reform technology into practical applications, and problems encountered in the applications.

1. Introduction

As described in Figure 1, surface reform of a material can be carried out using a high-temperature process involving heating of the material, and using a low-temperature process in which the reform is effected by a photochemical reaction induced by short-wavelength laser light having high light quantum energy.

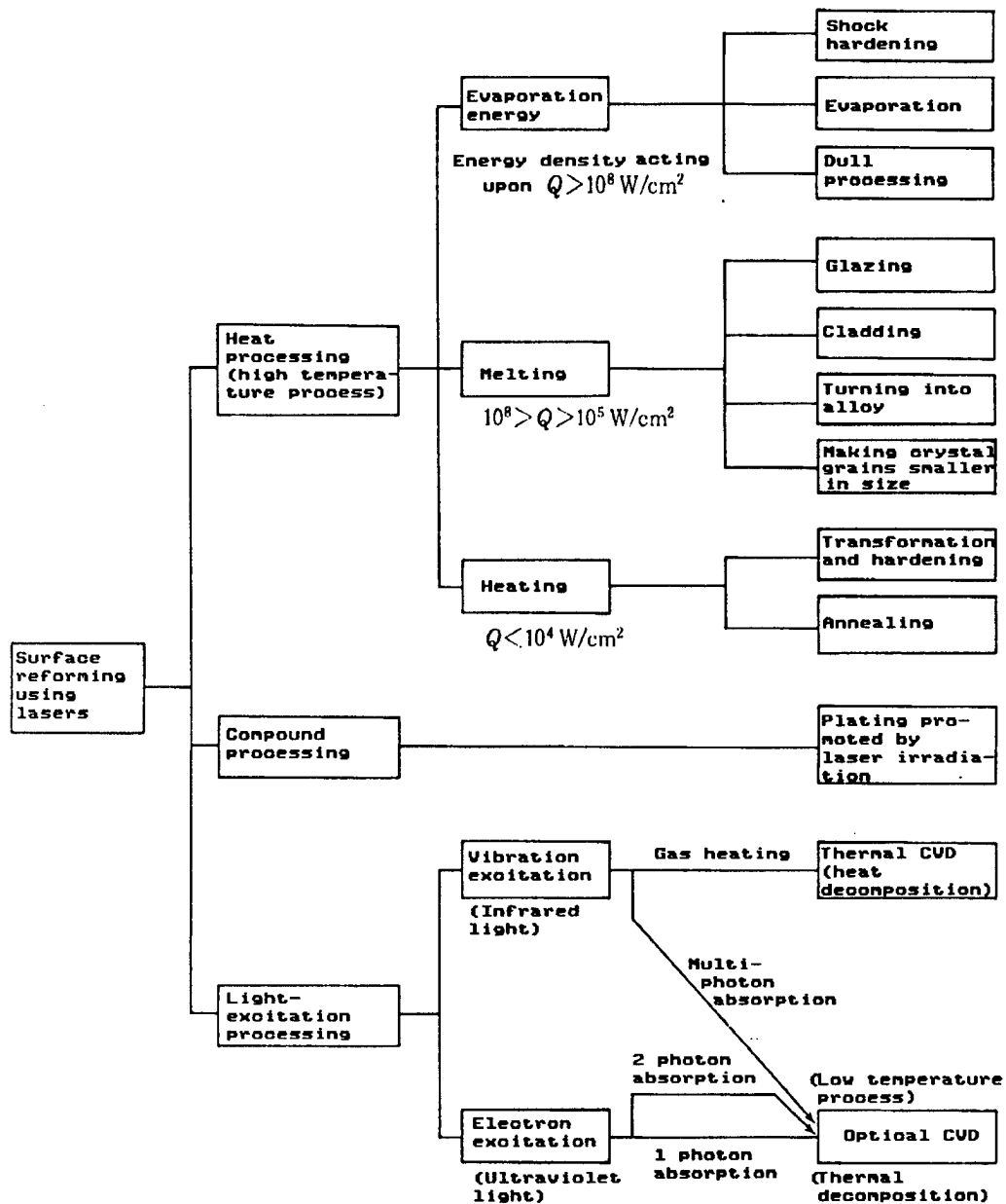


Figure 1. Ways of Surface Reforming of Material
(Values of Q are approximate)

At present, the high-temperature process is being used mainly in the steel and automobile production lines. In reforming materials, the process currently in use causes transformation and hardening of those materials. Significant progress has been made in recent years in the research on cladding and transforming material surface into an alloy, as part of the high-temperature process technology. Under the circumstances, it is expected that those surface reform techniques would be put into practical applications in the near future.

On the other hand, in the low-temperature process, the high light quantum energy makes it possible to directly coat the surface of a material with the metal atoms of an organic metal compound or other kinds of materials, by breaking the chemical binding in the materials. In recent years, this process began to be used actively in various applications, including repairing of pin-hole defects in the transcribing masks in LSI production. In addition to those two principal processes, a new process combining the features of the processes has appeared.

2. Hardening by Lasers

Surface hardening using a laser beam is achieved by irradiating a localized surface area of a material, where the hardening is supposed to be done, for a short time until the surface temperature rises higher than A1 transformation point; cooling of the heated surface occurs as a result of the heat on the surface dispersing into deeper depths of the material, after the laser beam moved away. The hard martensite is formed through these processes.

Itemized in the following are the merits of surface hardening using a laser beam: 1) Laser surface hardening method calls for heating the surface of a material to a shallow depth and this requires a smaller heat input. The smaller heat input means a smaller degree of deformation caused by the heater, and this in turn leads to reducing the necessity for the post-heating treatment of the material to correct the deformations; 2) it is possible to harden inside of a pipe, or only part of an object having complex shape; 3) different from electron beam processing or the carburization hardening method, which requires the use of a vacuum chamber or a carburization furnace, the laser beam method allows conducting processing in the air, and this is suitable for treating a bulk object; 4) the laser method requires no water or oil to dip the heated object in for cooling, producing no industrial wastes; 5) the method allows controlling the depth of hardening and the area of hardening precisely; and 6) the method enables treating a method in a very short time, and this makes it possible to conduct on-line processing.

But the laser beam hardening method has disadvantages, too. They are:

1) difficulty in hardening to a greater depth; 2) the necessity to condition a material so that carbons can be diffused within it easily for a better hardening result, because of the short time of the temperature of the material staying higher than the A1 point at the irradiated area; and 3) the necessity for a measure to prevent reflection of a laser beam, when a metal object to be treated has a highly smooth surface.

So far, a number of other material surface hardening methods have been developed, with some of them already being used in practical applications, including high-frequency hardening method, electron-beam hardening method, and flame hardening method. Under these circumstances, there would be no advantage in introducing the laser beam hardening method, unless the above-mentioned advantages of the laser method are realized in practical applications. For example, in the production of a precision gear, the methods used so far involved processing the material using expensive grinding machines and taking a long time after the material was surface-hardened. (In fact it took a very long time because the surface was hardened.) By using laser beam, precision cutting of the gear material can be performed while it is still relatively soft. The necessity for no corrective treatment after the heating contributes greatly to cutting the processing time, and consequently the production costs. The short time required for the processing makes it possible to conduct the processing on-line. In introducing the laser beam method, it is necessary to evaluate the advantages of the method from an overall point of view. In applying the method to manufacturing of industrial products, it is important to pick the right kinds of products to which the method is applicable, by paying attention to the tolerable degrees of deformation caused by heat.

In Japan, the laser beam hardening method is being used by Yanmar Diesel Engine Co., Ltd., for the hardening of the piston ring groove of the diesel engines the firm produces. Besides the company, the laser beam hardening method seems being used by an automobile maker for the hardening of the cam lobe of a cam shaft, though the firm has not revealed introduction of the method for such an application. In the United States, GM introduced 1-kw CO₂ laser systems at its Saginaw, Michigan plant for the hardening of inner surface of the steering gear housing in 1977. Using 15 such machines, the car maker is reported to be producing the hardened housings at a daily output of 30,000 units.

3. Conditions for Surface Hardening

Before putting the laser beam hardening method to industrial applications on a commercial basis, it is important to fully understand the following conditions: 1) proper heating conditions; 2) relationship between the heat history and the material component of a metal involved; and 3) the mechanical character of a material to be hardened, by experiments. As items which must be taken into account concerning the heating conditions, there are beam feed speed V , diameter of a beam spot D , laser output power P , thermal constant of a metal to be heated, and temperature distribution within a material when it is being heated. As items which must be considered regarding the mechanical character, there are residual stress, and abilities against wear, corrosion, and shock.

4. Consideration From Viewpoint of Thermal Conduction

Another problem in applying the laser beam hardening method to practical applications concerns the distribution of laser beam energy on the surface of a material being irradiated. Figure 2 shows the various mode of laser beam. Among those modes, TEM_{mm}* mode and TEM₀₁* mode are being used for

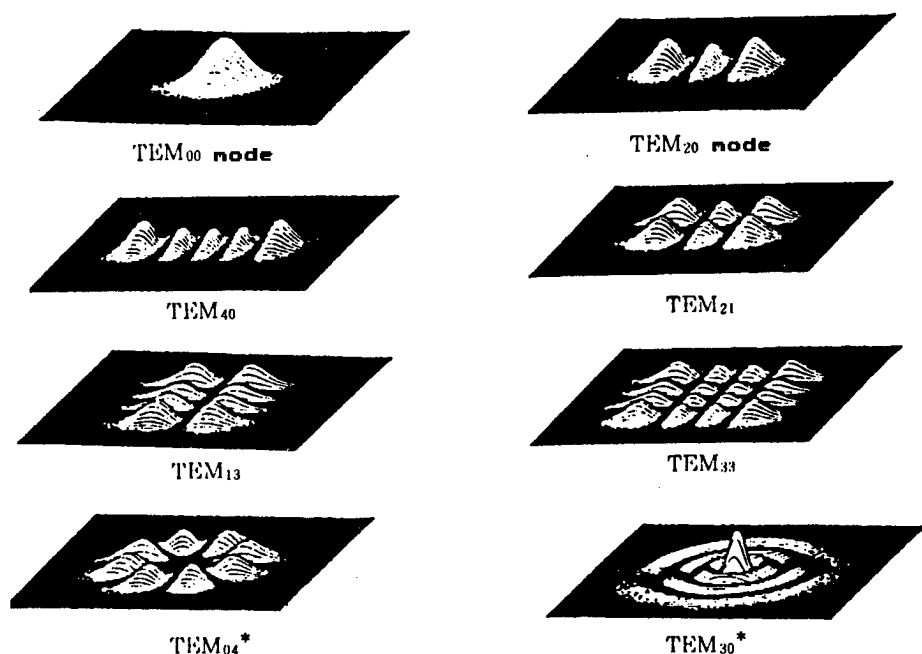


Figure 2. Various Modes of Laser Beam

material surface reforming applications. The TEM_{mm} mode is also called higher mode; mathematically, it can be approximated by rectangles. On the other hand, the TEM_{01} mode is also called a doughnut mode, and the energy distribution in the mode looks like a cluster of neatly arranged doughnuts after having been cut in halves.

In case no modes other than Gauss mode can be obtained, oscillation beam mode (Figure 3) which was employed by S.L. Engel can also be used. The processes involved in the method are similar to electron beam hardening method, and the oscillation method is used when hardening is required to be carried out to a shallow depth but in a wider width. On the other hand, when hardening is required at a deeper depth and wider width, the oblique beam irradiation method developed by this author could be used.

Figure 4 and Figure 5 show the results of calculations conducted by this author to obtain the temperature distribution patterns within a three-dimensional object, when it was heated by a rectangular-mode laser beam. The calculations were conducted by assuming that the object had uniform and isotropic structure, and that it was heated at a rate of $Q(x, y, z, t)$ per a unit length of time.

In Figure 4, the heating period is the duration until the temperature rise reaches the peak in the curves, and the cooling period are the durations on the curves after the temperature peaked. For a faster cooling, a laser beam with the trailing edge of the waveform of its energy density having a steeper slope must be used. At the same time, for hardening of a material to a deeper depth, it is important to use a laser beam having proper shape of beam spot. The curves in Figure 5 represent the depth of hardening obtained in a material model by setting irradiation conditions the same as irradiation conditions used for Figure 4.

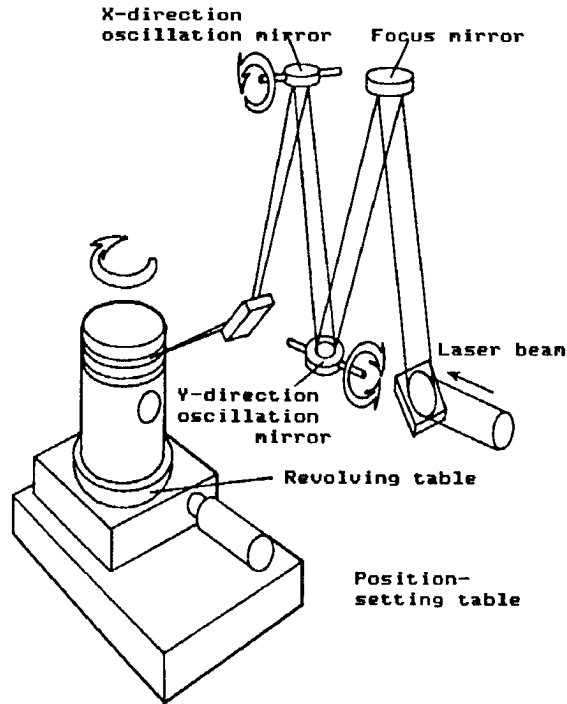


Figure 3. Oscillation Beam Method Employed by A.S. Bransden, et al., in Hardening Piston Ring Grooves

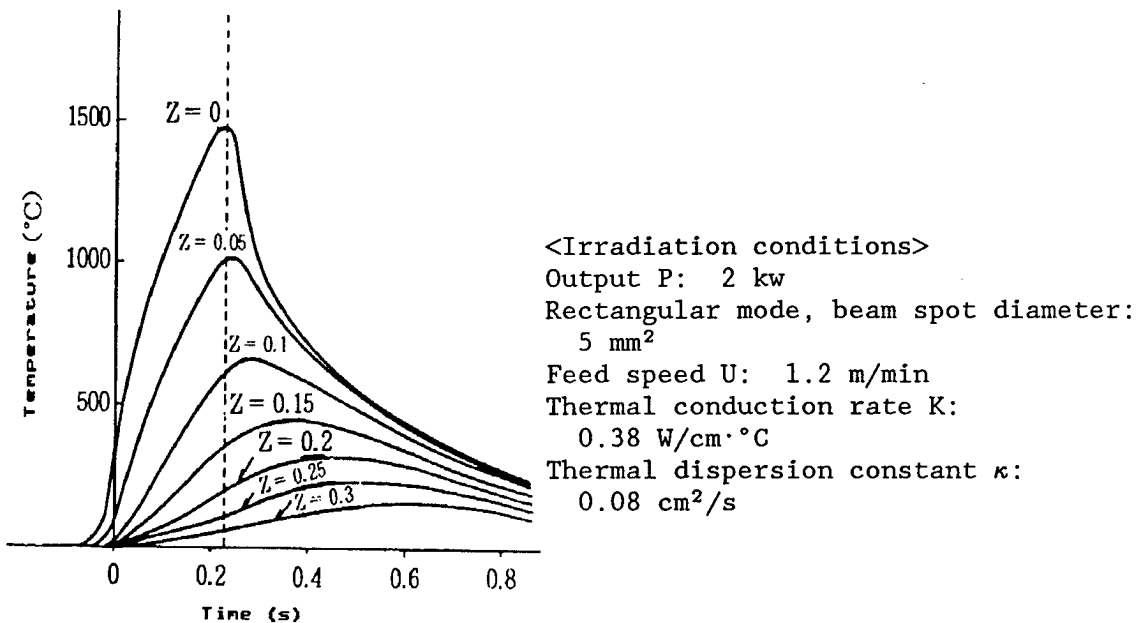


Figure 4. Heating/Cooling-Elapsed Time Characteristic Curves for Three-Dimensional Model of Mild Steel (S45C)

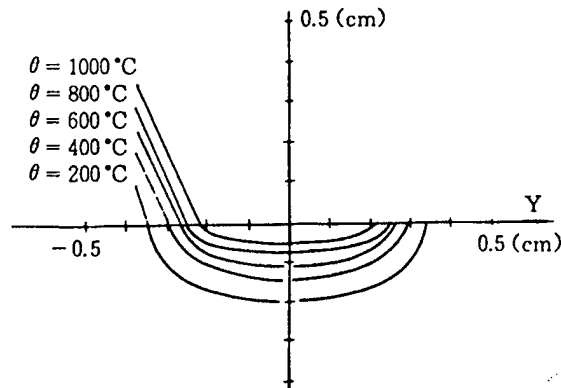


Figure 5. Curves of Temperature Distribution on Cross Section of Three-Dimensional Material Model Perpendicular to Direction to Which Heat Disperses

<Irradiation conditions>

Output P: 2 kw

Rectangular mode, beam spot diameter: 5 mm²

Feed speed U: 1.2 m/min

Thermal conduction rate K: 0.38 W/cm·°C

Thermal dispersion constant κ : 0.08 cm²/s

When a material, in which either the laser beam feed speed v is very large or the thermal diffusion rate is very small, is to be hardened by a laser beam irradiation, the surface temperature T_{\max} of the material is given by the following equation:

$$T_{\max} = \frac{2Q}{\kappa} \left(\frac{\kappa t}{\pi} \right)^{1/2} \dots\dots\dots (1)$$

The equation indicates that the surface temperature increase in proportion to the density of irradiation laser energy, and in proportion to square root of the length of irradiation time. This means that the thickness of hardened layer on the surface of the material increases approximately in proportion to square root of the length of irradiation time.

By calculations and experiment, this author found that hardening of the surface of a thin plate-form material can be conducted with satisfactory results, as long as the depth of the hardening is confined to less than one-tenth of the thickness of the material.

5. Consideration From Metallurgical Point of View

Two conditions must be met in hardening steel. One of the conditions is that the maximum heating temperature T_{\max} for conducting the surface hardening must be higher than the A_1 transformation point of steel, but

lower than the metal's melting temperature T_{melt} was surpassed, the smoothness of the surface of the hardened material could be harmed, and consequently the advantages of using a laser beam could be diminished too. (Recently, a new method has been developed in which hardening temperature is raised deliberately beyond T_{melt} to increase the depth of hardening, and the deformations caused by this are corrected in post-hardening treatment. But utilization of the method is confined to very limited applications.) The other of the two conditions concerns the necessity to cool the heated material from temperatures higher than the A_1 transformation point at a speed faster than the critical cooling speed.

In hardening a material using a laser beam, the material is heated to a high temperature rapidly (faster than 10^3°C/s). This gives the carbons within the material not enough time to disperse, and the material is rapidly cooled without the transformation having been completed. I will consider this problem using CCT curve chart, though the setting conditions in the chart are a little different from conditions in the conventional chart. The hardening using a laser beam is different from conventional hardening methods in that the laser version relies on self-cooling for cooling of the heated material. Consequently, cooling on the surface of the material progresses like curve I in Figure 6, while cooling inside the material progresses like curve II. Due to this, the greatest hardness of the material is achieved at a depth a bit inside from the surface.

Masao Kikuchi, et al., conducted experiments in which the same kind of cast iron samples were hardened using high-frequency hardening method and laser beam hardening method, respectively. As a result, it was found that the high-frequency hardening method could attain hardening to a deeper depth, but caused a considerably larger portion of incomplete hardening compared with the laser method. As regards the hardness achieved, the laser method could attain a higher hardness--50 or so larger in terms of Hv hardness. It is believed that this resulted from the faster cooling speed of the laser-beam method.

6. Hardening of Steel and Cast Iron

Figure 7 [omitted] is the photo of a cross section of a sample of carbon steel S45C, after the surface sample was hardened using a laser beam under optimum conditions. (The cross section shows a face of the sample perpendicular to the irradiation direction of the laser beam.)

The irradiation was conducted under the following conditions: laser power output--1.6 kw, TEM₀₀ mode; beam spot diameter--13.3 mm; feed speed--2 m/min; assisting gas--argon with a pressure of 2 kgf/cm² and with a flow rate of 50 l/min. In general, in laser-hardened carbon steel, a clear boundary is formed between the hardened portion and the rest of the parent material not hardened. Figure 8 gives the hardness distribution patterns in laser-hardened carbon steel samples. In the boundary regions, hardness suddenly drops, and this is a feature of laser beam hardening method. The figure shows that under optimum irradiation conditions (feed speed: 2.0-2.5 m/min) comparatively uniform hardness is obtained, with very few portions of incomplete hardening. When the feed speed is increased further,

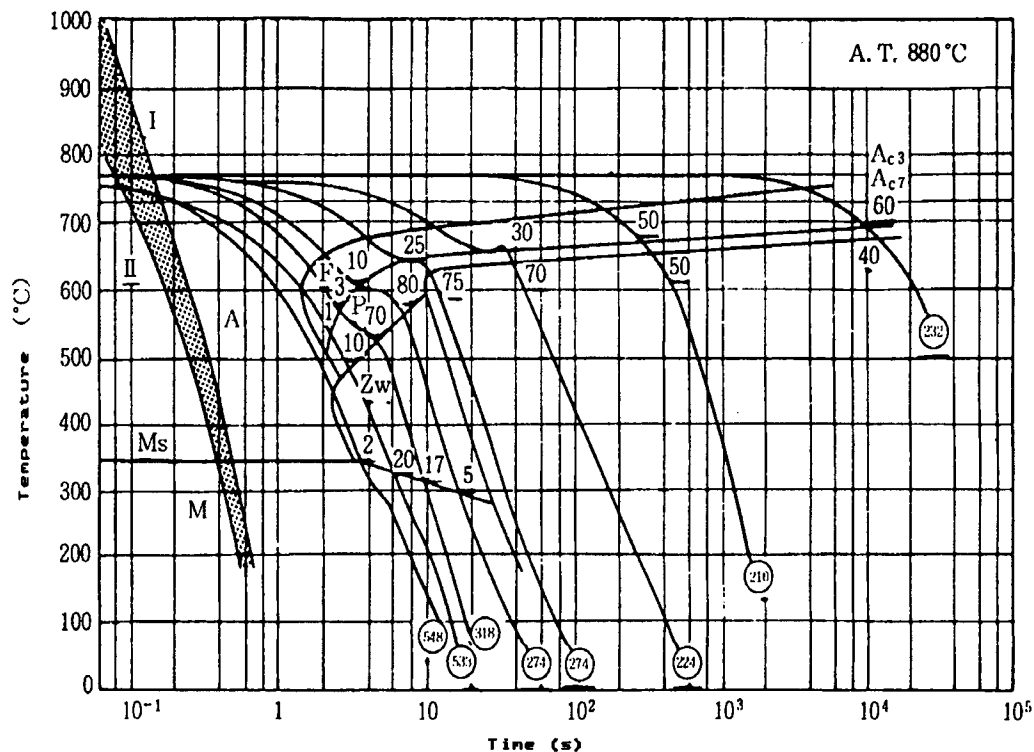


Figure 6. CCT Curve Chart (S45C-equivalent material)
<Irradiation conditions>

Rectangular mode, beam spot diameter: 5.0 mm²

Feed speed: 1.2 m/min

Compared with a Gauss-mode laser beam, a rectangular-mode beam has a steeper slope of the trailing edge of the waveform of the beam energy. This makes the cooling curves for the rectangular mode to shift toward the left in the chart compared with the Gauss-mode curves.

Output: 2 kw

nonuniformity in the hardness achieved tends to appear due to presence of portions within a material where carbons can be diffused easily or not so easily. Figure 9 [omitted], Figure 10(a) and (b) [both omitted] and Figure 11 (a) and (b) [both omitted] show the photos of the cross sections of a cast iron sample for high-frequency hardening, a black heart malleable cast iron sample and a perlite cast iron sample, respectively, after they were hardened using a laser beam. Table 1 and Table 2 give the results obtained from experiments to harden those material samples.

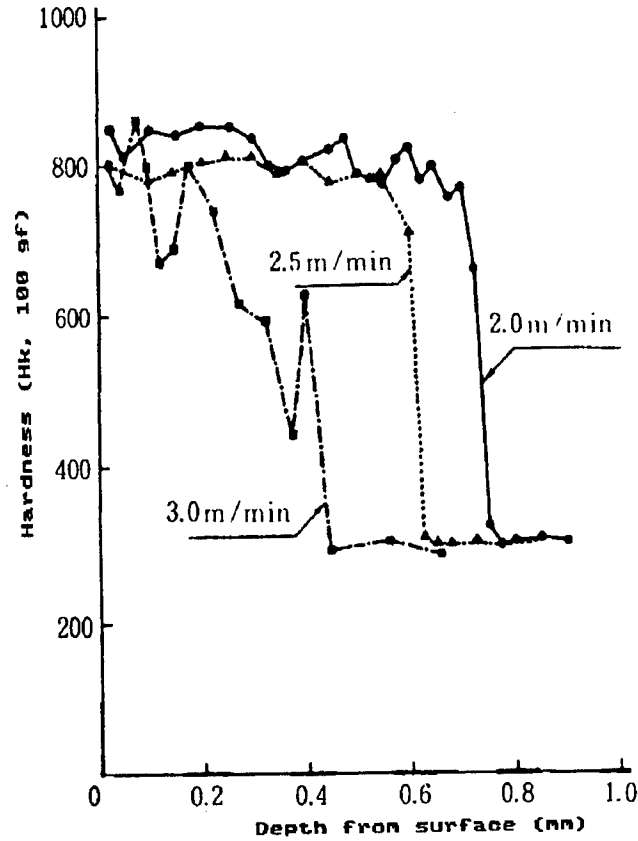


Figure 8. Hardening Depth-Hardness Curves for S45C Carbon Steel Samples
(Parameter represents laser beam feed speed)
Laser power output P: 2 kw
TEM₀₀ mode, 10 mm in beam diameter
Assisting gas: Ar

Table 1. Hardening Conditions for Various Kind of Steel and Widths and Depths of Hardened Layers (Surfaces were given (lubrication) treatment)

Material names	Output P (kW)	Feed speeds U (cm/s)	Hardened widths W (mm)	Hardened depths h (mm)	Hardness (HRC)	Metal composition	Modes
Hard steel 1045	2	0.83	6.8	1.0	60	Surface melting a little, mostly martensite	TEM ₁₁ + TEM ₀₀ Mix mode
Bearing steel SUJ2	1	2.0	2.6	0.44	65	Globular annealed material	TEM ₁₁ + TEM ₀₀ Mix mode
	1	2.5	1.3	0.18	60~64		
Tool steel	1	0.5	5.5	0.9	65	Untreated material	TEM ₁₁ + TEM ₀₀ Mix mode
Alloyed steel 4340	1	1.9	2.5	0.4	57~59	Globular annealed material	Doughnut mode
8620 SNCH 220	1	1.9	2.3	0.36	50	Very fine martensite	Doughnut mode

Table 2. Results of Experiments of Hardening of Various Kinds of Cast Iron
(Laser output: 2 kw, TEM₀₀ mode)

Material names	Feed speed U (m/min)	Hardened depth h (min)	Hardened width W (mm)	Hardness (max value) (HV)	Metal composition
FC25	2.5	0.30	2.54	791	Thick flake-like graphite within perlite base
Cast iron for high-frequency hardening	2.5	0.34	2.90	694	Flake-like graphite within perlite base
Ductile cast iron	1.0	0.46	3.18	722	Ferrite around globular graphite
FCMB	1.0	0.28	2.56	644	Globular graphite within ferrite base
FCMP	2.5	0.44	3.38	796	Globular graphite within perlite base
S45C	2.5	0.60	3.98	719	Ferrite and perlite

(Note) Laser beam spot diameter for S45C is 5.0 mm.

7. Points of Consideration in Laser Beam Hardening

From the results of experiments described above, it is important to pay attention to the following things:

(1) Highly smooth surface of a metal reflects the 10.6 μm laser beam well, and this makes it necessary to give a treatment to the surface to prevent the reflection.

(2) As seen in Table 1, in the case of bearing steel SU2 there appear large differences reaching higher than 1 to 2 in ratio in hardened widths and depths, between the globular annealed material and untreated material. A higher width and depth was attained in the treated material, in which carbons had been diffused well, showing the importance of a preparatory treatment prior to hardening. To attain a hardening to a deeper depth, it is necessary to use the rectangular mode or doughnut mode, modes suitable for a deeper hardening. At the same time, it is important to pick a kind of material which keeps heat longer and exhibits good results of hardening.

(3) In general, good hardening results can be obtained when the composition of the parent material is perlite based, but not when it is ferrite based. In modular cast iron and black heart malleable cast iron, the ferrite-based portions cannot be hardened easily, causing complex contours of hardened portions.

(4) Good hardening results were obtained in perlite malleable cast iron, cast iron for high-frequency hardening, and centrifugal cast iron. In all of those irons the attained hardness reached higher than 700 in HV values.

(5) As described so far, in laser beam hardening method, heating and cooling of a material occurs in a very short time, and the result of hardening depend greatly on the amounts of the carbons usable. The maximum hardness attained also depends on the amounts of carbons contained, and it is affected little by other material components. Consequently, as far as the results of hardening are concerned, attention should be paid to only the contents of carbons and their distribution pattern within the material. In the meantime, in hardening malleable cast iron, a time consuming prehardening treatment must be given to the metal. This pushes up cost for hardening the cast iron to the level equivalent to a cost for hardening low-alloy steel. For those reasons, whether or not the laser beam hardening method can be used must be decided by taking into account various elements affecting cost and the results of hardening.

8. Examples of Practical Applications of Laser Beam Hardening

In recent years, the quality of fuel oil used in low- and medium-speed diesel engines is becoming worse. This causes an increased friction between the piston rings and the piston ring grooves due to the hard residues of the oil. At present, hardening of piston material to ease wear on the ring groove surface is carried out using high-frequency hardening method for nodular graphite cast-iron pistons with a width of the groove higher than 5 mm (about 250 mm or higher in diameter of a piston). With the pistons having a groove width smaller than 5 mm, the high-frequency hardening method is unsuitable, and laser beam hardening method is being used instead. Yanmar Diesel Engine Co., Ltd., began applying the laser method to hardening of the piston ring grooves with a width of 4.5 mm. In 1 year, the company produced 4,000 units of the pistons having the ring groove width, and the company is satisfied with the low single-digit failures of such pistons. The diagrams in Figure 12(a) and (b) are based on a test-piece piston offered by the company. The piston is made of thin nodular graphite cast iron, and has a diameter of 200 mm with a ring groove width of 4.5 mm. Wear in the ring grooves occurs on the upper and lower faces of the grooves and in the first and second grooves closer to the combustion chamber. By taking this into account, Arita, et al., in their research calculated the depth of hardening in their experimental pistons to be 0.2 ± 0.05 mm, by allowing a tolerance aimed at lengthening the operative life of the piston slightly. They used an oscillator with a maximum output of 1.2 kw. The beam mode of the oscillator was a mixed mode of TEM_{00} and TEM_{01} (top-hat type).

In irradiating the grooves of the piston, a laser beam cannot help but be fired at the grooves from an oblique direction, and this causes a limit in the maximum width of the groove faces which can be hardened.

In the process of conducting hardening of the piston ring grooves, an important fact concerning the tolerance of the groove width was discovered.

As a result of hardening the first and second grooves using the overlapping heating method, there occurred a significantly large shrinkage (Figure 13) in the width of the second groove reaching 30μ (25μ in allowed tolerance).

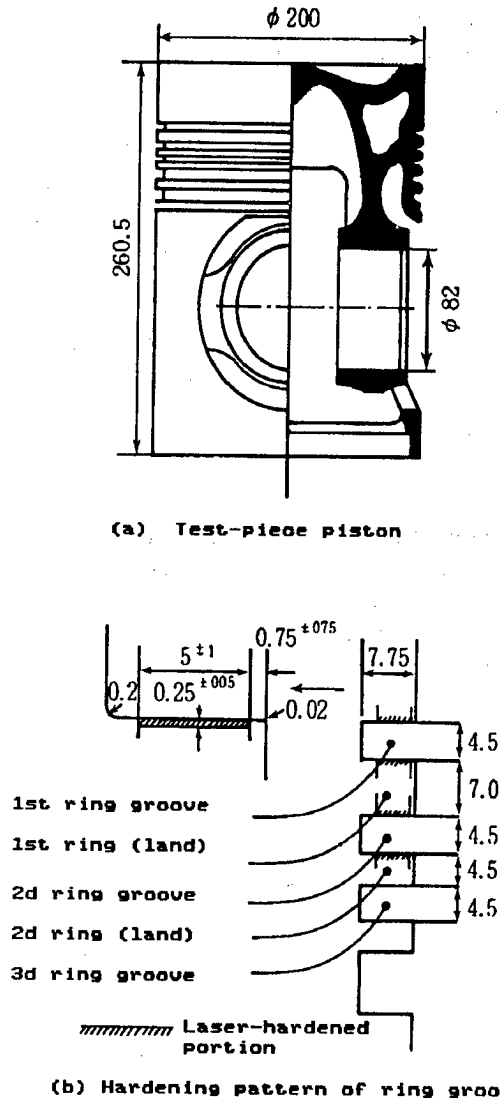


Figure 12. Dimensional Drawing of Piston Copied From Yanmar Diesel Engine Co. Used in Hardening Piston Ring Grooves Using a Laser Beam

This shrinkage was caused as a result of the second ring (land), forming part of the second and third grooves, having been hardened in only one side of the ring (land) (lower face of the second ring groove) and consequently a slant occurring in the ring (land). In a bid to offset the slant, the upper face of the third groove (lower face of the second ring (land)) was additionally heated. As a result the unwanted slant caused due to an expansion of the martensite was removed successfully.

The overall change (shrinkage) in the width of a piston ring groove after the slant was removed was larger than the degree of expansion caused as a result of the hardened portion's turning into martensite. The degree of change is said to have reached 12-15 μ , about twice as large as an expected change of the width of the groove ranging from 6 to 8 μ (for an upper and

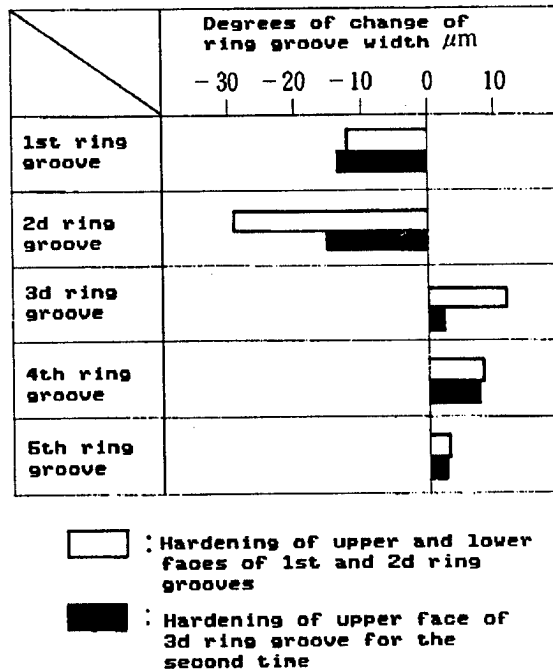


Figure 13. Changes of Widths of Piston Ring Grooves as Result of Laser-Beam Hardening of Grooves
(Results of distortion-canceling measure)

a lower face), due to turning of the hardened portions into martensite. Similar results have been reported by many other researchers, but causes for the large changes of width of the grooves have not been known well yet.

In practical applications, efforts to keep the change of width of the grooves within the tolerance values are made by giving mechanical processing to the piston grooves by taking into consideration the expected expansion rate and the degree of contraction.

Arita, et al., in their report declare, based on the results of above-mentioned example of processing, that laser heat processing should be recognized as a processing method causing comparatively low distortions to a product being processed. However, efforts must be made to reduce the distortions further. As seen in the examples discussed above, laser heat processing method, different from conventional processing methods, keeps a reference point to measure the degree of distortion in the treated product even after the distortions occur. This makes it possible to measure the absolute degree of distortion easily, and this in turn makes it easy to find the cause of distortions caused by laser beam hardening.

9. Turning Material Surface Into Alloy

The surface of a metal material can be turned into an alloy easily and in a very short time, by putting an alloy in powder form on the surface, plating the surface with the alloy or depositing the alloy element on the surface, and then irradiating the surface with a laser beam. A thin film of the

alloy is formed on the surface in a short time ranging from 10^{-3} to 10 sec or so, as a result of the alloy element dispersing into the base material. This method enables the formation of a film of alloy with a desired material composition at a desired place of a part or material.

By using the method it is possible to impart good capabilities against wear, corrosion, and high temperature to an inexpensive carbon steel base material by forming a film of high alloy steel at localized places on the material. This reduces the use of expensive alloy elements. In the United States, active research has been done on the alloy film with a view to conserving strategic metals.

For forming the alloy film, various kinds of elements can be used.

Figure 14 shows the relationship between the laser output and the depth of a film of alloy formed on an AISI-1018 steel.

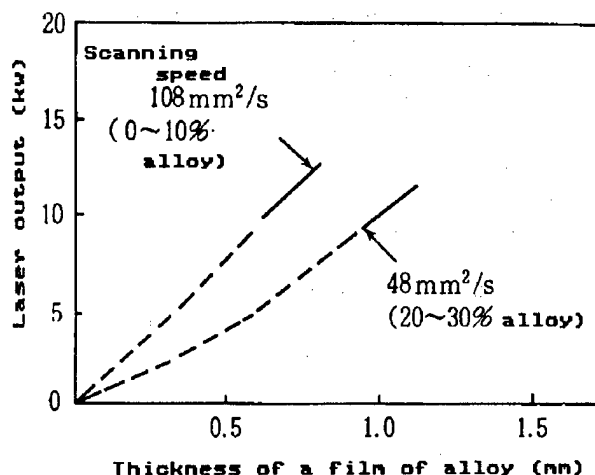


Figure 14. Relationship Between Laser Output and Depths of Film of Alloy Formed on AISI-1018 Steel Using 6.35 x 12.7 mm Beam (Parameter: scanning speeds)

The laser power input required for the formation of a film of alloy is about three times as large as one required for attaining the transformation hardening (thermal treatment) for a given unit area.

The gray cast-iron valve sheet for use in a large diesel engine, shown in Figure 15, could not withstand continued use under a temperature of 540°C, when only a transformation hardening had been given to it. To deal with this problem, the vital portions of the part were turned to alloy using a laser beam. To minimize the degree of necessary grinding, the work for forming the alloy was done after a mechanical processing was applied to the part. The deformation resulting from the work to form the alloy layer was confined within the permissible tolerance of 0.13 mm. The hardness achieved surpassed Rc55.

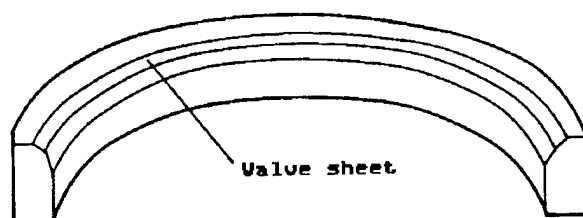


Figure 15. Valve Sheets for Large Diesel Engine, With Sheets Hardened by Laser Beam Irradiation (AVCO Corp.)

Table 3 gives the conditions for turning the surface of AISI1018 steel to alloy using a laser beam, and the results of an attempt to form the alloy, with the listed data obtained by D.S. Gnanamuthu.

Table 3. Conditions for Forming Alloys on Surface of AISI1018 Steel, Results of Attempt To Form Such Alloy (D.S. Gnanamuthu)

Powders of alloy elements pasted (wt %)	85 Cr - 15 C	25 Cr - 50 C - 25 Mn	24 Cr - 48 C - 24 Mn - 4 Al
Conditions			
Thickness of pasted mixture of elements (mm)	0.75	0.025	0.125
Shape of surface of base material Beam mode	Barrel-shaped $6.4 \times 19 \text{ mm}^2$		
Oscillation beam method	690 Hz		
Laser output (kw)	5.80	3.40	5.00
Feed speed mm/s	21.17	8.47	8.47
Depth of alloy layer mm	0.38	0.13	0.66
Component of alloy layer (wt%)	43.0Cr --4.4C --0.5Mn	3.5Cr -1.9C -1.3Mn	0.9Cr -1.4C -1.0Mn -0.5Al
Hardness		64	56

On the other hand, the Agency of Industrial Science and Technology's Mechanical Engineering Lab succeeded in directly coating the surface of mild steel with copper using a powerful CO_2 laser beam. The coating process involved pasting the surface of the steel with a mixture of copper powder and boron nitride (BN), and then irradiating the surface with a laser beam.

As a result of the irradiation, the copper melts and then solidifies on the surface. Firm adherence of the copper to the steel surface cannot be achieved when only copper is used. It was found that introduction of BN powder, with its ratio less than 50 percent of the copper, could achieve the strong adherence. It is expected that this coating technique could be applied to the production of large-diameter metal mirrors. The mild steel used for the coating is a kind called SS41, a commonly available material. The copper powder used in the coating had a diameter of about $20\ \mu$ and the BN powder a diameter of about $5\ \mu$. The mixture was composed of 70 percent copper powder and 30 percent BN powder in volume, and they were mixed by adding alcohol. The mixture was then pasted to the surface of the steel sample at a thickness of $25\ \mu$. After the alcohol evaporated, the sample was irradiated with a beam power of about 4 kw. While being irradiated, the sample was moved along at a rate of 50 cm per minute, and as a result a copper film strip measuring about 10 mm in width was coated on the surface of the steel sample.

The governmental Mechanical Engineering Lab announced that it also succeeded in coating other kinds of materials with copper using the same method. Those material included germanium glass, CC composite (a new material produced by baking carbon-fiber-reinforced plastic by shutting oxygen supply) and other kind of materials having light weights or low thermal expansion rates.

10. Cladding

It is known that a laser has a capability of cladding a parent material having a relatively low melting temperature with an alloy having a higher melting temperature.

Using a mild steel sample as the parent material, Akira Nakamura of Toshiba succeeded in cladding the steel with a 10 mm NiCr-system material strip using laser. The Ni-Cr material in powder form was pasted to the surface of the steel sample, and the cladding was carried out using oscillation beam method under a laser output of 5 kw with a feed speed of 0.2 m/min. As shown in Figure 16 [omitted], a diffusion layer having firm adherence was formed between the cladding layer and the parent material.

The hardness of the cladding layer increased from Hv 600 on the surface of the melted and then solidified layer of Ni-Cr-system material to 700 toward the parent material (Figure 17).

It is possible to form a cladding layer up to the thickness of 2 mm using lasers. In the Nakamura's cladding formation method, cracks tend to develop on the layer. To prevent cracks from developing, it is important to change the irradiation power slowly by giving adequate preheating to the materials to be treated.

Nakamura also succeeded in creating a steel plate enveloped by a film of Al_2O_3 having good anticorrosion ability (Figure 18 [omitted]). For the formation of the film, first a film of Al was formed on the surface of a

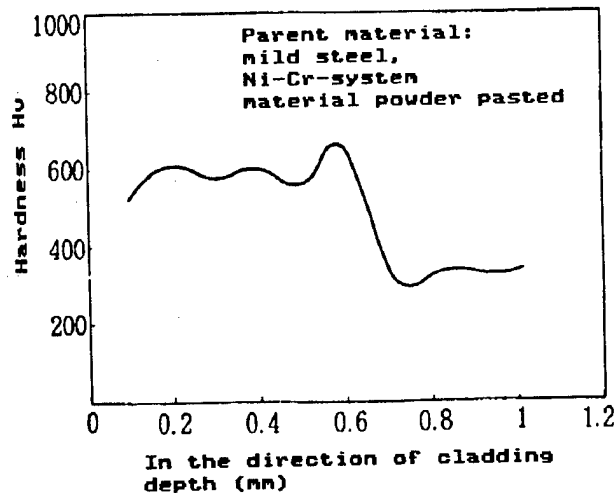


Figure 17. Hardness Distribution Pattern Within Cladding Layer Formed by Laser Irradiation

steel sample. Then the sample was irradiated with a laser beam within an oxidizing atmosphere to create a stable film of Al_2O_3 .

11. Glazing

Glazing is a surface reform technology developed by United Technologies Corp. The reform method calls for scanning the surface of a material with a laser beam at high speed, to form a thin melted and then solidified layer of the ZrO_2 - HfO_2 material by adjusting for the beam spot to have an energy density ranging from 10^5 to 10^7 w/cm². The melted layer solidifies at a very high speed, as the parent material surface is scanned while the material is kept cool. When the thickness of the melted layer ranges from 1 to 10 μ , the cooling speed reaches 10^8 °C/s, and either superfine material composition or amorphous phase structure is formed within the solidified layer. By reforming the material surface, it is possible to make a material having good characteristics against corrosion, wear or material fatigue.

12. Conclusion

Today, laser beam hardening technology has been established as a surface reform technology for mass-production application. Recently, a new processing technology which is difficult to regard as a surface reform technology began to be used as a mass-production technology. An example of such a technology is seen in the production of the electromagnetic steel of lower power loss for use in transformers. The procedure for producing the steel involves making craters on the surface of the steel in a regular pattern by irradiating the surface with a laser beam of very fine spot. Such craters narrow the width of the magnetic domains, due to the residual stress fields present when the steel is used as the iron core in transformers, reducing the power loss in the core. At present, Nippon Steel Corp. turns out electromagnetic steel with the laser-produced craters, and the production volume attains a few hundred thousand tons per year. Another example is seen in the steel for use in the exterior panels

of automobiles. On the steel for such an application, similar craters are formed in a regular pattern using an equally small-spot laser beam. Such craters serve as the oil sumps in stamping the steel. In painting the car body, the use of the steel with the depressions on the surface enhances the results of the paint work by making the painted surface shine better. The steel product with the laser-produced depressions is currently mass-produced under the trade name of "laser-mirror steel plate." Those examples of the application of laser technology suggest that a new major mass-production technology could bloom around the laser surface reform technology in the future.

20102/9365

END

10

This is a U.S. Government publication. Its contents in no way represent the policies, views, or attitudes of the U.S. Government. Users of this publication may cite FBIS or JPRS provided they do so in a manner clearly identifying them as the secondary source.

Foreign Broadcast Information Service (FBIS) and Joint Publications Research Service (JPRS) publications contain political, economic, military, and sociological news, commentary, and other information, as well as scientific and technical data and reports. All information has been obtained from foreign radio and television broadcasts, news agency transmissions, newspapers, books, and periodicals. Items generally are processed from the first or best available source; it should not be inferred that they have been disseminated only in the medium, in the language, or to the area indicated. Items from foreign language sources are translated. Those from English-language sources are transcribed, with the original phrasing and other characteristics retained.

Headlines, editorial reports, and material enclosed in brackets [] are supplied by FBIS/JPRS. Processing indicators such as [Text] or [Excerpts] in the first line of each item indicate how the information was processed from the original. Unfamiliar names which are rendered phonetically or transliterated by FBIS/JPRS are enclosed in parentheses. Words or names preceded by a question mark and enclosed in parentheses were not clear from the original source but have been supplied as appropriate to the context. Other unattributed parenthetical notes within the body of an item originate with the source. Times within items are as given by the source.

SUBSCRIPTION/PROCUREMENT INFORMATION

The FBIS DAILY REPORT contains current news and information and is published Monday through Friday in 8 volumes: China, East Europe, Soviet Union, East Asia, Near East & South Asia, Africa (Sub-Sahara), Latin America, and West Europe. Supplements to the DAILY REPORTs may also be available periodically and will be distributed to regular DAILY REPORT subscribers. JPRS publications generally contain less time-sensitive information and are published periodically. Current JPRS publications are listed in *Government Reports Announcements* issued semi-monthly by the National Technical Information Service (NTIS), 5285 Port Royal Road, Springfield, Virginia 22161 and the *Monthly Catalog of U.S. Government Publications* issued by the Superintendent of Documents, U.S. Government Printing Office, Washington, D.C. 20402.

U.S. Government offices may obtain subscriptions to the DAILY REPORTs or JPRS publications (hardcovers or microfiche) at no charge through their sponsoring organizations. DOD consumers are required to submit requests through appropriate

command validation channels to DIA, RTS-2C, Washington, D.C. 20301. (Telephone: (202) 373-3771, Autovon: 243-3771.) For additional information or assistance, call FBIS, (703) 527-2368, or write to P.O. Box 2604, Washington, D.C. 20013.

The public may subscribe to either hardcover or microfiche versions of the DAILY REPORTs and JPRS publications through NTIS at the above address or by calling (703) 487-4630. Subscription rates will be provided by NTIS upon request. Subscriptions are available outside the United States from NTIS or appointed foreign dealers. Back issues or single copies of the DAILY REPORTs and JPRS publications are not available. New subscribers should expect a 30-day delay in receipt of the first issue.

Both the DAILY REPORTs and the JPRS publications are on file for public reference at the Library of Congress and at many Federal Depository Libraries. Reference copies may also be seen at many public and university libraries throughout the United States.